THE EFFECT OF HIGH VOLTAGE FIELDS ON EPOXY LAMINATES

Thesis Submitted for the degree of
Doctor of Philosophy
at the University of Leicester

By

Mohammed Nasser Ajour
Department of Engineering
University of Leicester

July 2003

THE EFFECT OF HIGH VOLTAGE FIELDS ON EPOXY LAMINATES

By

Mohammed Nasser Ajour

DECLARATION OF ORIGINALITY

This thesis is submitted in fulfilment of the requirements of Doctor of Philosophy in the Department of Engineering, University of Leicester, United Kingdom. All work recorded in this thesis is original unless otherwise is acknowledged in the text reference. No part of this thesis has been submitted for any other degree either to the University of Leicester or to any other University.

Signed

Mohammed Nasser Ajour

July 2003

ACKNOWLEDGEMENT

I would sincerely like to thank my supervisor professor John Fothergill for his encouragements, guidance, support, and supervision. I wish to thank professor Len Dissado. I would sincerely like to thank Dr Phil Norman and his staff at Alcatel Submarine Networks for their help and support during my visits to London. I wish to thank Alcatel Submarine Networks for their financial support. I wish to thank the EPSRC for their financial student award.

I wish to thank all the staff at the Engineering Department for making my time at the Department very enjoyable.

I wish to dedicate this thesis to my father Nasser, and my daughter Sara for all what they gave me in life. I wish to express my gratitude for all of my brothers and sisters for all their support.

I would like to give my thanks to all of my friends for their spiritual support.

Finally I would like to express my appreciation to Roger Shirly-Elgood for his technical support. To the many people who have not been mentioned but have contributed in some way to my research work, I hope the lack of acknowledgment will not be taken as lack of gratitude.

Mohammed Nasser Ajour.

THE EFFECT OF HIGH VOLTAGE FIELDS ON EPOXY LAMINATES

By

Mohammed Nasser Ajour

Abstract

This thesis describes the characterisation of epoxy/glass fibre composite material before and progressively through electrical and thermal ageing. Glass fibre reinforced epoxy (GFRE) material is used in pressboard transformers for optical telecommunication systems, typically at voltages between 1 and 2kV. The material was characterised by means of space charge measurements using the Pulsed Electro-acoustic (PEA) technique, Dielectric response, Dynamic Mechanical Analysis (DMA), Differential Scanning Calorimetry (DSC), and Scanning Electronic Microscopy (SEM). An ageing programme was set up to follow the thermal and electrical ageing (at DC fields) of the GFRE by the same means.

The results show a q-dc transport process with an activation energy of 1.1eV. The q-dc process is associated with a charge transport process on the surface of the fibres. The results for the aged samples show delamination and debonding between the epoxy and the glass fibre at the glass epoxy interface. The delamination creates free volumes and voids which lead to partial discharge and hence failure. Electrical ageing can be characterised in term of dielectric, PEA, and DSC responses. Thermal ageing does not produce the same effect as electrical ageing. The samples that were only thermally aged behave in the same way as un-aged samples.

CONTENT

CHAPTER 1

INTRODUCTION

1.1 General Introduction.

Electrical and electronic insulating materials, also called dielectrics, are essential for the proper operation and reliability of all electrical and electronic equipment. The type and size of dielectrics used determine the size and the operational limitations of the electrical equipment [1]. The prime objective of insulating materials is to prevent the flow of electric current where it is not wanted and to support high electric fields. The main requirement of the material is to have the lowest electrical conductance coupled with the maximum resistance to electrical breakdown, long life, low cost, mechanical strength, high corrosion resistance, ease of forming and manufacturing, chemical inertness, and the ability to withstand elevated temperatures [1]. There is a need and desire to reduce the size, enhance reliability, reduce degradation, and increase the life of electrical power equipment. This has resulted in a search for new types of equipment and a need for a fundamental understanding of the effect of increased electrical stress inside the equipment. Printed circuit boards (PCBs) are no exception. There has been a density revolution in PCB technology. There is a continuous evolution towards a smaller and more efficient board [2].

Significant advances have been achieved in the research of electrical breakdown of insulating materials in the last thirty years. However the subject is very complicated and not fully understood. More research is needed to fundamentally understand the mechanism of electrical breakdown and the way in which an applied voltage causes degradation. Degradation and breakdown need to be characterised as a function of parameters such as electrical field, temperature, time of voltage application, and thickness. This will lead to better component design.

Polymers are the most widely used insulation in electrical machines. In order to fundamentally understand the physics of ageing process in polymers, it is vital to understand polymer's morphology and structure, the chemistry of the polymer, and charge trapping and transport in polymers.

The behaviour of insulations in printed circuit boards has been intensively studied in the last ten years. The research is driven by the spectacular rise of High Density PCBs in domestic and commercial electric machines; Kaore Fukunaga has investigated charge migration from electrodes to epoxy [3]. She found that ions might migrate from copper to insulation material. Helgeson looked at the dielectric response of epoxy resin during curing [4]. Y.Yamano studied dielectric losses and ion migration to PCBs [5]. Hitachi –Shi looked at the Breakdown strength in epoxy resin at high temperatures [6]. Sheiretov and Zahn investigated moisture dynamic in PCBs [7]. S. Grzybowski studied accelerated ageing of high voltage encapsulated transformers [8].

The existing knowledge falls short of giving a full picture of the behaviour of epoxy /glass fibre composite in printed circuit boards. More research is needed in the area to gain the fundamental understanding in order to keep pace with the technological advances in the high density printed circuit boards.

Epoxy- glass composite material is investigated in this thesis. The results show that ageing can be characterised by dielectric response, space charge measurements and DSC. The results also show that ageing causes delamination between epoxy and glass fibre. This delamination creates free volume and facilitate for degradation and hence breakdown.

1.2 Modern Printed Circuit Boards.

All electrical and electronic components must be interconnected and assembled so as to be able to perform a function and create an operational system. Since the 1950s the basic building block for assembly is the printed circuit board (PCB) and it will remain so for the foreseeable future [9]. PCBs are also known as printed wiring boards (PWBs). In this thesis we shall refer to them as PCBs.

PCBs are made single side, double side or multilayer. This can go up to 40 layers [2]. Multilayer printed boards are the most widely used now. Multilayer printed circuit boards consist of a number of layers of thin, flexible, or laminate systems stacked together with an orderly registration. The characteristics of multilayer PCBs are large volume production capability, exact reproduction of circuitry from board to board, high density of circuitry and terminal points, increased freedom of conductor routings, shorter conductor paths, integral shielding and heat sink planes, and improved environmental performance by locating all conductors within a homogenous dielectric material. This enables the highest component densities, and reduces the size. Layers may be reserved for power distribution or shielding.

Shielding is implemented by interposing a ground foil layer between two wiring planes, the signals of which would otherwise interfere with each other. This implies that wiring has been carefully grouped so that incompatible signals do not occupy the same layer. Multilayer PCBs require very close attention to dimensional tolerance, as they are virtually impossible to repair.

Layer to layer connection on multilayer PCBs can be formed by

- Plated through-holes (PTH)
- Clearance holes.
- Sequential build-up (SBU) process.

Plated through holes is the most commonly used method. It commences after the individual layers have been laminated together, only then are the holes drilled, etched back and plated. Since holes are drilled at the same time, PTH construction is more convenient than the clearance holes method. The SBU process emerged around 1988. The technology is based on interlayer connection and is limited only by the required layers. This enables higher wiring densities and greater wiring freedom [2,9].

1.2.1 PCB Design

Central to the design of every modern circuit board is the use of a grid system as an aid to the placement of components. Choosing the substrate material is one of the

most important design decisions. Epoxy/glass fibre is one of the most desirable materials to be used. Considerations must be given to removal of heat from the system [2, 9]. For multilayer PCB design it is recommended that no wiring be placed on the outer layer, just heat sinks, ground planes or pads that marks the holes locations.
Outer layer wiring is avoided because defects produced in the etching may ruin the whole board. The thickness of the multilayer PCB should be limited to a maximum of 3 times the diameter of the smallest plated through hole.
It is imperative that the board does not expand or contract excessively in the z-axis direction as the temperature change would crack and ruin the plated through holes.

1.2.2 PCB Fabrication:

Fabrication of circuit boards varies from one manufacturer to another; each manufacturer has his own recipe [2].
The basic manufacturing steps are:

- Circuits are etched on a thin laminate (less than 0.8mm).
- The laminates are then laid up to the desired construction with two or three bonding layers of prepreg between circuit layers.
- These multilayer books are cut to size and positioned in a moulding frame by the means of locating pins.
- The frame with the lay-up is placed in press; making sure platens are parallel to within 0.025mm.
- The press is closed and heated to the desired temperature, usually in the range of 149-232 °C at pressures of about 3.50MPa.
- After approximately one hour, the press contents are cooled under pressure to about 49 °C.
- The frame is unloaded from the press and the circuits removed.

Each step must be carefully monitored to ensure the circuit quality. Causes of rejects include voids, blisters, displaced layers, delamination, and board distortion.

1.2.3 Insulating materials used in PCBs

The choice of insulating material is crucial to the design of PCBs. The reinforcement type, the resin system used, and the glass transition temperature Tg can classify the various types of base materials [2, 9].
The most commonly used classifications are:
National electrical manufacturers association (NEMA) grades.
IPC-4101 specification for base materials for rigid and multilayer boards

Some of the most commonly used materials are FR-2, FR-3, CEM-1, and CEM-3 FR-4.

- FR-2 is made from piles of papers impregnated with flame resistance phenolic resin. It is cheap. It is used for simple applications [2].
- FR-3 is made from piles of paper used in epoxy resin system [2].
- CEM-1 is paper with woven glass cloth on the surface. It is used in home and industrial electronics [2].
- CME-3 is a composite made from dissimilar core materials. It is more expensive than CEM-1 [2].
- FR-4 is the most commonly used material for PCBs. It is made of woven fibreglass cloths impregnated with an epoxy resin. FR-4 has excellent electrical, mechanical, thermal properties [2].

1.2.4 Polymers:

Polymers have large molecules in the form of long chains. Each chain consists of a large number of small molecules, known as monomers. The chains may be linear, branched or cross-linked [10]. A simple example of a polymer chain is that of polyethylene shown in Fig1.1.

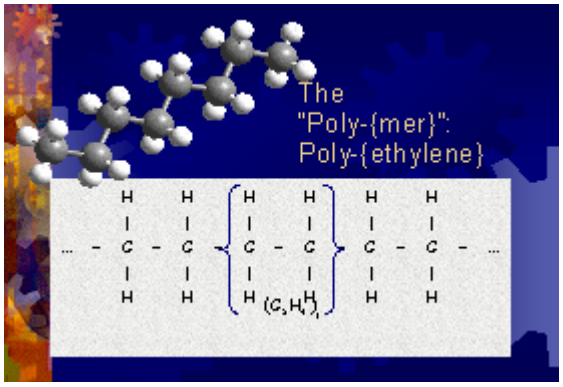

Figure 1. 1

Polymer chains may contain of the order 10^3-10^5 monomer units [10]. The end groups' effect on the properties of the bulk material is very small. Nevertheless they may have a significant effect on space charge by acting as charge traps. All polymers can be assigned to one or two groups based upon their processing characteristics or type of polymerisation mechanism. More specific classifications can be made on the basis of polymer structure [11, 12, 13].

The shape of the building block monomer unit and the degree of cross-linking are the main factors affecting the polymer chain structure. The properties of polymers are strongly influenced by details of chain structure.

Many polymers are semi-crystalline, consisting of both crystalline and amorphous regions.

In crystalline solids the atoms are arranged in a regular three-dimensional array. There is a basic unit, called the unit cell, which is repeated throughout the structure in all three dimensions. Crystalline solids have a well-defined transition melting point. The reason for having a well-defined melting point is that crystalline molecules are bound by similar forces: the energy needed to break the bonds is the same. Polymer chains are very long; it is very difficult for the chains to fit into a perfect crystalline arrangement.

Amorphous materials are materials whose molecules have no regular order structure. Glass is an example of this structure; the forces binding the molecules together will vary. Thus the material will not have a well-defined melting temperature. These materials go through a glass transition state with an average temperature Tg [11].

Semi-crystalline structure: most polymers are made of a mixture of crystalline and amorphous parts. So polymers possess the properties of both structures. They go through melting and glass transition temperatures.

The crystalline region of polymer forms what are called *lamellae* and a group of lamellae can then form spherulites as shown in Fig 1.2 [10, 11, 12, 13]. Lamellae are large parallel chains of polymers molecules. Lamellae formations achieve a very high degree of crystallisation surrounded by amorphous region. The amorphous region contains most of the physical and chemical impurities.

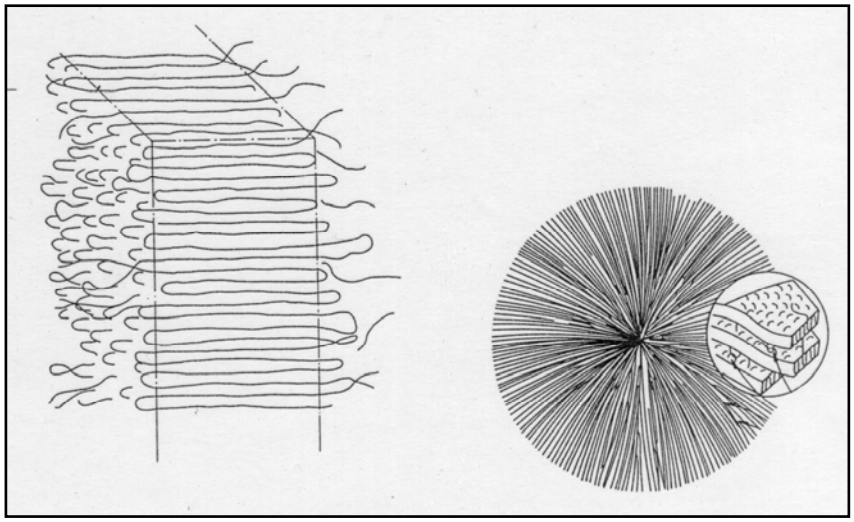

Figure 1. 2. From [10]

1.2.5 Epoxy resin:

Epoxy resins are polymers in which the end groups contain an epoxide ring shown in Fig 1.3 [14].

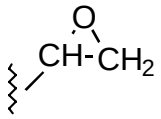

Figure 1. 3

Epoxies represent a special type of polymer and they are among the most widely used dielectrics, they are very important from the commercial standpoint.

Epoxies are used in many industrial applications, (PCB, transformers, motors, generators, switchgear, coil, capacitors, resistors) because of their many outstanding characteristics:

- Excellent dielectric properties.
- Superior adhesion to most surfaces.
- Low shrinking during cure.
- Good thermal properties.
- Good chemical resistance.
- Good moisture resistance, depending on fillers.
- Their properties may be varied widely to suit specific end uses.
- Can be moulded.

1.2.5 Epoxy resin Chemistry:

The exact details of the epoxy resin or the hardener used in the multilayer PCB are not available, because the manufacturers do not supply the details of their products for commercial reasons.

However the material used is N4000-2 which is an FR-4 system flame retardant epoxy /glass [15] .The resin is a reaction product of Epichlorohydrin and tetrabromobisphenol-A.

The epoxide group serves as a terminal linear polymerisation point in all epoxy resins. Crosslinking of epoxide molecules occurs at the epoxide group and at the hydroxyl groups that may be present in the molecules.

Although there are many variations in epoxies, the basic epoxy resin is the polycondensation product of bisphenol-A and epichlorohydrin, see Figure 1.4 [14].

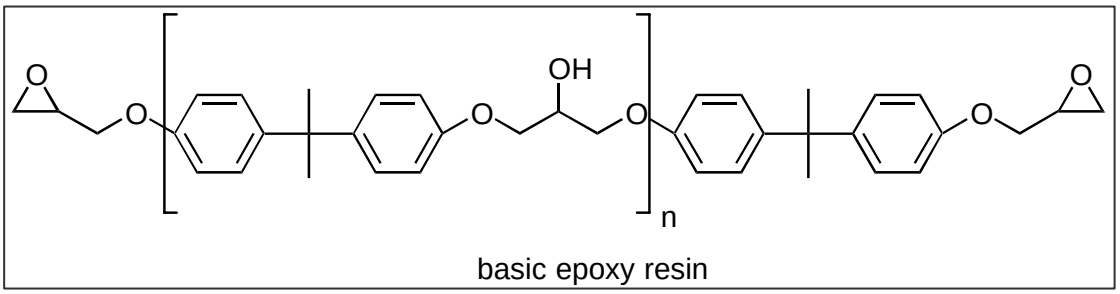

Figure 1. 4. From [14]

1.2.6 Epoxy processing:

The base resin is a mixture of Diglycidyl Ether-Bisphenol-A (DGEBA) and Iso-Octyl Glycidyl Ether (IOGE).

Epoxies have a sophisticated molecular network and are formed in a two-procedure process. Initially pre-polymer Diglycidyl Ether-bishphenol A (DGEBA) is prepared by a base catalysed step-growth reaction of dihydroxy compound such as bisphenol-A

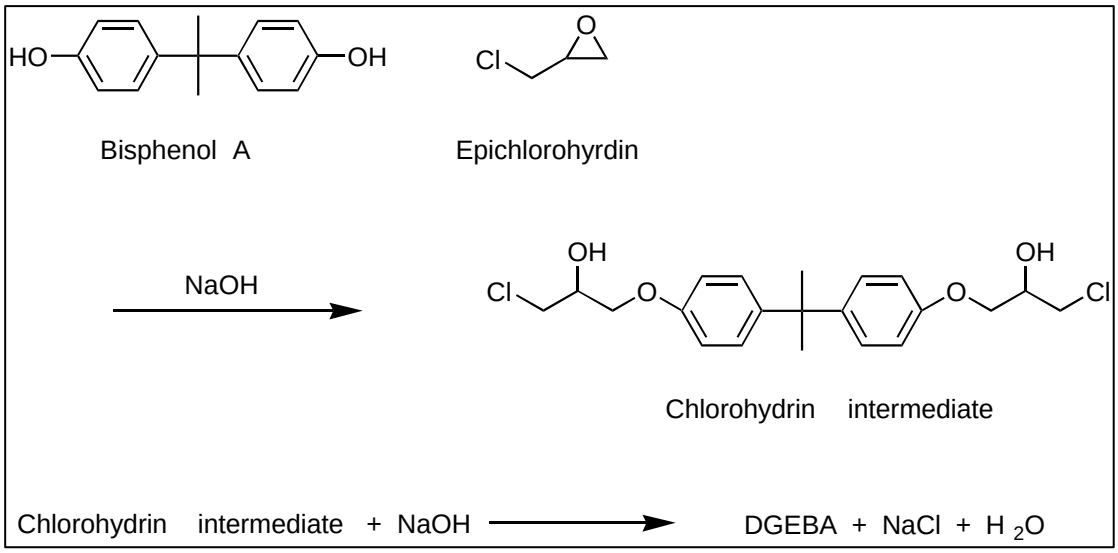

Figure.1.5

with an epoxide like Epichlorohydrin [14, 16]

The Epochlorohydrin is made from propylene and Allyl Chloride.

The Bisphenol A is a product of acetone with phenol in a condensation reaction producing water.

DGBA is prepared as follow:

Epichlorohydrin reacts with phenolic hydroxyl groups of the Bisphenol-A. This reaction is catalysed by NaOH to give a chlorohydrin intermediate component.The chlorohydrin intermediate then reacts with NaOH to get rid of the hydrogen and chlorine, which produces a new epoxy group. The ratio of Epichlorohydrin to Bisphenol determines the molecular weight of the resin produced see Figure1.5.

1.2.7 Epoxy curing

Epoxies must be cured by the action of a hardener to be made into useful end products [16]. Epoxies can be cured in two ways:

The hardener can react with the epoxide group and become part of the epoxy. The hardener can promote the resin's self- polymerisation by a catalytic action.

The final curing of epoxy involves the chemical reaction of hardening agent such as a diamine with the terminal epoxide group creating a cross-linked polymer structure.

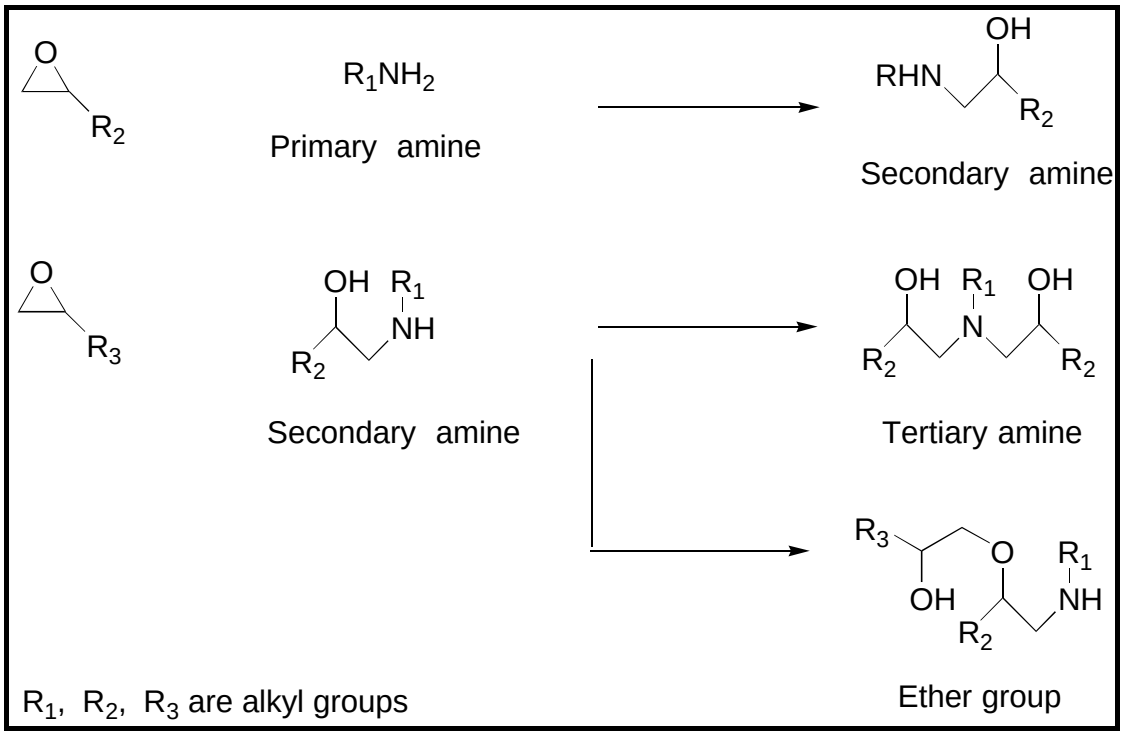

Figure 1.6

Figure 1.6 is a polymerisation reaction between molecules with amine group and epoxide group. It shows primary amine to secondary amine reaction, secondary amine to tertiary amine reaction and secondary amine to ether reaction.

There are several types of hardeners [16]:

Primary, secondary and tertiary aliphatic amines are the most commonly used hardeners in concentrations of 4 to 20 parts per 100. Curing proceeds at room temperature. Systems may be toxic.

Primary, secondary and tertiary aromatic amines require high temperatures. They impart longer pot life and improve thermal properties, mechanical strength and chemical resistance properties. They produce a harder cured system than aliphatic amines. The system may be toxic.

Polyamides affect curing at room temperature, producing a tough resilient system with good moisture resistance and excellent adhesive properties. The ratio of epoxy to polyamides may range from 80/20 to 40/60 by weight.

Anhydrides, derived from dicarboxylic acid, require a temperature of 120 degree C for rapid curing, the hardener concentration of 30 to 140 per 100 parts of resin. These produce good thermal, mechanical and dielectric properties.

Flame resistance of the epoxy system may be improved by incorporating into recipes phenols and anhydrides containing bromine, chlorine, and phosphorous as well as antimony oxide.

The viscosity of the liquid may be reduced by reactive dilutants such as allyl butyl, and phenyl glycidyl ether, or styrene oxide. Unreactive dilutants such as dibutyl phthalate are also used for this purpose, acting also to plasticize and add flexibility to the cured system.

The most commonly used ratio of epoxy resin to hardener is one to one. However in practice it could be as high as 100 parts epoxy to one part hardener.

To facilitate uniform mixing resin and hardener are usually of different colours.

Proper precautions are required to handle epoxy systems safety hazards include the following:

- Skin irritation.
- Ingestion- materials are toxic.
- Inhalation (toxic materials).
- Percutaneous absorption.
- Material my cause severe eye burns.
- Flammability.
- For some room temperature curing epoxies, measures should be taken to ensure that temperature rise is controlled.

1.2.8 Glass fibres:

Epoxy resin properties are often improved significantly by compounding with reinforcements and fillers.

Glass is an amorphous material. It is the most common of reinforcing fibres. It significantly improves the mechanical strength and electrical insulation properties of

the composite material. The Young modulus of the epoxy on it own is 3GPa, of glass it is 80GPa, and for the composite it is 24GPa. This is a very significant increase. Chopped standards of glass in length of 3-6 mm comprise 10-50 percent of the compound weight for optimum results.
The most common reinforcement used for resins is known as “E” glass. This glass was especially designed for dielectric applications, although it is now more widely used. E glass has 50-55 percent SiO_2, which is less than in most other glasses. Boric oxide (B_2O_3) content in the E glass is 8-13 percent, among the highest of all glasses. Other major ingredients are Al_2O_3, Fe_2O_3 and CaO.

All glass fibres must have a surface treatment, or sizing, that serve as the lubricant and bonding agent.
Glass fibre reinforcements are supplied in many different forms. It is supplied to the manufactures of the PCBs studied in the form of cloth woven on textile looms in a variety of thicknesses. Unidirectional properties are obtained by emphasizing warp (lengthwise) yarns over weft (filling) yarns.

1.2.9 E Glass Fibre processing

Glass fibres are generally produced using melt-spinning techniques. These involve melting the glass composition into a platinum crown, which has small holes for the molten glass to flow. Continuous fibres can be drawn out through the holes and wound onto spindles, while short fibres may be produced by spinning the crown, which forces molten glass out through the holes centrifugally. Fibres are cut to length using mechanical means or air jets.

Fibre dimensions and to some extent properties can be controlled by the process variables such as melt temperature (hence viscosity) and drawing/spinning rate. The temperature window that can be used to produce a melt of suitable viscosity is quite large, making this composition suitable for fibre forming.

As fibres are being produced, they are normally treated with sizing and coupling agents. These reduce the effects of fibre-fibre abrasion, which can significantly

degrade the mechanical strength of the individual fibres. Other treatments may also be used to promote wetting and adherence of the matrix material to the fibre.

Properties that have made E-glass so popular in fibreglass and other glass fibre reinforced composite include low cost, high production rates, high strength, high stiffness, relatively, low density, non-flammable, resistant to heat, good chemical resistance, relatively insensitive to moisture, able to maintain strength properties over a wide range of conditions, good electrical insulation

1.3 Charge conduction and transport in polymers

Polymers are insulators and they are not supposed to conduct electrical current. The polymers electrical properties change when subjected to high electric fields and temperatures for long time. Consequently insulators conduct electrical current. The classical conduction and transport mechanism found in conductors and semiconductors are not found in polymers. This is due to the difference of morphology and chemistry of the polymer. Consequently different mechanisms operate. Charge injection from electrodes into polymer, traps and volumetric conduction, tunnelling and hopping conduction were found to play an important role in conduction and charge transport in polymers It is important to investigate charge transport processes in polymers in order to understand ageing, degradation, and breakdown mechanisms. In the last thirty years extensive research has been made into charge conduction and transport in polymers [17, 18, 19, 20, 21, 22].

1.3.1 Charge injection from electrodes into polymer.

The electrode-insulator interface is very complicated [10, 22]. Electrical, chemical and physical defects are likely to exist at the interface. Such defects include protrusions, imperfect contact, dangling bonds, and local polarisation, contaminate, and traps. The main two theories that describe the interface phenomenon are Schottky and Fowler Nordheim. Electrons are injected from electrodes into the bulk of material. Electrons need to overcome a potential barrier to cross from electrode into insulator. Crossing the barrier depends on applied electric field and the interface defects [19].

1.3.2 Schottky injection.

Schottky injection describe one way electrons are transferred from electrodes into dielectric [18, 19, 22]. At electrode-insulator interface electrons overcome the potential barrier, leave the metal electrode and move to the adjacent insulation material. The barrier is assumed to be abrupt between the metal and the insulator. In Schottky injection the barrier is modified by the electrostatic attraction between the

positively charged electrode, since it has lost an electron, and the electron. This electrostatic attraction leads to a change in the barrier due to the electron potential energy.

1.3.3 Fowler-Nordheim injection

At high fields and short distances the potential barrier become very thin and non-classical mechanism come into existence. Classical physics is no longer valid in this situation. Particles exhibit the particle- wave duality and the principle of uncertainty comes into play [18. 22]. This is will lead to electrons tunnelling through a potential energy despite not having enough energy to overcome them normally. Also electrons will have a finite probability of existing at two different localised states. When this occurs at the contact barrier it is known as Fowler-Nordheim injection.

1.3.4 Traps and volumetric conduction.

Polymer conductivity is very low. It is usually less than 10^{-13} $\Omega^{-1}m^{-1}$ [10]. Consequently charge will find it very difficult to travel in the polymer by normal conduction mechanisms. In amorphous solids the band structure is ill defined .

Polymer molecules are joined together by strong primary covalent bonds. As the polymer chain is made up, degenerate monomer molecular orbitals form a series of extended electronic states. Band theory is therefore applicable along chains. However the band gap is very large (in the order of 9eV) and it is very difficult to create mobile charge [17, 21].

Polymer chains are joined by secondary weak (van der Waals) attractions. Therefore there is no valance band between chains. This changes the classic band theory and limits the movement of charge.

Charge conduction is limited even further by the existence of what are called traps. Traps are region-localised states of low potential energy. They could be structural, physical or chemical. Imperfections can also act as traps. For charge carriers to leave traps, they must have enough energy to overcome a large potential barrier. Charges can reside in traps from seconds to antiquity. Charges can move from one trap to another in a nearby localised state by hopping and tunnelling. The probability of

hopping and tunnelling is highly dependant on the inter-site distance. The existence of traps alters the band gap model as shown in Fig (1.7).

Charge in the traps makes large increases in net space charge. This may have a significant effect on electrical ageing.

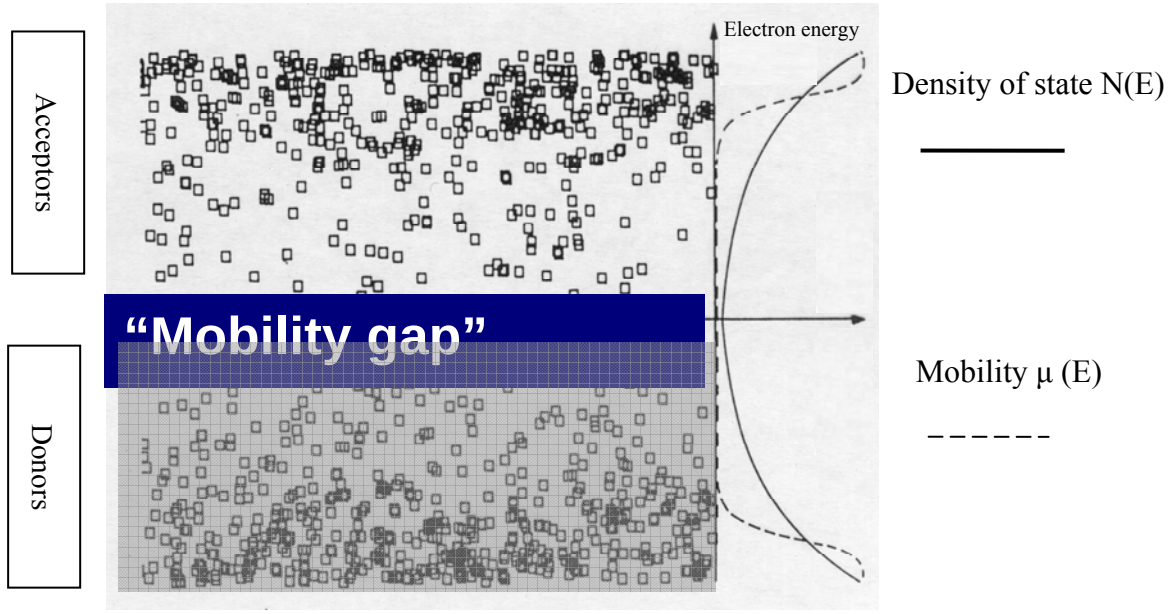

Figure 1. 7. From [10].

Fig 1.7 shows localised states in a non-crystalline material (indicated by squares) as a function of electron energy together with the density of states N (E), and the mobility μ (E). The band gap is not well defined. The effective mobility decreases sharply near the centre of the gap where the concentration of state is very low. Overlapping squares show the states between which charge transport is likely.

1.3.5 Tunnelling and hopping conduction.

Trapped charge can lead to the polarisation and distortion of the lattice structure. This will result in local energy band deformation making it very hard for trapped charge to be free. Consequently different transport mechanisms are involved in polymers. Charge carriers in polymers may move from one site to another by hopping over a potential barrier, tunnelling through it, or a combination of both [18, 19, 21].

Hopping is the transfer of a thermally activated charge carriers between localised sites. Carriers acquire enough energy from the lattice by means of thermal fluctuations to overcome the potential barrier.

Tunnelling is a quantum mechanical process. In accordance with the uncertainty principle, the position of an electron is not fully determinate. If the energy barrier is thin enough, then the spatially distributed uncertainty of location of the electron may actually pass through the energy barrier and have non-zero probability on the "other" side of the boundary. Electrons, in this manner, can "tunnel" out of traps that they do not have enough energy to simply overcome and hop into another trap.

1.4 Ageing

1.4.1 Introduction

Ageing is an instinctive concept. It affects everything around us. In this research the interest is in electrical ageing that occurs in electrical insulation.

Ageing is a gradual change of state and property that usually leads to a degree of malfunction. The ageing process is that chemical and physical bonds between atoms of the substance are repeatedly broken, reorganised and reform into new configurations [23, 23]. The two main bonds between a polymer's atoms are primary bond (usually covalent) and a weaker secondary (van der Waals). Ageing sets up the conditions for degradation and hence eventually breakdown.

Electrical ageing is a very complicated process. Therefore understanding the fundamental aspects of ageing mechanism is very complex. Nevertheless, there are underlying physico-chemical principles that apply to ageing. There are three main electrical ageing models: Dissado-Montanari-Mazzanti Model [DMM] [25,26, 27, 28], Lewis Model [23, 29, 30], and Crine Model [31, 32]. All three models are thermodynamic. DMM and Lewis are explicitly kinetic and Crine is implicitly kinetic, but only DMM is Space charge. The aim of electrical ageing models is to predict the working lifetime of polymer, to aid resource management and in improving material and systems. [25] The three models differ in their physical details and their mathematical developments but they approximately agree with their predictions. [33]. The three models consider that a region of the polymer can transfer between different local states by crossing an energy barrier.

DMM and Lewis models try to predict insulation lifetime by mathematically describing an ageing process in terms of applied electric field and temperature, and by specifying an end point at which the process is considered to have ended the life of polymer. Crine model does not define an end point. It is one of the major differences. Crine model just relates the lifetime to the inverse of the rate of ageing under the assumption that there is no balancing processes.

In these models ageing is assumed to be a lengthy process ended with rapid breakdown.

All of the three models have been successfully fitted to characteristic lifetime data from ageing experiment involving thin film specimens [33]

1.4.2 DMM Model

The development of the DMM model is not restricted to any specific physical process that causes ageing. It can be applied to any ageing mechanism as long as it is described by a chemical rate reaction [26, 27, 28]. A polymer is made of many moieties, or groups of atoms. Moieties that are thermally activated may change their free energy level to another. This process is reversible for each moiety.

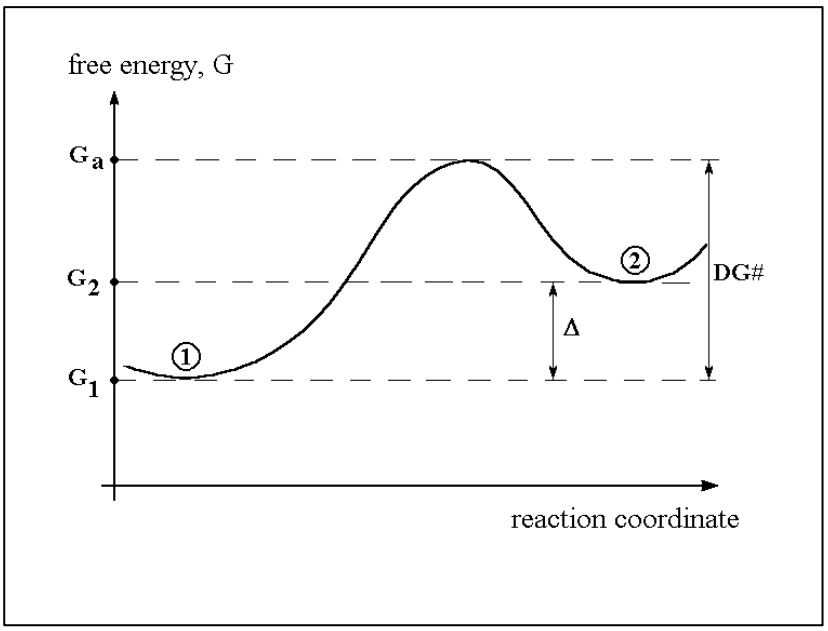

Figure 1.8. *DMM model. Ageing in the absence of electrical field.*

G_1 and G_2 are the free energies of the unaged and aged states respectively; G_a is the free energy for a short-lived state. The difference between the aged and unaged free energies Δ is denoted as K_d. G# is the difference between G_a and the mean of G_1 and G_2. G# is defined as the activation energy barrier and it is made of enthalpy part, H_{dk}, and an entropy part, S_d. G# is not the same for all moieties due to microstructural inhomogeneity [26]

DMM model assumes that the overall system begins in a non-equilibrium state and moves progressively towards an equilibrium state by means of local changes of the moiety state that are themselves reversible. An end point is defined in terms of critical concentration of converted moieties. When the overall state reaches this concentration the changes become irreversible and a rapid failure occurs. Below a given field, called the threshold field, the critical state cannot be reached and the material will not fail, i.e. the local reversibility is retained overall. It assumes that ageing occurs due to space charge trapped in defects in the polymer.

The DMM life expression is given in equation 1.

$$t_c = \frac{\frac{h}{2kT}\exp\left[\frac{-S_d}{k}\right]\exp\left[\frac{H_{dk} - \frac{C_d E^{4b}}{2}}{T}\right]\left[-\ln\left(\frac{Aeq - A^*}{Aeq}\right)\right]}{\cosh\left[\frac{K_d - C_d E^{4b}}{2T}\right]}$$

Equation 1.1 ***DMM*** *lifetime equation.*

t_c (in sec) is life time of polymer.

h is Planck's constant.

k is Boltzmann's constant .

T is temperature (in Kelvin).

S_d is entropy parameter (in Kelvin). It is likely to be material dependent.

H_{dk} is enthalpy parameter (in Kelvin). It is likely to be material dependent.

A^* is critical fraction of moieties that need to be in the aged state in any localised area for ageing process to cause breakdown of the polymer. This is likely to be dependent on material.

K_d is the difference in free energy between aged and unaged states in Kelvin. It is likely to be material dependent.

C_d links the applied electrical field, E, to the change in free energy of the unaged moiety state. It is material dependent.

The necessary steps that need to take place for change to occur are:

Electro-mechanical Strain: the change from state G_1 to state G_2 ,see fig 1.8, will generate elemental strain. This strain will result in a change of volume occupied by the moiety and create free volume. The number of moieties per unit volume might change due to this [28]. Morphological changes are expected as a result of ageing. Trapped space charge has electromechanical energy that can cause chain rearrangements. In this case the local field is enhanced. Microscopic defects such as impurities cluster of chemical additives, and cavities can form space charge traps. In this model a minimum threshold electric field is required to make this process irreversible. The repeat of this process will create low-density regions.

Low-Density regions: low-density regions will have voids and free volume. These can act as charge trapping centres.

Ageing at macroscopic scale: When the voids and free volume become big enough failure (thermal, mechanical, electrical) can occur.

1.4.3 Lewis Model.

The Lewis model is based on bonds breaking. The moiety chemical bonds to the polymer matrix are changing with time [30]. Bonds are weakened or broken for aged states. In this model the two states will have broken and unbroken bonds. So a broken chemical bond is the starting point for ageing see Figure 1.9. The application of electrical field assumed to accelerate the ageing process. This process is reversible in the absence of a critical electric field. Lewis model assumes that electromechanical stress causes bonds between molecules and lamella to break. This will cause other unbroken bonds to weaken and break. Above the critical electric field the ageing process becomes irreversible. For breakdown to occur a critical fraction of the bonds that take part in ageing must be broken.

Voids and free volume are created when moieties move from state one (unbroken bonds) to state two (broken bonds). The size of the voids will increase causing degradation and failure [30]. This comes from a change with time of

$$b(t) = [1 - \exp\{-(K_f - K_b)t\}]b_{eq} \qquad 1.2$$

so that when $t \to \infty$ $\qquad b \to b_{eq}$

Failure occurs when $b(t) = b^*$ $\qquad$ and $t = t_c$

Giving

$$b^* = [1 - \exp\{-(K_f - K_b)t_c\}]b_{eq} \qquad 1.3$$

$$\frac{b^*}{b_{eq}} = [1 - \exp\{-(K_f - K_b)t_c\}]$$

$$\exp\{-(K_f - K_b)t_c\} = 1 - \frac{b^*}{b_{eq}} = \frac{b_{eq} - b^*}{b_{eq}}$$

$$-(K_f - K_b)t_c = \ln[\frac{b_{eq} - b^*}{b_{eq}}]$$

$$t_c = \frac{1}{K_f - K_b} \times \left[-\ln\left(\frac{b_{eq} - b*}{b_{eq}} \right) \right]$$

Equation 1.4. *Lewis's Model Life Time Equation*

t_c is the life time of polymer.

K_f is the rate at which bonds are broken or weakened.

K_b is the rate at which bonds are repaired.

b^* is the critical fraction of bonds that needs to be broken for breakdown to start.

b_{eq} is the equilibrium fraction of broken bonds.

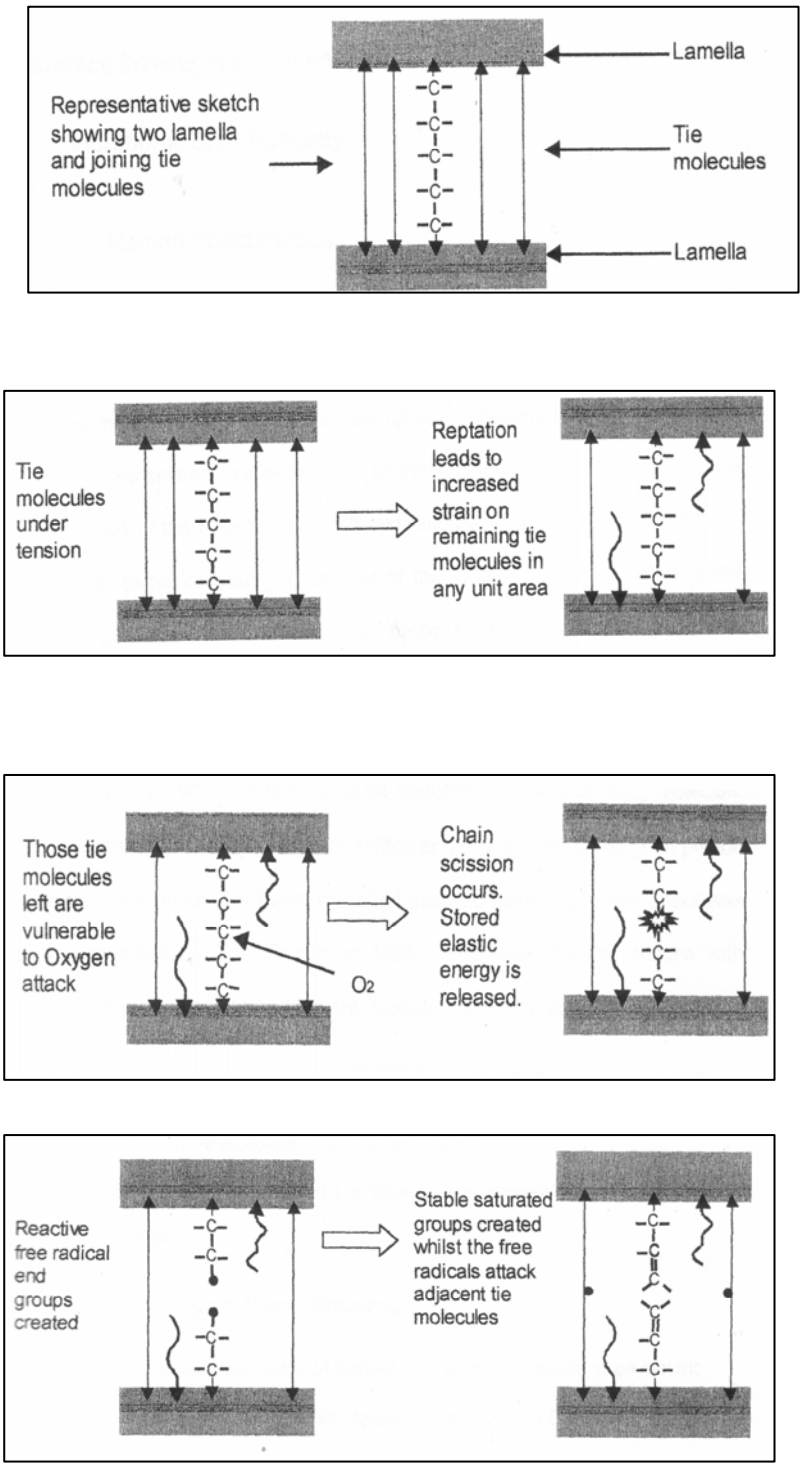

Figure 1.9. *After PWC SAYERS [34]. It shows the process of ageing in Lewis's model.*

1.4.4 Crine Model

The Crine model is based on moieties moving alternatively from state1 to state 2 overcoming an energy barrier. The life prediction is in terms of electrical field and temperature [31, 32]. In Crine model there is no threshold field as found in the DMM, and Lewis models, instead there is a critical field for the ageing process to begin. The value of critical electrical field depends on the energy of cohesion of the polymer. Nanocavities (with more ageing can become sub-microcavities), space charge, bond breaking are created as a result of ageing at low to moderate fields. Electrons can then move within the cavities and this may lead to further degradation. This eventually leads to breakdown and failure. The model assumes molecular chain deformation is essentially a fatigue process and therefore, at high frequencies it generates more defects and thus reduces polymer life.

Crine theory is based on thermodynamic concept in the Eyring rate theory. It also includes the concept of sub-microcavity formation proposed by Zhurkov[31]. The rate constant in the Eyring rate theory can only be calculated a priori for the reaction

$H + H - H \rightarrow H - H + H$

In any other situation $\Delta G = \Delta H - T\Delta S$ contains two adjustable parameters.

The rate theory states that the time t to cross an activation energy barrier of height ΔG is given by:

$$t \approx \frac{h}{kT}\exp[\Delta G / kT] \approx \frac{h}{kT}\exp[\frac{-\Delta S}{k}]\exp[\frac{\Delta H}{kT}]$$

Equation 1.5. *The Rate Theory Equation.*

where h is Planck's constant, ΔS is activation entropy and ΔH the activation enthalpy. The lifetime equation for Crine theory is

$$t \approx \frac{h}{2kT}\exp[\frac{\Delta G_0}{kT}]\operatorname{csch}[\frac{e\lambda E}{kT}]$$

Equation 1.6. *Crine's Model Life Time Equation*.

Where ΔG_0 is the activation energy at zero electric field, e is electron charge, λ is the submicrocavity size, E is electric field strength.

The mechanical deformation of intermolecular (van der Waals) bonds created by electrical stress is the first step to electrical ageing [32].

The three major parameters describing the ageing process are the activation energy of interchain bond breaking, $\Delta G_0 = \Delta H_0 - T\Delta S_0$, and the length of the submicrocavities $\lambda_{\max}$. These three parameters vary with applied electric fields (magnitude and frequency), polymer morphology, impurities and applied pressure.

The energy needed to break the interchain binding must be bigger than the energy of cohesion of polymer. This may occur at fields higher than a critical field.

At a field lower than the critical field very few or no submicrocavities form, resulting in a long lifetime [31, 32].

1.4.5 A brief comparison between the three models.

The three models give good results. The life to failure prediction from all three models is very similar.

The common features of these models are elemental electro mechanical strain, growth of low-density regions, ageing at macroscopic scale, chemical instability of insulation.

Treeing and discharging occur in low-density regions

The differences can be summarised in the following table.

Dissado and Motanari	Lewis	Crine
Failure due to nanocavities induced by the high field of space charge.	Failure by bond breaking.	Failure due to nanocavities at low to moderate fields and bond breaking at high fields introduced by Maxwell stress.
There is a threshold field for ageing to start becoming irreversible.	Threshold field is required.	No threshold field is required. There is a critical field instead.
Life equation	No explicit life equation.	Life equation.
Define an end point.	Define an end point.	Does not define an end point.

Table 1.1

1.5 Forms of electrical degradation

Electrical breakdown is usually preceded by ageing and degradation. So the breakdown sequence is

Ageing ⟶ Degradation ⟶ Breakdown

The most important forms of electrical degradation are:

Electrical trees: Electrical trees are narrow branched hollow channels in the insulation [10]. They are formed in regions of high electrical local field such as metallic asperities; conducting contaminants, and structural irregularities, electrical trees can also be formed by partial discharge in voids. Electrical trees lead directly to breakdown. The main two types are branch and bush trees. The growth rate of trees depends on the shape of the tree. The shape of tree depends on voltage, temperature, and mechanical stress.

Water trees: Water trees are diffused collections of voids in insulation material [35]. They grow in presence of water and AC field. They do not lead directly to breakdown but they often lead to electrical trees, and discharge channels.

Partial discharge is called partial because the discharge does not bridge the insulation between electrodes [10]. Partial discharges occur in voids within the insulating material. They occur because voids are filled with gas; since gas has a lower permittivity than the insulator field intensification occurs inside the voids. This could cause gas to become ionised and hence discharges occur across the voids. Factors that could affect partial discharge are gas content, gas pressure; void shape and size. Partial discharges do not necessarily result in breakdown; they could produce electrical trees and act as a degradation mechanism.

The electrical and mechanical degradation are interrelated in a very complicated way [36,37]. For an amorphous epoxy /glass composite the electrical breakdown strength increases with increasing compressive stress and decreases steadily with increasing tensile stress up to a yield point where it decreases rapidly. A small elongation of the epoxy results in a big drop in electrical breakdown strength.

The explanation for this behaviour could be due to the fact that compressive stresses increase the density of the material by eliminating voids and increasing molecular packing, while tensile stress can create voids and defects.

1.5.1 Electrical stress in gaseous cavities

Electrical discharge in gaseous cavities is one of the most important types of dielectric breakdown [38]. The electric stress is enhanced in such low permittivity areas as cavities, cracks, and delaminations within the dielectric. The study of electric field distribution in and around cavities is very important for the design of electrical equipment. The high stress value is an important parameter to control [39].

The field enhancement in cavities is highly dependent on the shape of the cavity and its axis of orientation with respect to the applied electric field. A cavity with its axis parallel to the direction of the applied electric field produces the highest stress enhancement. The cavity stress increases as the permittivity of the surrounding dielectric increases.

The electrical stress E in a gaseous inclusion in the solid insulation is

$$E = \frac{3\varepsilon E_0}{1+2\varepsilon} \qquad 1.7$$

in a spherical void in alternating voltage, and

$$E = \frac{3}{2}E_0 \qquad 1.8$$

in direct voltage.

$$E = \frac{\varepsilon(1+\frac{m}{n})}{\varepsilon+\frac{m}{n}}E_0 \qquad 1.9$$

in elliptic cylindrical cavity in alternating voltage

and, $E = 2E_0$ 1.10 in direct voltage.

E is the electric field in the cavity; E_0 is the electric field in the insulation. ε is the permittivity of the insulation. m and n are the semimajor and semiminor axis of the cross-section of an elliptical cylindrical cavity.

1.5.2 Electrical breakdown processes

Electrical breakdown in polymer insulators is always catastrophic in the sense that it is destructive and irreversible. [10]. The main mechanisms for electrical breakdown are: thermal, electromechanical, avalanche, mixed mode breakdown [10].

A common feature of all breakdown mechanism is positive feedback.

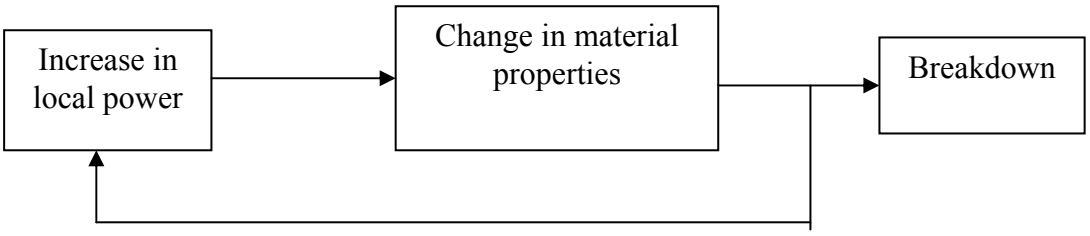

Thermal breakdown occurs due to thermal stress in the insulating material. Thermal stress is caused by an increase in temperature due to power dissipation in the insulation, this is caused by the flow of current however small it is ($P= I^2R$). This could:

- Increase conductivity as more carriers become available for conduction.
- Increase the segmental motion which could increase the mobility for intrinsic ion conduction

When the insulating material is exposed to this for a long time the current density will increase, which will increase the temperature further, and hence thermal runaway will occur.

Electromechanical breakdown occurs when the mechanical compressive stress on the dielectric caused by the electrostatic attraction of the electrodes (or, more accurately, by electrostriction) exceeds a critical value, which cannot be balanced by the dielectric's elasticity.

The breakdown of polymer due to mechanical and electrically produced mechanical stress has been studied extensively [40]. The initial stages of such failure are considered to involve the scission of main polymeric bonds, and generation of free

radicals, which induced bond-breaking chain reactions, and the consequent growth of a population of sub-microscopic voids, which ultimately leads to breakdown.

Mixed mode breakdown is where more than one mechanism operates. For example the thermal breakdown mechanism starts to soften the material but perhaps the voltage isn't big enough for the thermal runaway to occur. However, the softened material might reduce the Young's modulus sufficiently for the electro-mechanical mechanism to operate. Normally if the temperature was increased a little then only one mechanism would operate (in this case the electro-thermal mechanism)

CHAPTER 2

MATERIAL CHARACTERISATION

2.1 Problem Definition

In recent years the power feed line for optical telecommunications systems has moved over to the use of copper track transformer coils embedded in an epoxy laminate. This gives considerable saving in space and cost. They are currently operated at voltages of about 500Vac/300dc and temperatures of (70-90)ºC**.**

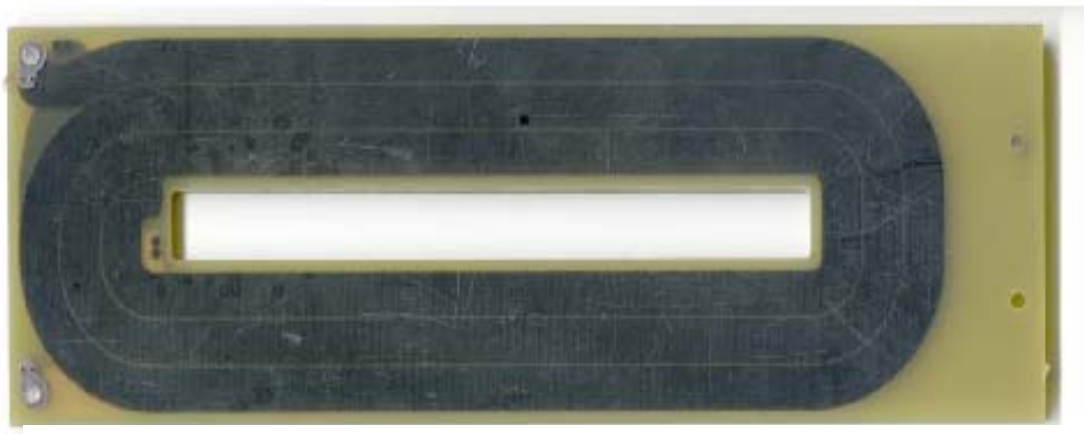

Figure 2- 1. *Power copper track transformer in a multilayer printed circuit board. This transformer consists of eight layers. It is used by Alcatel Submarine Networks as part of a circuitry for power inverters and converters.*

Alcatel Submarine Networks is intending to improve the power converters they are using at the present time by:

- Increasing the voltage of the system power feed by 75% in the next five years.
- Improving the multilayer printed circuit boards design (PCB) used in the power converters to include encapsulated transformer wirings.

As a result of this the PCB components will experience A.C and D.C fields much higher than they are used to now.

The main difficulty in achieving this is the lack of knowledge of how the insulating material (epoxy/glass fibres composite) is going to react to these higher fields, so the

potential problem is insulation failure. It is therefore necessary to define the electrical reliability of the insulating material and hence set a limit for their design and operation.

The main objective of this research is to gain a fundamental understanding of the electrical aging mechanism of the insulating material and its electrical performance as wire encapsulation. In order to achieve our objective the following aims were set:

- To measures the epoxy /glass composite material electrical properties before ageing.
- Measurements of epoxy core, pre-preg materials, and glass fibre mat properties
- To age composite material under high fields and temperatures.
- Progressively measure electrical properties of aged composite material.
- Liaison with Alcatel Submarine Networks for technology transfer.

2.2 Material description

The material investigated in this thesis is FR4 .It is a well-established material in the manufacturing of PCBs. It is a product of Nelco Ltd. The product line is N4000-2. This is a system of multifunctional epoxy-laminate and pre-preg. It is designed for use in high-density multilayer boards. The material is 50% epoxy and 50% glass w/w. The following table gives some of the engineering properties of this material

Property	Epoxy	Glass	Composite
Relative pemittivity	Approximately 2.9 At 1MHz	6.4 at 1GHZ 6.7 at 1MHz	4.1 at 1GHZ 4.4 at 1MHz
Young Modulus	3Gpa	80Gpa	24Gpa
Coefficient of thermal expansion	$70*10^{-6}$ /m/°C	$5*10^{-6}$ /m/°C	
Specific Volume	$0.83*10^{-3}$ m^3/kg	$0.39*10^{-3}$ m^3/kg	$0.52*10^{-3}$ m^3/kg

Table 2.1 *Engineering properties of this material [15].*

2.3 PCB Specimen and experimental program

Wrekin Ltd makes PCBs. A visit was made to Wrekin where they demonstrated how the PCB boards were made and what material they were made out of.

After some consideration of the experiments to be performed the following samples were designed and manufactured by Wrekin in the same way as the PCBs:

All samples were circular shape samples

- Specimen with no electrode, shown in Figure 2.2a.
- Specimens of radius 50 mm and of 400 μm thickness shown in Figure2.2b. These samples were designed with electrode arrangements to be used for the thin film PEA system.
- Specimens for conductivity/dielectric spectroscopy measurements of 80 mm radius and 400 μm thickness, to be used in conductivity cell, shown in Figure 2.2c.

A large number of different samples (200), have been made and some of them characterised (25) by:

- Dielectric response
- Dynamic mechanical response (DMA).
- Space charge measurements.
- Differential Scanning Calorimeters (DSC).
- Scanning Electronic Microscopy (SEM) analysis.

Dielectric response and DMA gives information about the internal motions of chains, dipoles, and charges. DSC and SEM give structural and morphological information about the material. PEA gives information about space charge formation and traps.

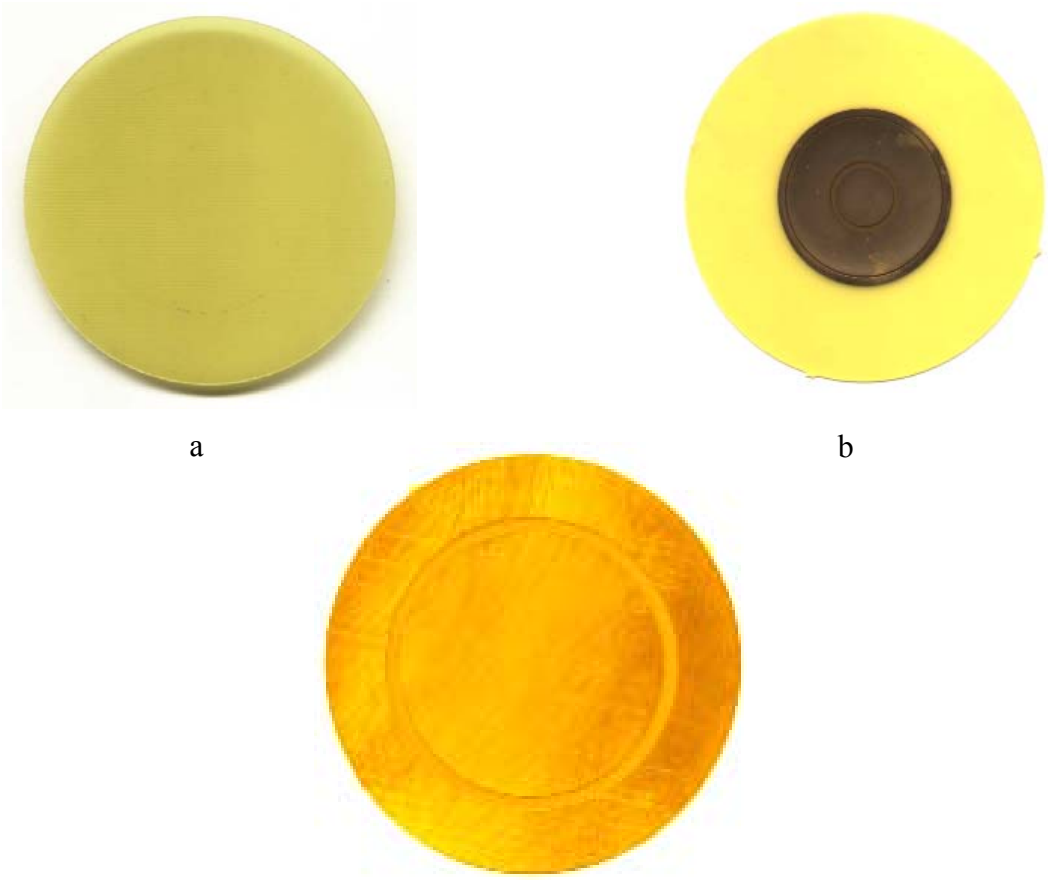

Figure 2- 2. *Samples used to perform measurements. a) Specimen with no electrode, b) specimen with two electrode rings, c) specimen with one electrode ring.*

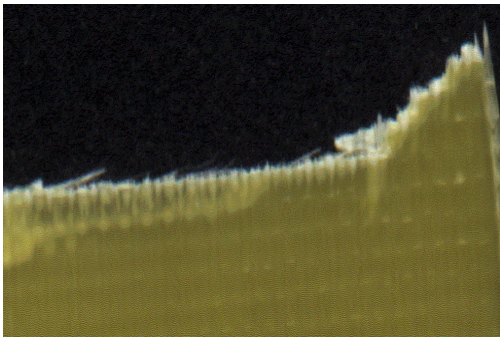

Figure 2- 3. *Cut sample to show fibres in the epoxy/glass composite. Shown actual size.*

2.4 Dielectric Spectroscopy

Dielectric spectroscopy has been widely used by experimentalists for many years [1]. For example Jonscher (1983) refers to work on ferroelectrics and the silicon p-n junction, (Deguchi et al 1982), (Mason et al 1974) to work on water. Dielectric experiments have been performed by (Dissado and Hill 1981) on many materials. Dissado and Hill have also developed a theory of the dielectric response [2 - 7].

Dielectric spectroscopy depends on the polarisation, which is induced in the material due to the effect of an external electrical stress.

Dielectric spectroscopy is used because it is a good tool to probe the internal structure of systems by means of observing macroscopic parameters, which are easily measurable. It is also non- invasive making it suitable for materials, which change characteristics when subjected to any form of stress.

Dielectric materials were initially investigated by J.C Maxwell. This work was continued by Debye at the beginning of the last century (Debye 1912). Debye's theory is based on dielectric losses, which is concerned with polarisation and relaxation of electric dipoles. His model is based on non-interacting dipoles floating freely in a viscous medium and assumes that the rate of polarisation relaxation is directly proportional to polarisation, i.e. $\frac{dP}{dt} \propto -P$. Experiments, which the model was based on, were performed on dilute solutions. Later investigations showed that this theory is not applicable to solid materials [1].

In solid dielectrics morphology as well as chemistry affects the dielectric properties of the material. Dielectric spectroscopy is used to investigate the conformation and dynamics of amorphous polymers; it has also been used to follow the polymerisation reaction.

This chapter presents the dielectric characteristics of the epoxy/glass composite material in the frequency domain. Measurements were made on the samples before being subjected to thermal and electric field; temperature was used as an experimental variable. The aim is to characterise the system before ageing.

2.4.1 Source of polarisation

In order to describe the dielectric properties of the material consider a thin parallel plate capacitor held in a vacuum. If the capacitor is charged the potential established across the capacitor would be

$$V_0 = \frac{Q_0}{C_0} \qquad 2.1$$

Q_0, C_0 are the charge and capacitance of the capacitor in vacuum.

If a dielectric is inserted between the plates of the capacitor and the charge Q_0 is maintained the voltage is reduced to V.

The ratio of the voltages defines the permittivity of the dielectric, ε,

$$\varepsilon = \frac{V_0}{V} = \frac{C}{C_0} \qquad 2.2$$

C is the capacitance of the capacitor with the dielectric inserted.

The voltage across the capacitor can be written as

$$V = \frac{Q_0}{\varepsilon C_0} = \frac{Q}{C_0}$$

Q_0 is known as the true charge, Q is known as the free charge since it is the portion of true charge which contributes to the voltage. The difference between the true and free charge is the bound charge ($Q_0 - Q$). The charge is bound by an adjacent charge of equal magnitude and opposite sign, which lies in the surface of the dielectric. Polarisation, P, is defined as the surface density of the bound charge.

Polarisation is the difference in charge density contributed by the material, see Figure 2.4.

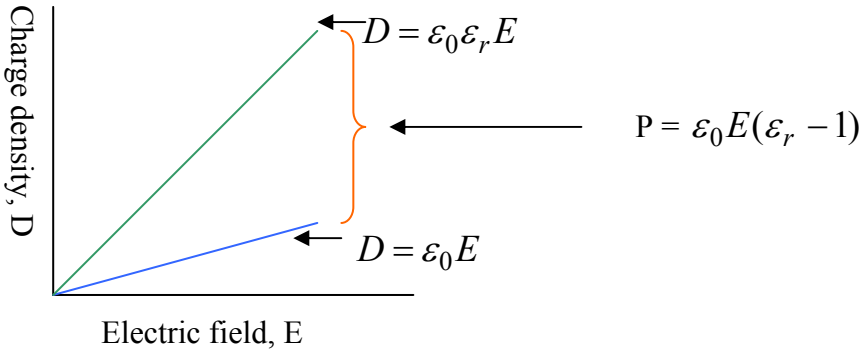

Figure 2.4. *Charge density, D, versus electric field E. Polarisation, P, is that part of the charge density contributed by the material.*

To understand the source of polarisation induced in the material by the electric field, polarisation unit can be thought of as the total dipole moment per unit volume.
Dipole moment, M , is the product of the charge Q, and the displacement, d, between the positive and negative charge [8 - 11].

$$M = Qd \qquad 2.3$$

C/ m^2 = C.m/m^3

There are four categories of polarisation, each having different mechanism depending on the type of dipole moment which is established.
Total polarisation is the sum of all polarisations.

Total polarisation = Integrated sum of all dipole moments per unit volume.

$$P = \sum(Me + Mi + Mo + Ms)/V \qquad 2.4$$

Me, Mi, Mo, Ms are dipole moments arises from electronic, ionic, orientational and space charge polarisation respectively, V is the volume.

$$P = Pe + Pi + P0 + Ps \qquad 2.5$$

Electronic polarisation P_e is electrons displacement inside the atom. Ideal situation is shown in Fig 2.5 a.

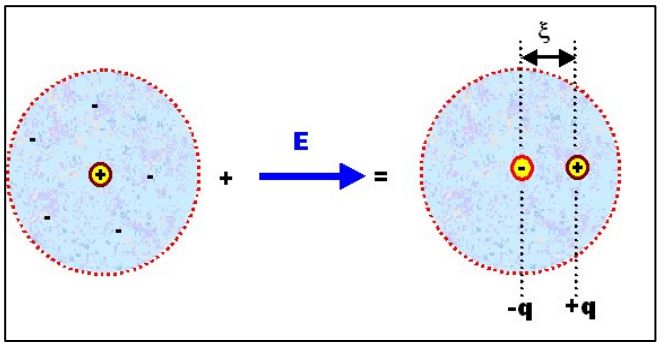

a) *Electronic polarisation*

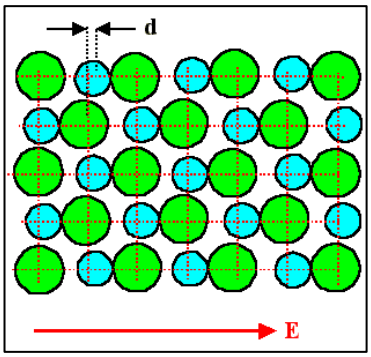

b) *Ionic polarisation*

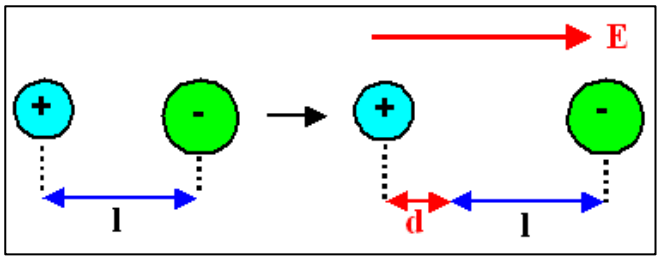

c) *The distance between the ions increases by d*

Figure 2.5. a) *Electronic polarisation, b and c ionic polarisation.*

In the absence of external electric field, on average the atoms have no net dipole moment and hence no polarisation. However, if subjected to an electric field the electrons (centre of negative charge), and the nuclei are shifted in opposite directions, creating polarisation, the length of the applied moment proportional to the applied field.

Ionic polarisation, P_i, originates from comparable displacement of ions and atoms. It is shown in Fig 2.5 b. In an electric field, the ions feel forces in opposite directions. For a field acting as shown, the lattice distorts a little bit (hugely exaggerated in the drawing). Figure 2.5c shows the situation where the distance between the ions increases by d. Electronic and Ionic polarisation are induced by electric field and both disappear when the external field is removed.

Orientational polarisation, P_o, originates from permanent dipoles that change orientation under an electric field to give a net dipole moment per unit volume. Space charge polarisation arises when charge accumulates, often at internal or external interfaces. Space charge polarisation arises only at high field. Experiments were carried out at low field so there is no space charge polarisation.

The current investigation is concerned only with ionic polarisation illustrated in Figure 2.5 and with orientational polarisation.

2.4.2 Theory of dielectric response

Dielectric relaxation is the polarisation of molecule or particle to form a dipole and/or alignment of an existing dipole by an electric field.

Dielectric relaxation is the recovery /decay of the polarisation after the applied electric field is removed [9].

Polarisation in the material is induced by the effect of an external electric field. Some materials such as ferroelectrics and electrets have permanent finite polarisation in the absence of external electric field, this form of polarisation does not exist in the epoxy /glass fibre composite investigated.

In general the relationship between polarisation $P(\omega)$ and electric field $E(\omega)$ as a function of frequency is [1]:

$$P(\omega) = P(0) + \varepsilon_0 \chi(\omega) E(\omega) + \text{ Higher terms in E} \qquad 2.6$$

$P(0)$ is the permanent polarisation, which is zero in our material.

ε_0 is the permittivity of free space, $\chi(\omega)$ is the susceptibility.

$$\chi(\omega) = \chi'(\omega) - i\chi''(\omega) \qquad 2.7$$

$$\chi' = \varepsilon_r' - 1 \qquad 2.8$$

Where ε_r' is the real part of the complex relative permittivity.

$$\chi'' = \varepsilon_r'' \qquad 2.9$$

$E(\omega)$ is the electric field.

The higher terms in E give rise to hyper- polarisation and exist only at higher fields such as that found in lasers.

High fields in epoxies may give rise to space charge build up. From the macroscopic view point this would give rise to non-linear dielectric effect. This may lead to quasi-permanent polarisation but this is counteracted by space charge [12].

The Complex form of susceptibility (and polarisation) is due to the fact that relaxing dipoles are out of phase with the applied AC field. At high frequency the molecular force impeding the dipole orientation dominate. Consequently the dipoles become unable to follow the field. This will lead to low polarisation and a very small contribution to the dielectric constant. At low frequency the polarisation can easily follow the field. This will give rise to a larger dielectric constant. The kinetic energy is dissipated and hence lost as polarisation lags behind the field [9, 10, 11].

Considering this, polarisation can be written as:

$$P(\omega) = \varepsilon_0 \chi(\omega) E(\omega) \qquad 2.10$$

The value of either $\chi'(\omega)$, $\chi''(\omega)$ may be expressed in term of the other throughout the entire frequency range $(-\infty, \infty)$ via Kramers-Kronig relations:

$$\chi'(\omega) = \frac{1}{\pi} \int_{-\infty}^{\infty} \frac{\chi''(\omega)}{\omega - x} dx \qquad 2.11$$

$$\chi''\omega) = \frac{1}{\pi} \int_{-\infty}^{\infty} \frac{\chi'(\omega)}{x - \omega} dx \qquad 2.12$$

The above two equations are very important in the study of dielectric behaviour and they are the Kramers-Kronig relations.

2.4.3 Dissado- Hill Theory

Dissado and Hill have developed a theory of dielectric relaxation based on a cooperative approach [3]. The dielectric material is considered as a localised structure. The dipoles relaxing effect is transmitted between the molecules. This is will cause fluctuations which spread out through the material. The cluster is a localised area near the dipole, which receives the dipole energy, as it is relaxing. This

allows for clusters diploes interactions when calculating the overall dielectric response of the material. The parameters in Dissado and Hill function are related directly to the processes occurring within the system.

Dissado and Hill have shown that the susceptibility can be expressed in the form:

$$\chi(\omega) = \chi(0)F(\frac{\omega}{\omega_x}) \qquad 2.13$$

$\chi(0)$ is magnitude of susceptibility dispersion ,i.e. the dielectric increment for a single process relaxation, $F(\omega/\omega_x)$ is the spectral shape function for this process with the frequency normalised to characteristic frequency ω_x .

For bound dipolar charge centres. Dissado and Hill have shown that the spectral shape function takes the form:

$$F(\omega/\omega_x) = F_0^{-1}(1+i\omega/\omega_x)^{n-1} \quad {}_2F_1(1-n;2-n;\frac{1}{1+i\omega/\omega_x}) \quad 2.14$$

where F_0 is a normalising parameter, ${}_2F_1$ is the hypergeometric function [15], and n lies between zero and one. In this equation n defines the degree to which the displacements of a dipole or charge couple to those of its environment to form a cluster. In one cluster relaxation occurs as a results of small rearrangements and the parameter n applies in this case. In systems where charges are not strongly bound, and charges are semi-free to move, the spectral shape function take the form

$$F(\omega/\omega_x) = F_0^{'-1}(1+i\omega/\omega_x)^{n-1}\ {}_2F_1(1-n,1+p;2-n;\frac{1}{1+i\omega/\omega_x}) \quad 2.15$$

where p is a measure of the ability of quasi free charges to transport between clusters, and $F_0^{'-1}$ is the equivalent normalising parameter.

2.4.4 Quasi- d.c behaviour (q-d.c)

Characterisation of dielectric response is possible by the dependence of the complex susceptibility, equation 2.7, on the frequency, ω, temperature, humidity, pressure etc. A loss peak is often observed in the frequency dependence of the imaginary part of the susceptibility, in company with a dielectric increment in the real part [4, 5, 6, 7]. The shape of the peak is generally given by.

$$\chi'(\omega) \propto \chi''(\omega) \propto \omega^{-(1-n)} \; ; \qquad \text{for } \omega > \omega_p \qquad 2.16a$$

$$\chi''(\omega) \propto \chi(0) - a\chi'(\omega) \propto \omega^{+m} \; ; \qquad \text{for } \omega < \omega_p \qquad 2.16b$$

where a is a constant, and $\chi(0)$ is the susceptibility at zero frequency. The constants n and m are between zero and one. ω_p is the reciprocal of the relaxation time and it is the peak frequency.

It can be shown that

$$\chi''(\omega)/\chi'(\omega) = \cot(n\pi/2) \text{ for } \omega > \omega_p \qquad 2.17$$

Jonscher found another form of response in which equation 2.16a is valid for both frequency ranges mentioned in equations 2.16a and 2.16b. No loss peak was observed in any of the frequency ranges. The response goes into a steeply rising branch towards the low frequency end. The susceptibility has been shown to be normalised with respect to its dependent variables in the same way as loss peak[1]. Jonscher called this behaviour anomalous low frequency dispersion (LFD). Dissado and Hill refer to it as quasi d.c conductance(q-dc).

q-dc can be explained by the dynamical possibilities inherent in the material structure and possessing limiting partial diffusion behaviour[4]. Dissado and Hill developed a model for this process. The model is based on the concept of clusters of quasimobile charges possessing partial structural regularity, which leads to a power law response [2, 4,5].

q-d.c is a charge transport process that exhibits a region of constant phase angle behaviour (CPA)[7]. Replacing 1-n by p in equation 2.16a yield to:

$$\chi'(\omega) \propto \chi''(\omega) \propto \omega^{-p} \qquad 2.18$$

$$0.5 < p < 1$$

This kind of behaviour can be explained by assuming self-similarity in the system or in its relaxation process. If p becomes equal to 1 then the process will be a d.c conductance.

Equation 2.18 can be written in terms of capacitance as

$$C'(\omega) \propto C''(\omega) \propto \omega^{-p} \qquad 2.19$$

where C' and C'' are the real and imaginary parts of capacitance.

To summarise:

- The familiar loss peak behaviour, which has a loss peak in the imaginary component of susceptibility together with dielectric increment in the real component. This form of response originates from dipoles relaxation that is out of phase with the applied electric field.
- No loss peak observed down to the lowest measurable frequency. The imaginary component of the susceptibility rises as f^{-1} at low frequency while the real component stay independent of frequency. This form of response gives rise to a dc conductivity and it originates from the presence of charge carriers in the material.
- No loss peak observed down to the lowest measurable frequency. The real and imaginary component of susceptibility rises steeply at low frequency at the same rate. This form of response originates from the presence of partially mobile charge carriers in the material.

2.5 Measurement System.

The frequency response analyser **FRA** used is a Solarton instrument 1255 H.F FRA. [12,13,14]. The measurements are based on measuring the current (amplitude and phase) in the material to an ac electric field and the voltage, V, in a capacitive element under the action of AC voltage signal.

The applied voltage is periodic function in the form of $\sin(\omega t)$, where ω is the frequency in radians. The applied voltage is produced by a digital generator with amplitude from 0 to 3V rms and applied to the sample by the means of two plain electrodes. The resulting current is measured by operational amplifier. The frequency range available is 10μHz to 20MHz. The amplifier is linked to the correlator of the FRA where the signal is integrated. The measurements give the complex impedance in term of frequency $Z^* = \frac{V^*}{I^*} = R + jX$ in the output file; this is transformed into complex capacitance $C^* = C' - jC''$, where V^*, I^* are voltage and current in complex form, R and X are the real and imaginary part of the impedance, C', C'' are real and imaginary parts of the capacitance.

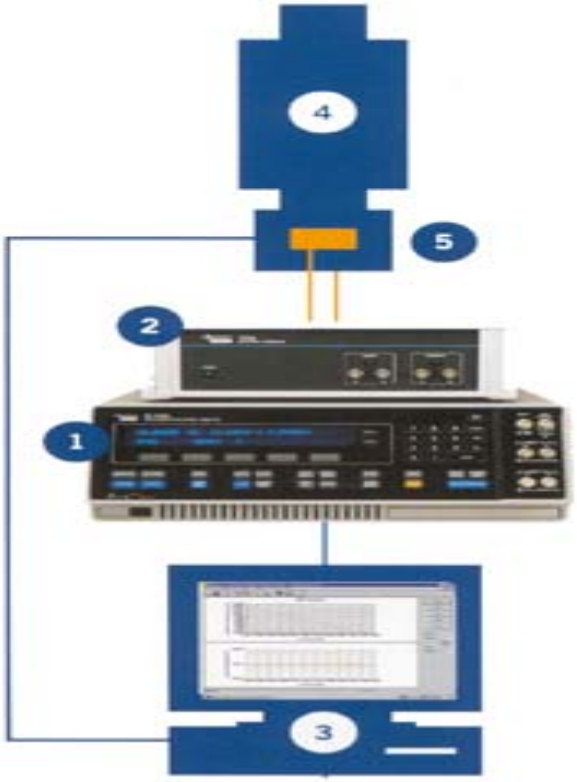

Figure 2.6. *Solarton instrument 1255 H.F* ***FRA*** **.**

1. Frequency Response Analyser (FRA) provides ac stimulus signal, and analyses the interface's response.
2. Dielectric/Impedance interface increases the sensitivity of the FRA.
3. PC provides system set up and control via easy to use software.
4. Sample holder for test material.
5. Temperature controller.

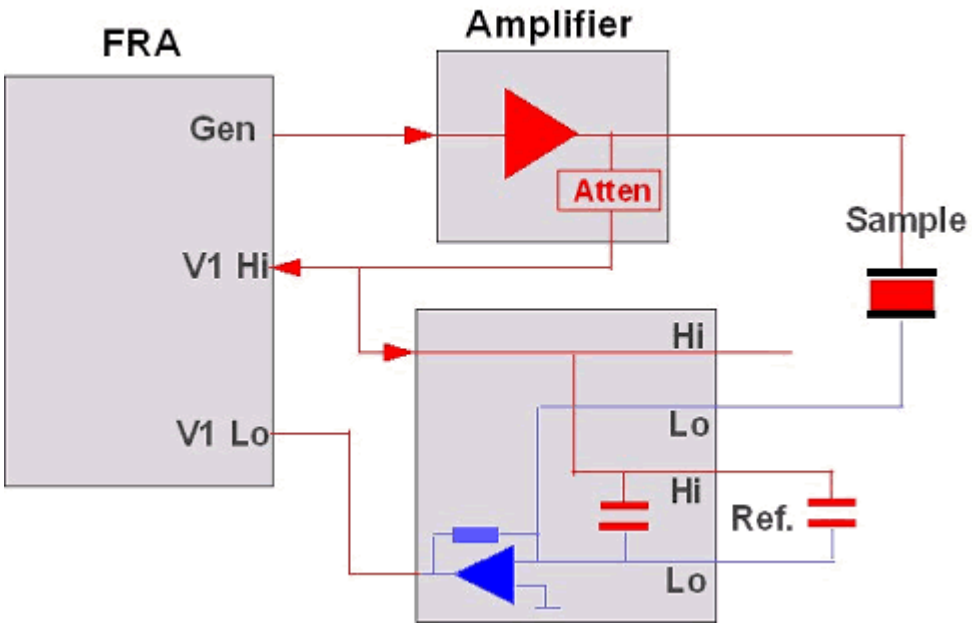

Figure 2.7. *FRA system configuration. In the experiments performed the applied voltage is (0-3) V and the amplification of the amplifier connected to the generator is 1.*

2.6 Dielectric Experimental results.

Dielectric spectroscopy measurements were performed on disc samples of composite material (glass/epoxy) of 54 mm diameter ranging in thickness from 200 to 400 μm. Capacitive and loss components were measured over a frequency range from 1 mHz to 100 kHz and from T= 20 C to 100 °C.

The aim of the experiment was to characterise the composite material prior to ageing. The measurement results of the experiment were obtained via a computer connected to the dielectric spectrometer, see Figure 2.6. The results give the real and imaginary part of the capacitance as a function of frequency.

The results for the composite, shown in Fig 2.8 as a Bode plot, show how the capacitance at low frequencies increases due to the increase of polarisation, which leads to an increase in the dielectric constant.

Fig 2.9 shows a master plot (Bode plot). This plot was obtained by a normalising technique. A temperature is chosen, and the response of each of the other temperatures is displaced in frequency and/or amplitude to bring them into coincidence with the response at the chosen temperature. The existence of a common master curve shows that the response observed exhibits a common frequency dependence over the temperature range investigated. The shift in frequency required to bring the curves into coincidence gives the relative change of the characteristic frequency for the process. A shift in amplitude would give the relative change of the magnitude of the process. In the present case only a shift in frequency is observed that can be interpreted as arising from the temperature dependence of the characteristic frequency of the process. In general the experimental data of the dielectric response can be satisfactorily normalised into reasonably single valued master curves. This proves that the spectral shape of the loss characteristic remains invariant with temperature. Normalisation technique is a very useful analytical tool of dielectric behaviour.

A low frequency process was found that possessed a constant phase angle (CPA) behaviour (i.e. $C' \propto C'' \propto \omega^{-p}$ with p between zero and one). The value of p determines the nature of process taking place in the material. [6]. For a dc conductance the value of p =-1, from the plot p=-0.8 which is a quasi-dc conductance.

A broad loss peak was found at high frequencies that were assigned to the β-process of the glassy epoxy. The β is a secondary loss relaxation process (α being the primary) results from motion within the polymer in the glass like state. In this state the main chains are effectively frozen in so that this process cannot be due to large-scale rearrangement of the main polymer chain. Since the molecules of most amorphous polymer contain side groups capable of undergoing hindered rotations independently of the chain backbone, the β relaxation is ascribed to such rotations. It applies to the relaxation region of low temperature and high frequency.

Figure 2.10 shows a master plot for this process.

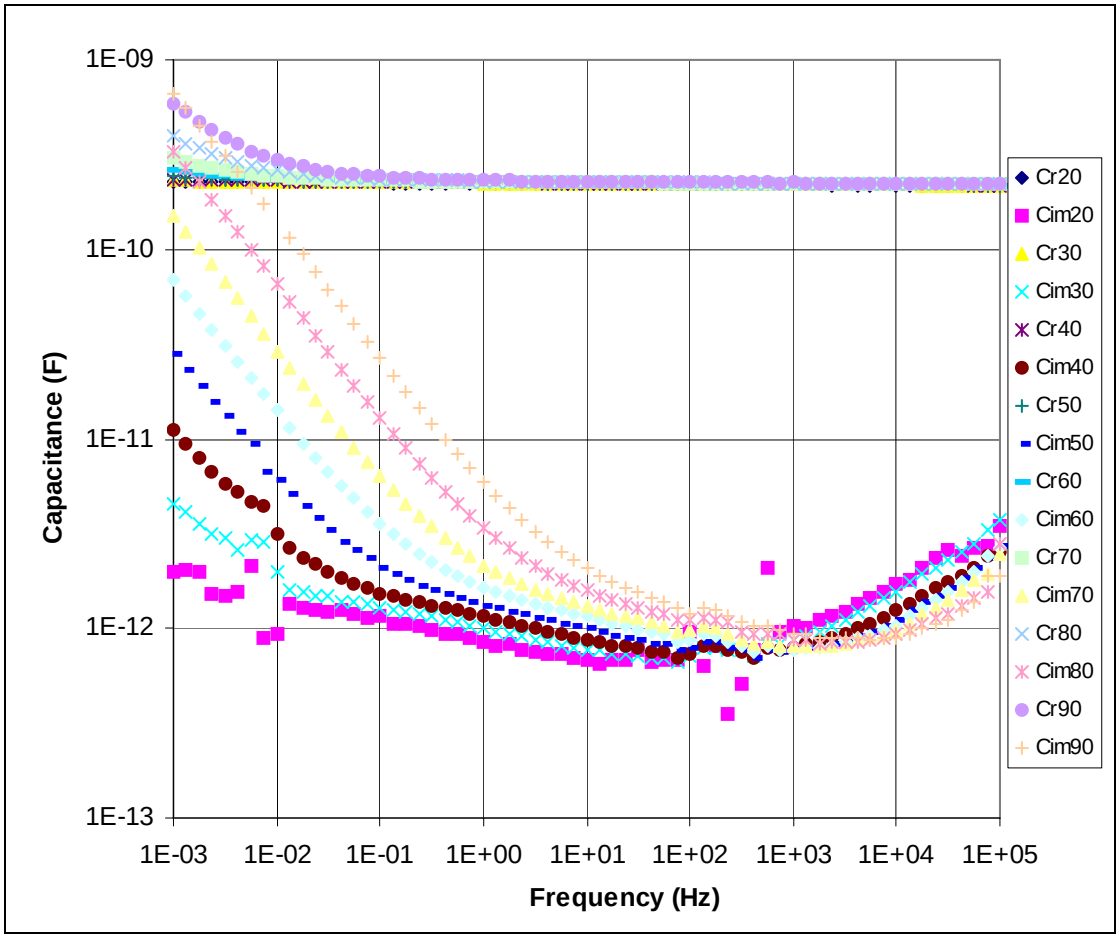

Figure 2.8: *Shows the real and imaginary part of the capacitance against frequency for the composite material for 8 temperatures 20-90˚C.*

The results show a constant real capacitance except at very low frequency, the capacitance starts to increase as frequency goes down. At low frequency the imaginary part of the capacitance increases as frequency goes down. These results were found to be typical.

.

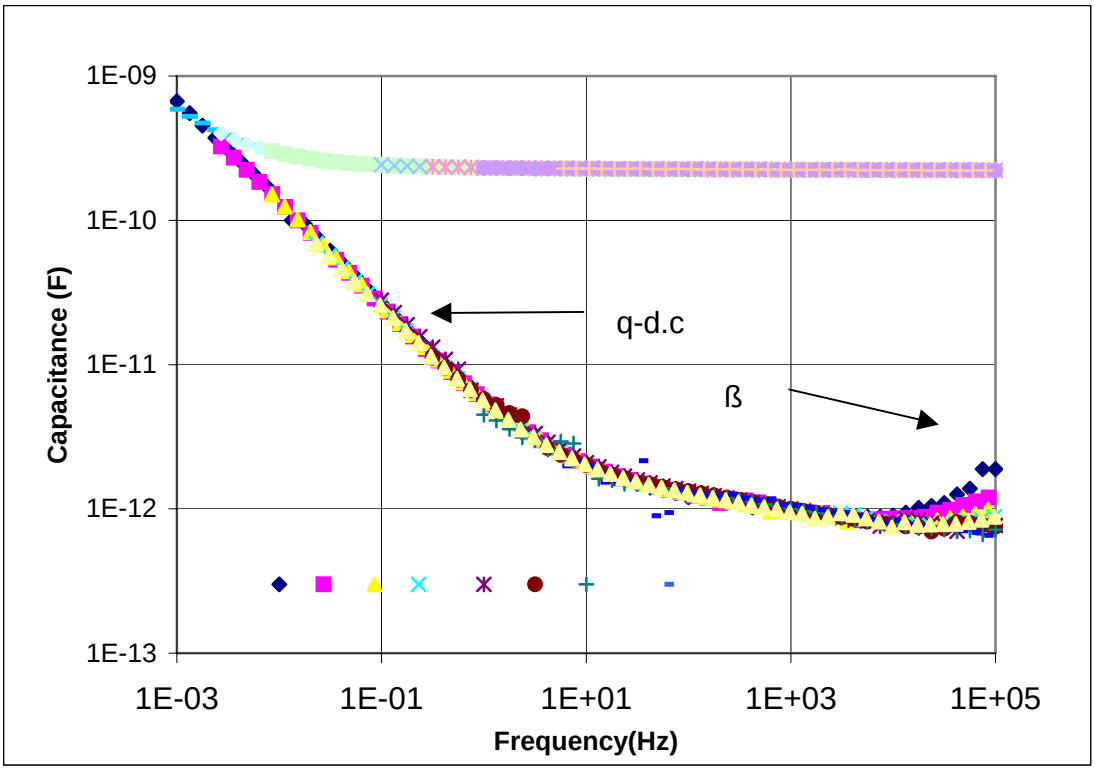

Figure 2.9 *Master plot of the dielectric response of composite for the low frequency process q-dc. For real (upper) and imaginary (lower) parts of capacitance, for 8 temperatures from 20-90˚ C. The amount of shift that was applied for each temperature to get the normalised plot is shown by the datum points below the curve. The frequency scale is exact for the data of the 90˚ C. the activation energy is 1.1±0.02eV*

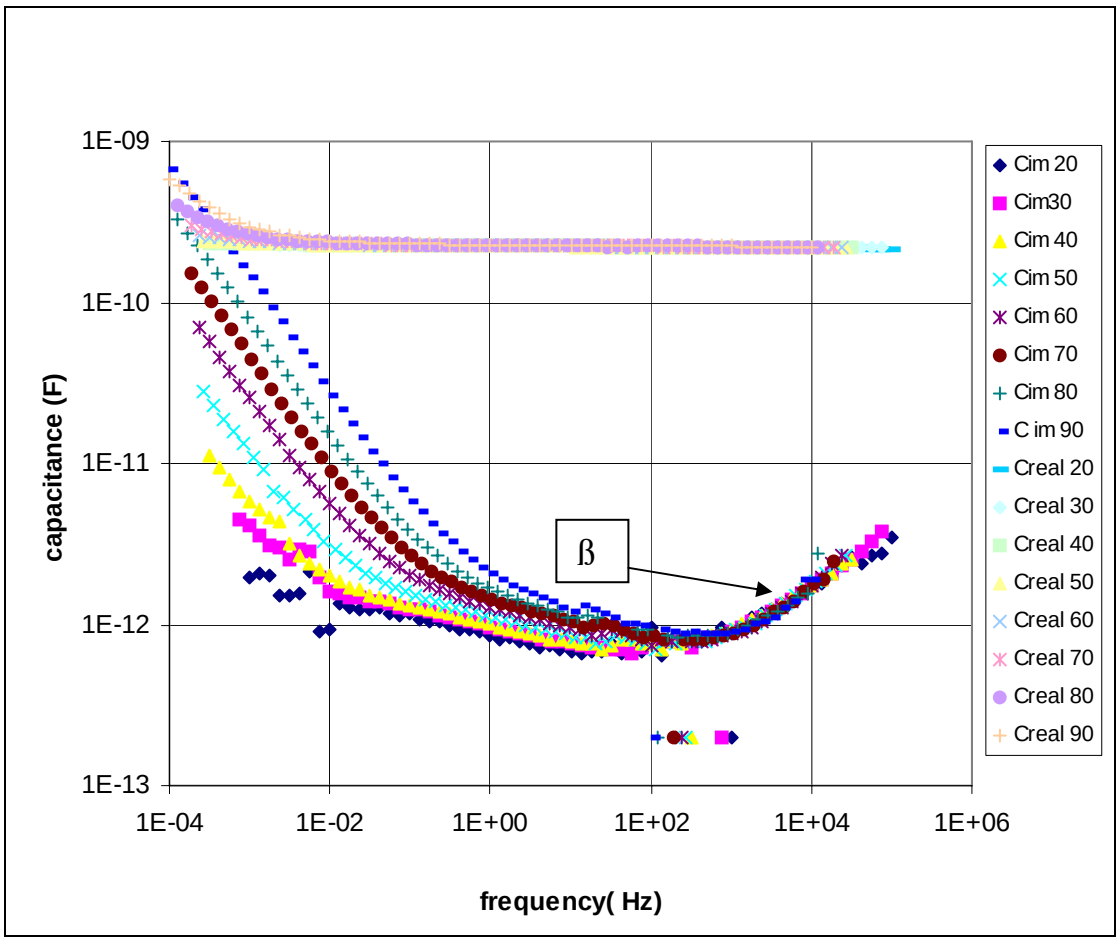

Figure 2.10. *Master plot of the dielectric response of the composite for the high frequency process being a β response. For real (upper) and imaginary (lower) parts of capacitance, for 8 temperatures from 20-90˚ C. The amount of shift that was applied for each temperature to get the normalised plot is shown by the datum points below the curve.*

The frequency scale is exact for the data of the 20˚ C.

A broad loss peak was found at high frequencies that was assigned to the β-process of the glassy epoxy. The activation energy of 0.3±0.03 eV found for the characteristic frequency is typical of such processes. Both the q-dc response and the β response have amplitudes that are not dependent upon temperature.

2.6.1 Arrhenius behaviour

The spectral shape function of the normalised relative characteristic frequency is strongly temperature dependant. It shows the characteristic activated or Arrhenius behaviour represented by the following equation [1]:

$$f = f_0 \exp(-W / kT) \qquad 2.20$$

Where f is the frequency that represents the probability of escape.

f_0 is frequency that represents the rate of attempts to escape, most of which are not successful.

W is the activation energy.

T is temperature in Kelvin .

k is Boltzmann's constant

The activation energy of the q-dc and the β processes found in the composite material can be calculated from the Arrhenius plot for each process.

Figure (2.11) shows the Arrhenius plot of the q-dc process, the plot is obtained from the master plot shown on Fig (2.9) by plotting the log of the reciprocal of shift against 1000/T, where T is the temperature in Kelvin. The shift is in the frequency axis and it relates to the characteristic frequency of the process studied. A Characteristic activation energy of 1.1±0.02 eV was found. The activation energy for the characteristic frequency gives an idea as to how the dipoles relax and how temperature affects their relaxation rate. In this case the process observed relates to the charge transport between clusters and the activation energy defines the barrier that has to be crossed for the charge to make the transport. Temperature dependent amplitude changes would show how the number of dipoles involved in the relaxation process changes with temperature. Here they are absent and hence the concentration of charge transfer process is independent of temperature.

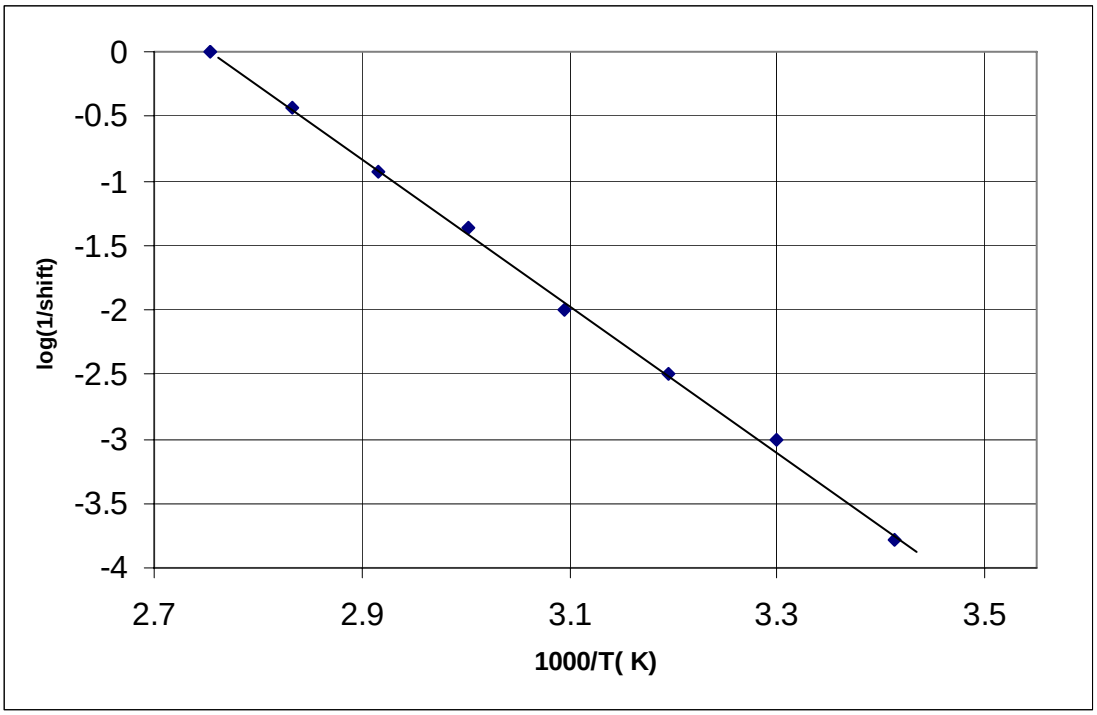

Figure 2.11. *Arrhenius plot of dielectric q-dc response for the composite material. The activation energy is 1.1±0.02 eV*

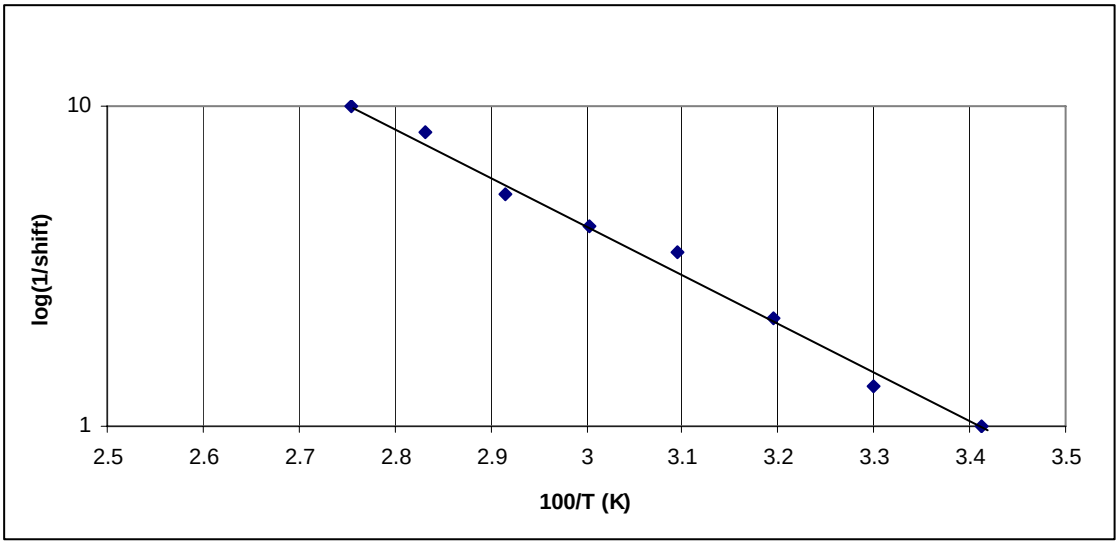

Figure. 2.12. *Arrhenius plot of dielectric β response*.

The activation energy of 0.3±0.03 eV found for the characteristic frequency of the β-relaxation is typical of such processes in glassy polymers.

The activation energy gives us a measure of how much the re-orientation rate of the contributing dipoles is dependent on temperature. The small value of activation energy indicates that the barrier to dipole re-orientation is small.

2.6.2 Dielectric Experiment On a Single and a Double Glass Fibre Mats

Dielectric measurements were carried out on single and double glass fibre mats of 200 and 400 μm thickness respectively over the frequency range [1mHZ to 100kHZ] and at selected temperatures in the range 20˚C and 50˚C.

These experiments were performed to try to understand the effect of the fibres on the dielectric response of the composite (glass fibre/epoxy), and by this means obtain a characterisation of the samples prior to electrical ageing.

The results obtained are plotted on a log-log scale, with the real and imaginary parts of the capacitance plotted as a function of frequency on the same graph, and are shown in Figure 2.13.

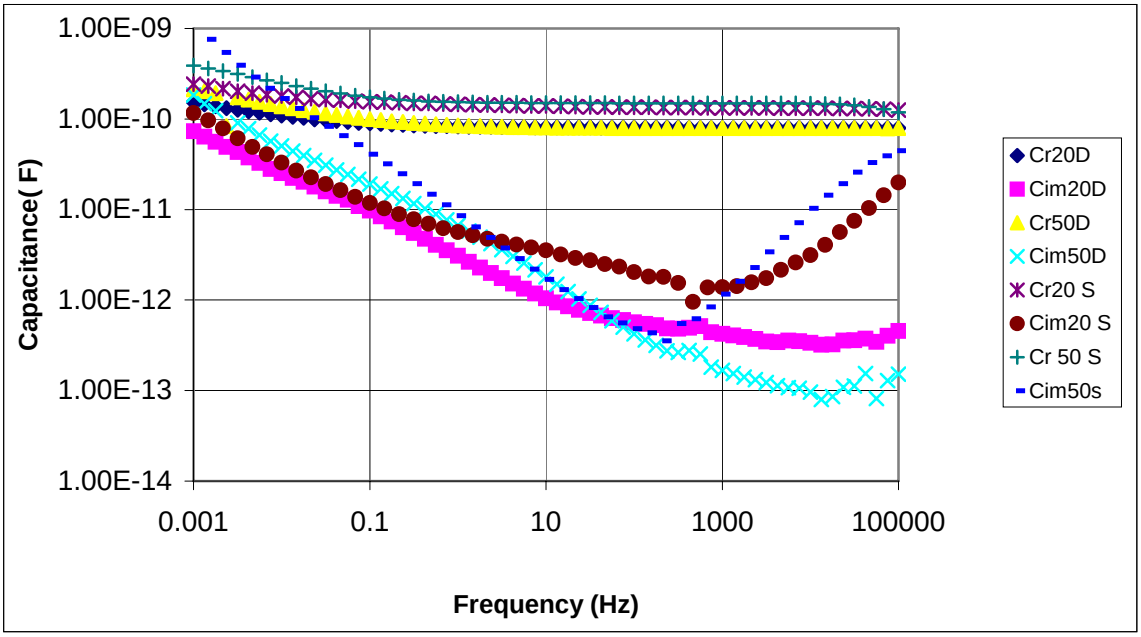

Figure. 2.13. *Shows the real and imaginary part of the capacitance against frequency for single and double glass fibre mats at temperatures 20 and 50˚C.*

Comparing the single and double glass fibre mats the only difference is the thickness, so in theory the real and imaginary parts of the capacitance ($C^{/}$, and $C^{//}$) of the single mat should be double that of the double mat. The real and imaginary parts of the double glass fibre mat were therefore multiplied by two and plotted together with the response of the single mat as shown in Figure 2.14.

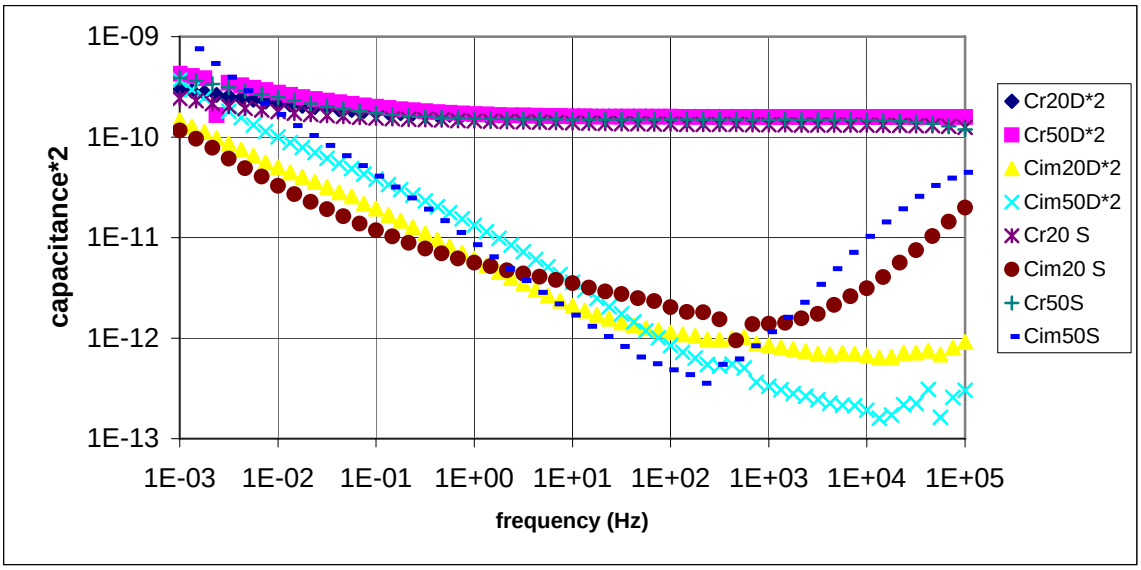

Figure. 2.14. *Shows the real and imaginary part of the capacitance against frequency for single and double glass fibre mats* ***multiplied by 2*** *at temperatures 20 and 50˚C.*

From the plot we can see that:

In the frequency range 1Hz to 100kHz the real part of the capacitance is almost the same for the single mat and 2x the doubled mat, and shows no real temperature dependence.

At frequencies below 1Hz there is a frequency dependent transport process ($C^{//}$ proportional to f^{p} and $C^{/}$ increasing with decreasing frequency) such as that observed in the composite.

2.6.3 Dielectric Experiment On Glass Fibre Mat.

Dielectric measurements were carried out on a glass fibre mat of 200 μm thickness and 54mm in diameter over a frequency range from 1 mHz to 100 kHz and from T= 20 C to 100 °C.

These experiments were performed to try to understand the effect of the fibres on the dielectric response of the composite (glass fibre/epoxy), and by this means obtain a characterisation of the samples prior to electrical ageing.

The results obtained are plotted on a log-log scale, with the real and imaginary parts of the capacitance plotted as a function of frequency on the same graph, and are shown in Figure 2.15.

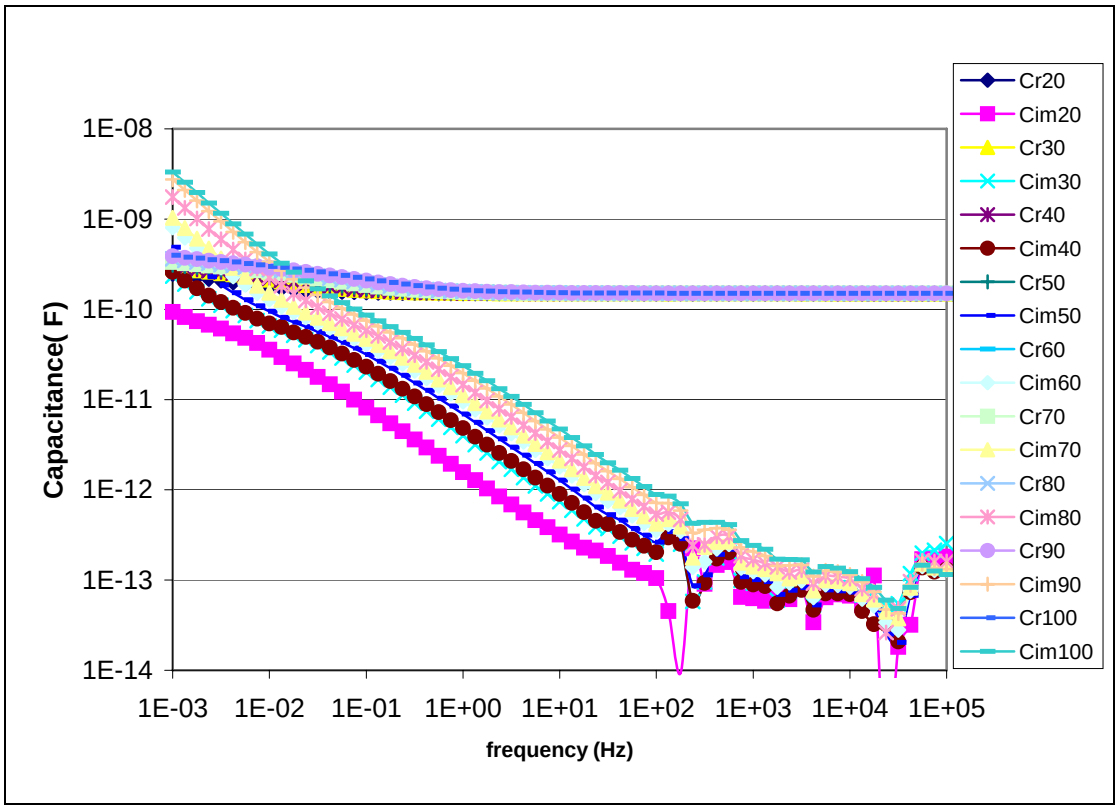

Figure 2.15. *Shows the real and imaginary part of the capacitance against frequency for the glass fibre mat for 9 temperatures 20-100˚C.*

A master curve was obtained as shown in fig (2.16), from which the Arrhenius behaviour was plotted fig (2.17).

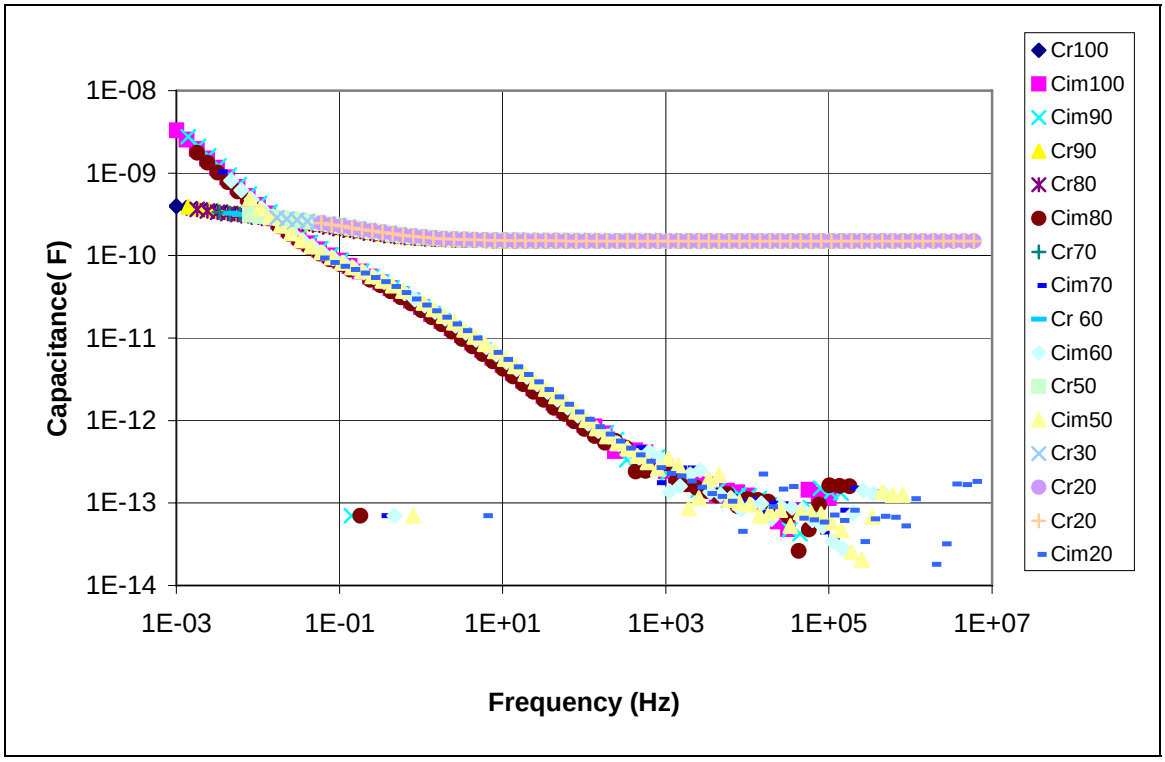

Figure 2.16. *Master plot of the dielectric response of glass fibre mat. For real (upper) and imaginary (lower) parts of capacitance, for 9 temperatures from 20-100˚ C at the low frequency region. The amount of shift applied for each temperature to get the normalised plot is shown.*

.

The results in fig 2.16 show

At low frequencies (below $1.3*10^{-2}$Hz) the slope of the line is -1±0.01, this shows a dc conductance.

At higher frequencies the slope of the line is 0.67±0.03, which is interpreted as a quasi-dc conductance. The inflection point shows the existence of a barrier layer, possibly the epoxy glass interface. This is caused by a build up of charge, which is transported by the quasi-dc charge transport process before the conversion to a dc conductance at the low frequencies.

The dc conductance and the quasi-dc conductance have the same temperature dependence, it may be that both processes have the same origin.

The activation energy was calculated 0.46±0.02eV; this is very much less than that corresponding to the quasi-dc process in the composite. If the process was transport inside the fibres the activation energy should be the same, this supports an argument

that the transport process is on the surface of the fibres. The charge transport will be more difficult in the composite where the fibres are coated with the epoxy, hence the higher activation energy. A dc conductance is not found in the composite because the fibres are insulated from the electrodes by the epoxy resin.

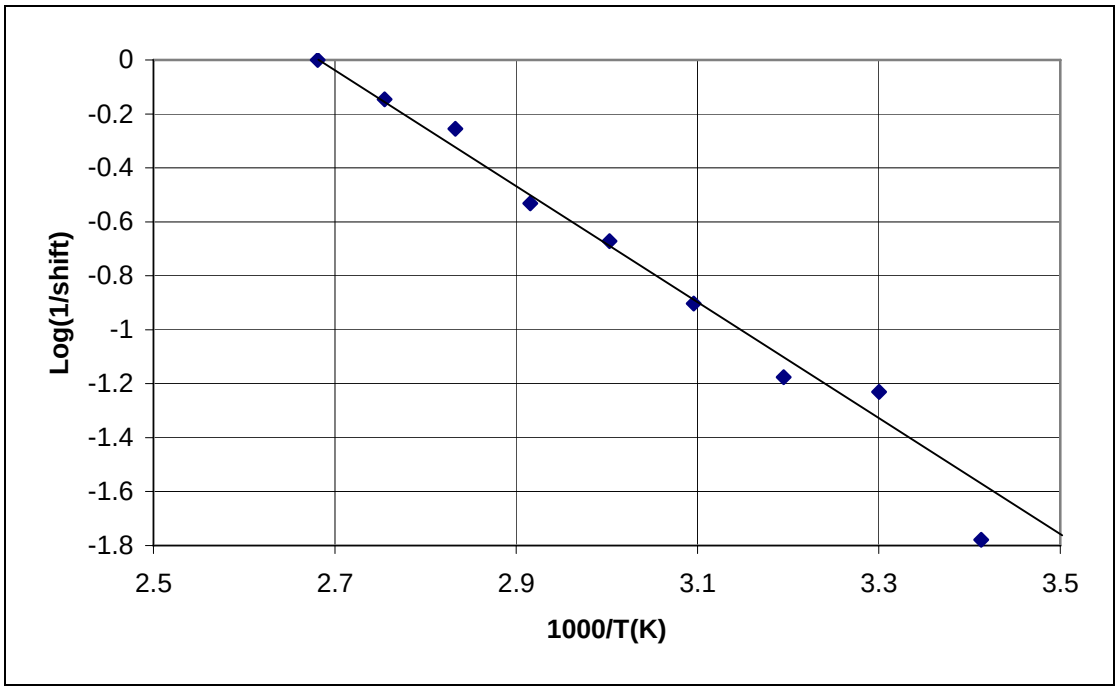

Figure 2.17. *Arrhenius plot of dielectric q-dc response for the glass fibre mat. The activation energy was calculated to be 0.46eV.*

2.7 Space Charge Experiments Using PEA.

2.7.1 Introduction.

The electrical properties of dielectric materials such as conduction, ageing, degradation and breakdown are closely related and significantly influenced by space charge distribution in the material [16 - 24]. Understanding space charge phenomena provide fundamental understanding of charge injection mechanisms, charge trapping and de-trapping, and charge transport process. The DMM ageing model is based on space charge. It is vital to investigate and characterise the behaviour of space charge in order to arrive at a better design for high voltage equipments. The role of space charge in insulating polymer, especially polyethylene, has been widely reported by many researchers.

Not many space charge measurements have been performed on epoxy glass composite material. In this thesis space charge measurements are made on such material using the PEA system.

Space charge is charge trapped in the insulating material; it could stay there for hours weeks or perhaps years.

Space charge is a function of space and time [ρ (x, t)].

The familiar space charge equations are as follow:

$$\nabla . J(x,t) + \partial \rho(x,t) / \partial t = 0 \quad \text{, Continuity} \qquad 2.21$$

$$J(x,t) = \mu \rho(x,t) E(x,t). \quad \text{, Transport} \qquad 2.22$$

$$\nabla . E(x,t) = \rho(x,t) / \varepsilon_0 \varepsilon_r \quad \text{, Poisson} \qquad 2.23$$

Where x is distance, t is time, ρ(x,t) is space charge, E(x,t) is field, μ is mobility, J(x,t) is current density , and $\varepsilon_0\varepsilon_r$ is permittivity, all in SI units.

Assume that the charge injection is uniform across the surface of the electrodes, and the capacitor edge effects are neglected, for a parallel plane geometry:

$$dE(x)/dx = \rho(x)/\varepsilon_0\varepsilon_r \qquad 2.24$$

This equation is a one-dimensional function of distance through the dielectric. The applied voltage $V(x)$, across the sample is related to the electric field within the sample $E(x)$, by:

$$V(x) = -\int_0^x E(x)dx. \qquad 2.25$$

Insulating material experience high electrical and thermal stress. Under such conditions electric charge (space charge) may be created from the impurities in the material or injected from the electrodes.

The understanding of the relationship between space charge and electrical breakdown is vital, as the existence of space charge in the material enhances the local electric field around the space charge and might lead into electrical failure.

2.7.2 Homocharge and hetrocharge.

Space charge can accumulate near electrodes. Charge of the same polarity as the electrode is called homocharge. Homocharge is injected by the electrode and therefore dependant upon electrode-insulator interface, temperature, and in DC fields the polarity. Polarity is considered in DC fields because some metals may inject carriers of one sign , while others support bipolar injection. Hetrocharge is defined as space charge that accumulates near an electrode with opposite polarity. It can be generated by charge migration from the bulk to the electrode. Homocharge and hetrocharge distort the electric field in insulators.

2.7.3 Measurement system.

Numerous techniques are used to perform space charge measurements: thermal pulse, thermal step, pressure wave propagation, laser-induced pressure pulse and pulsed electro-acoustic method. The technique that is used in this research is the pulsed electro-acoustic technique (PEA), see Figure 2.18

PEA is a non-destructive method, which has been developed in Japan and used to measure dynamically net charge density as a function of distance through solid insulating material under an applied voltage.
When a pulsed electric field is applied to a specimen containing space charges, the sudden movement of the charges generates acoustic waves, which propagate in the specimen.

A piezoelectric sensor under the electrode converts the acoustic wave into an electric signal that can be observed by an oscilloscope; the amplitude of the signal is related to the charge quantity and the delay indicates its distance from the electrode. In this way the internal space charge distribution can be observed
The pulse generator generates a pulse between 200 and 2000 volts for a duration of 5ns.
The typical size samples used for this system are 100-400μm thick and an applied voltage up to 19.5KV was used to generate the space charge. The pulse amplitude used was 400V.

Figure 2.18. *PEA measurement system and ancillary components for DC application.*

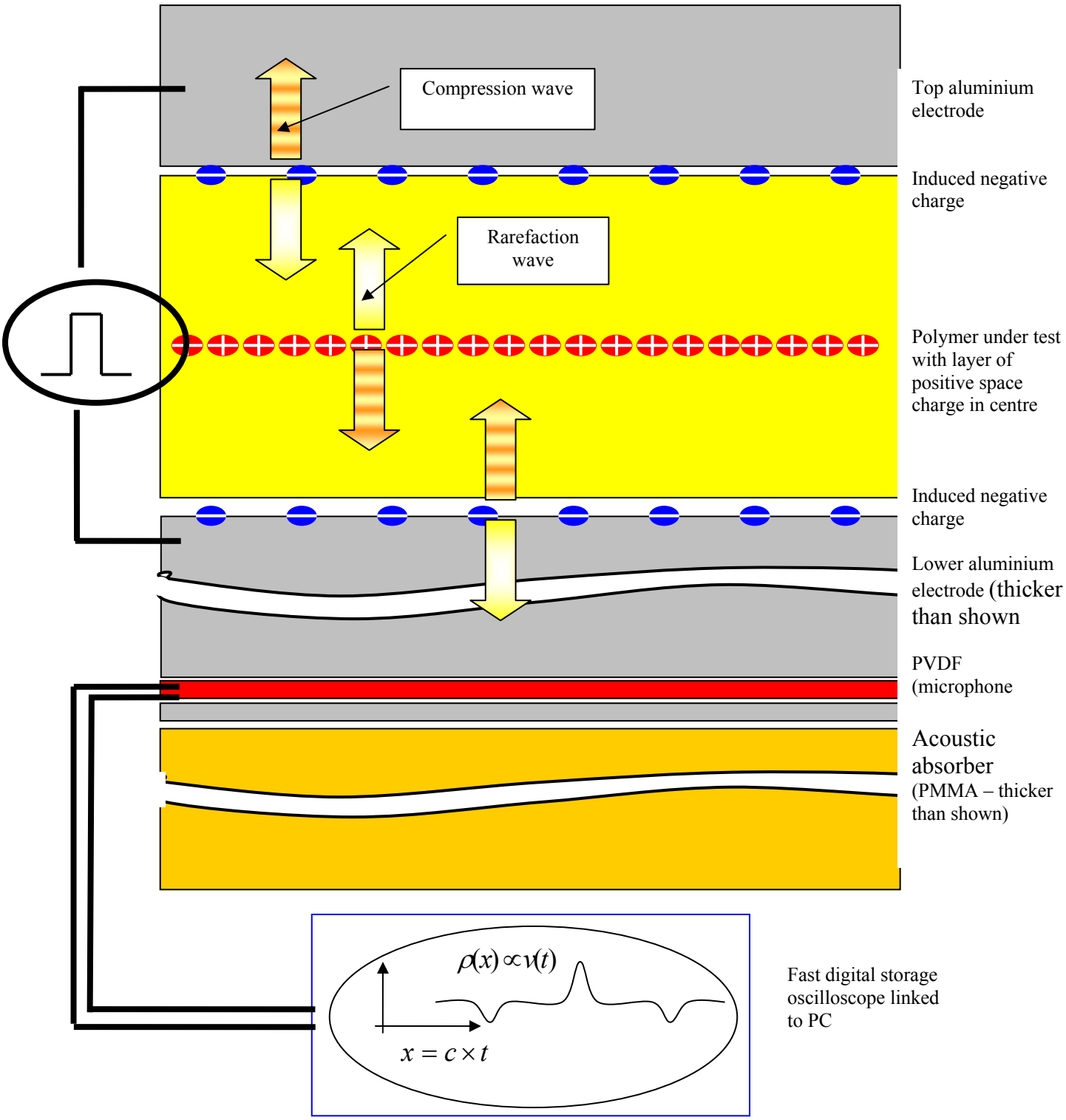

Figure 2.19. *A schematic diagram showing PEA measurement system. The speed of sound in the material is c.*

Figure 2.19 is a representation of the PEA system. The polymer under test is shown to have a layer of positive space charge in the centre and there is no DC applied voltage. The positive space charge has induced negative charges on the electrodes. A positive electrical pulse applied to the top electrode repels the positive space charge towards the bottom electrode. This results in a compression wave travelling from the positive space charge downwards and a rarefaction wave travelling upwards. Similar waves are seen emanating from the negative induced charges, but these are flowing in opposite directions. The waves travel through the lower electrode to a piezo-electric PVDF layer which converts the acoustic pulses to a voltage signal that can be stored on a high speed DSO. To a first approximation, the shape of the voltage signal as a function of time is proportional to the shape of the space charge density profile with respect to distance

2.7.4 PEA Results

Pulsed electro-acoustic (PEA) experiments were carried out on the composite material samples at 19kV (applied field 47.5kV/mm) and temperatures [20,30,40,50,60ºC]. The sample was subjected to the field for 24 hours at each temperature with the signal being measured at a number of selected times. The potential was then turned off (short circuited) and measurements taken during the period of decay.

The purpose of the experiment is to investigate the existence of space charge in the material under high DC fields, and to characterise its high field behaviour prior to ageing, also to measure decay after short circuit and charge condition close to the electrodes.

The composite material can be thought of as three layers of material in series as shown in fig 2.20.

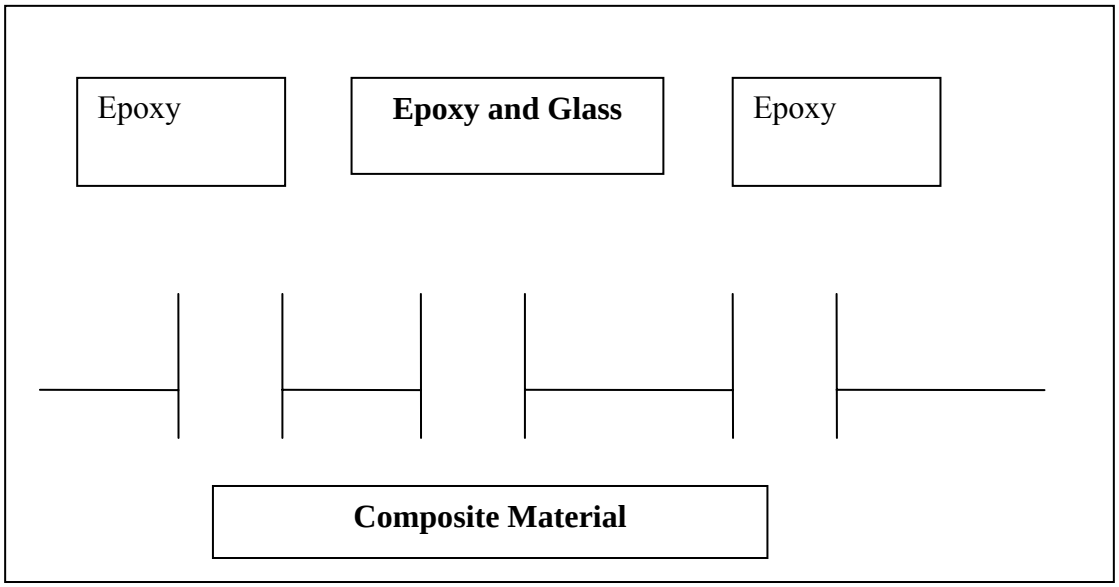

Figure 2.20. *Epoxy glass fibre composite material.*

Each of the materials will contribute a frequency dependent dielectric response; in particular the glass fibre gives a q-dc behaviour that can be expected to act rather like a conductance.

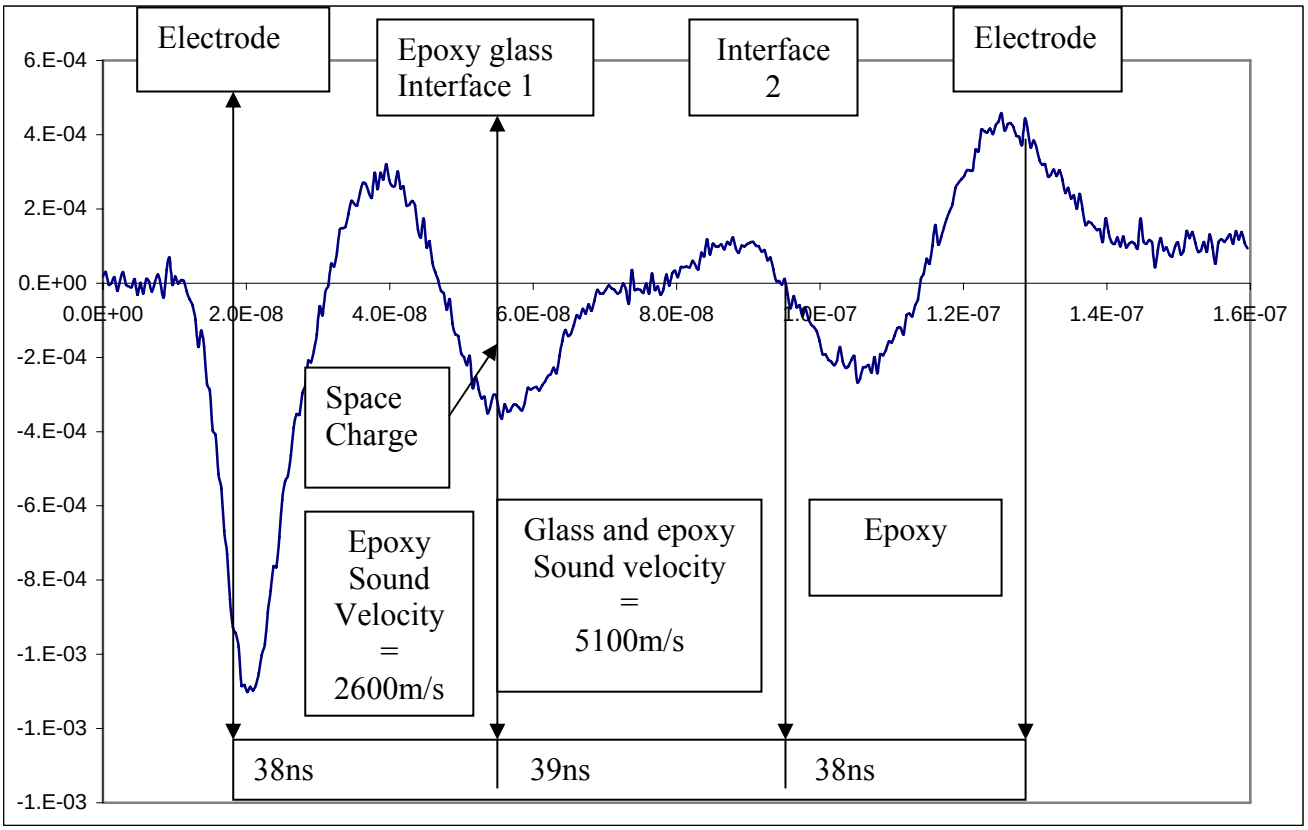

Figure 2.21. *A typical PEA signal profile.*

The first hump on the left shows the electrode near to the PEA sensor. The first 38-second shows the signal in 100μm of epoxy, after that it shows the epoxy glass interface. The middle part of the signal represents the glass epoxy layer, then glass epoxy interface, and the last hump represent the other electrode. Some space charge is found near the interface as shown.

The PEA response can be related to the three layers by using the speed of sound in each layer to find the time delay of the signal reaching the detector.

	Distance travelled (µm)	Sound velocity (m/s)	Time taken (ns)
Epoxy	100	2600	38
Glass mat and epoxy	200	(Dispersion, diffraction) occurs. In glass alone V=5100m/s	39
Epoxy	100	2600	38

Table 2.2 *It shows the distance travelled and the time taken for sound wave to travel in the composite material.*

The time taken for a sound wave to travel through two fibre layers is 39 ns, any wave through the epoxy is delayed and appears later as well as being diffracted

The results for each temperature are shown in Figures 2.22 - 2.31

For each temperature the graphs for different times are superimposed to show the way in which space charge builds up and decays.

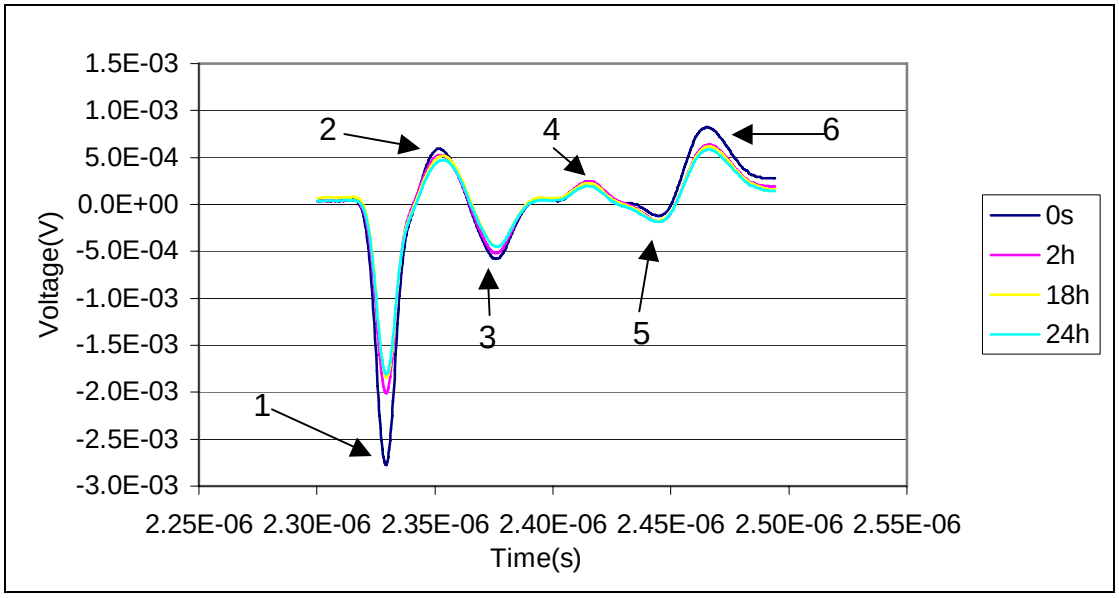

Figure. 2.22. *PEA signal at T=20ºC, and E=47.5V/mm, measurement times denoted in the inset (t=0 to 24 hours). Numbers 1-6 indicates the peaks.*

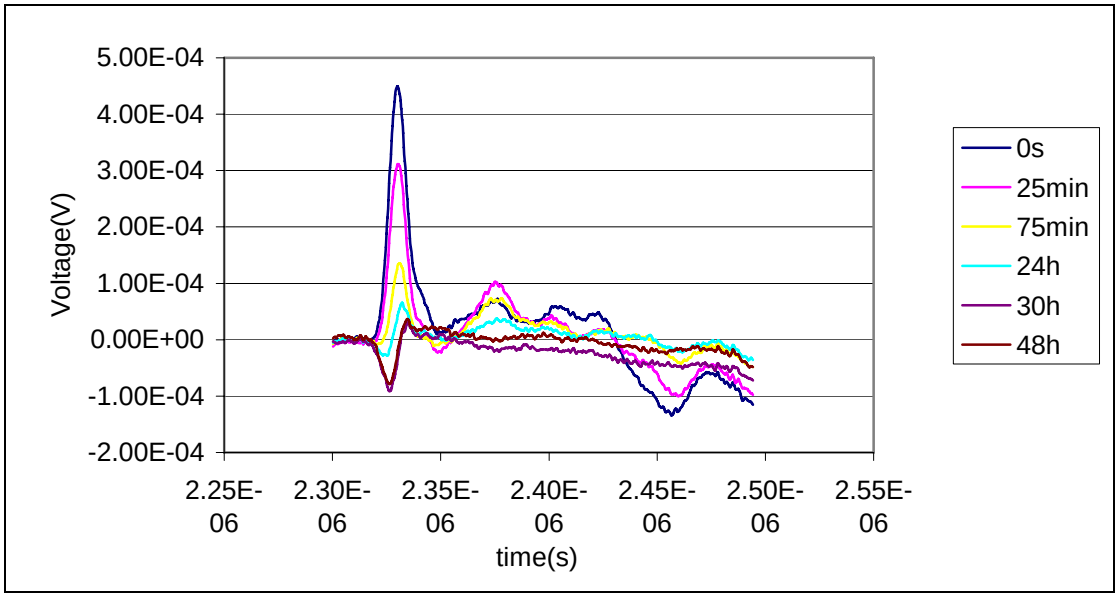

Figure 2.23. *Decay of PEA signal at T=20ºC on voltage removal, following 24hours at E=47.5V/mm, measurement times denoted in the inset.*

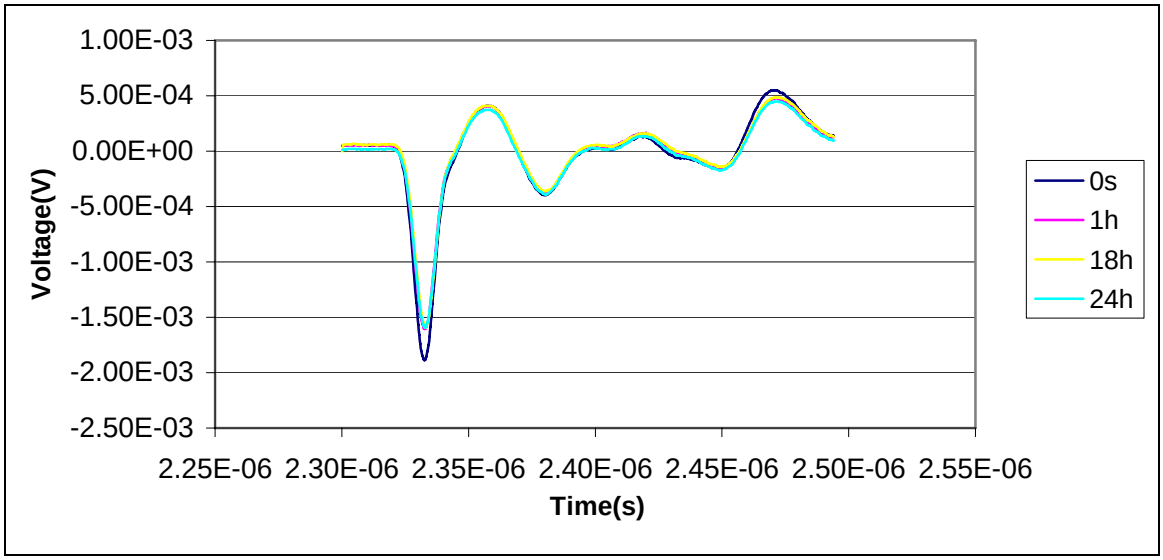

Figure 2.24. *PEA signal measured at E=47.5kV/mm and T=30ºC. time of measurements are shown in the inset.*

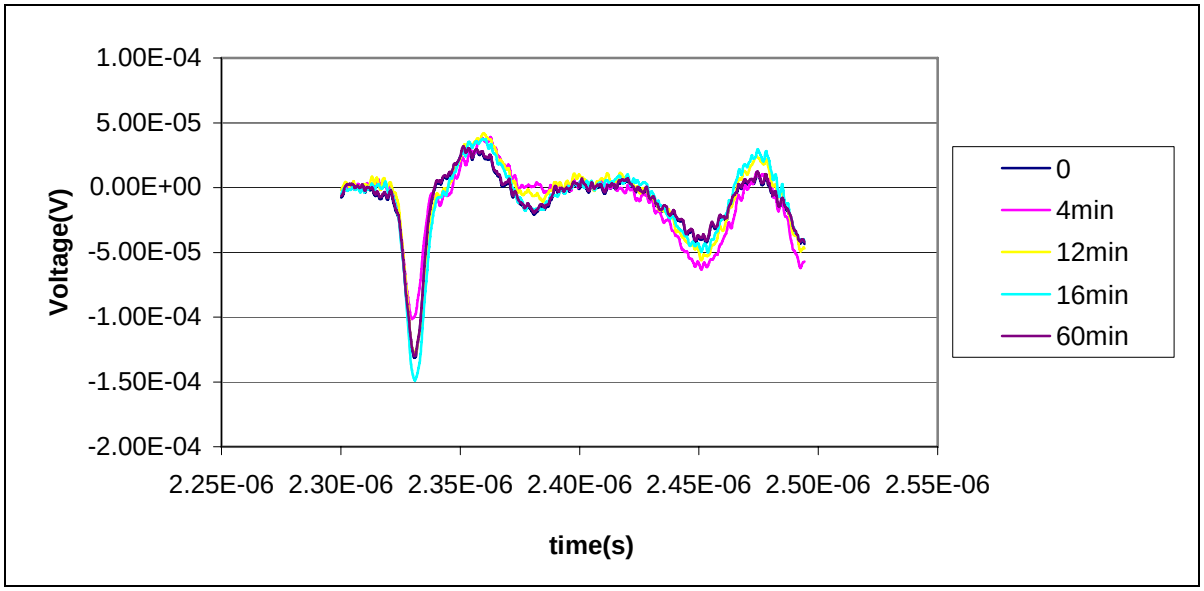

Figure 2.25. *Decay of PEA signal at 30°C following voltage removal at 24 hours.*

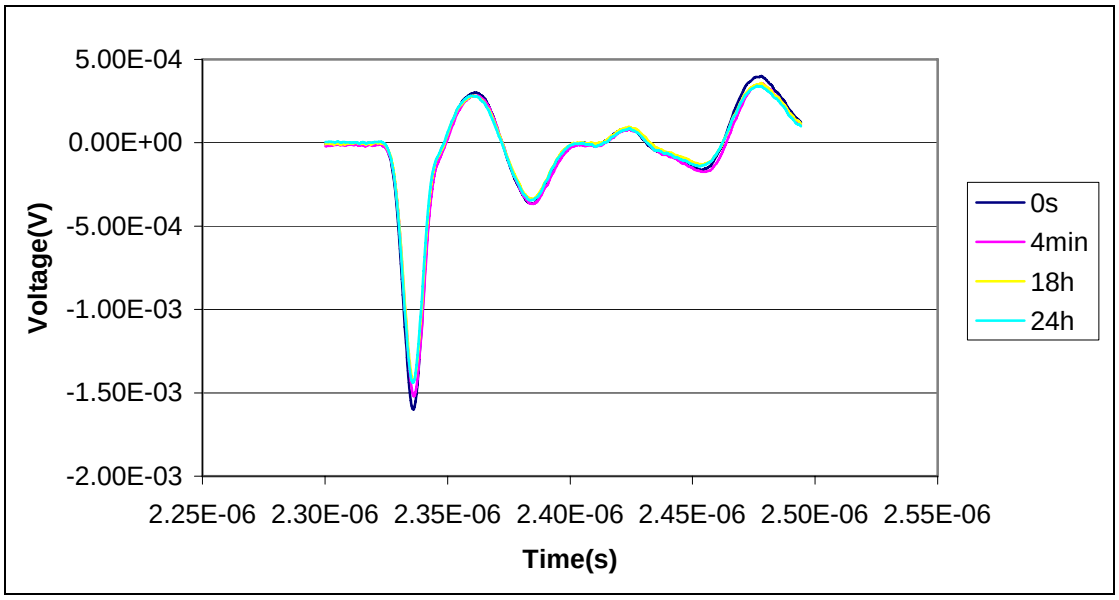

Figure 2.26. *Shows PEA signal measured at E=47.5kV/mm and T=40°C. Times of measurements are shown in the inset*

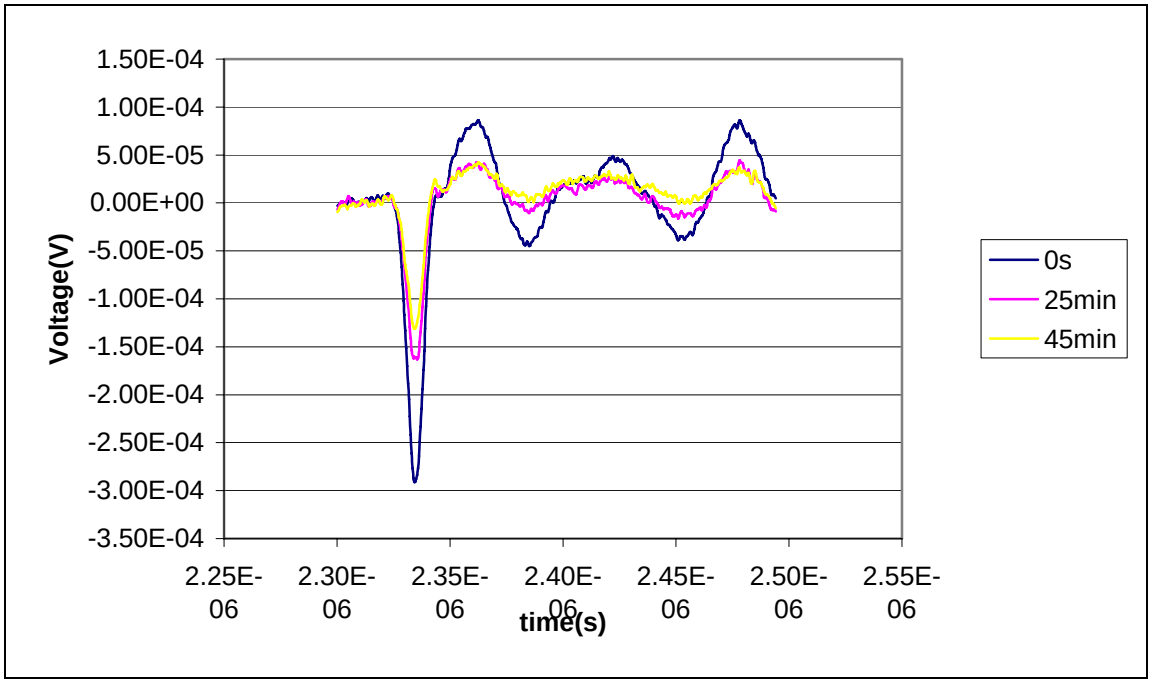

Figure 2.27. *It shows decay of PEA signal at 40ºC following voltage removal at 24hours.*

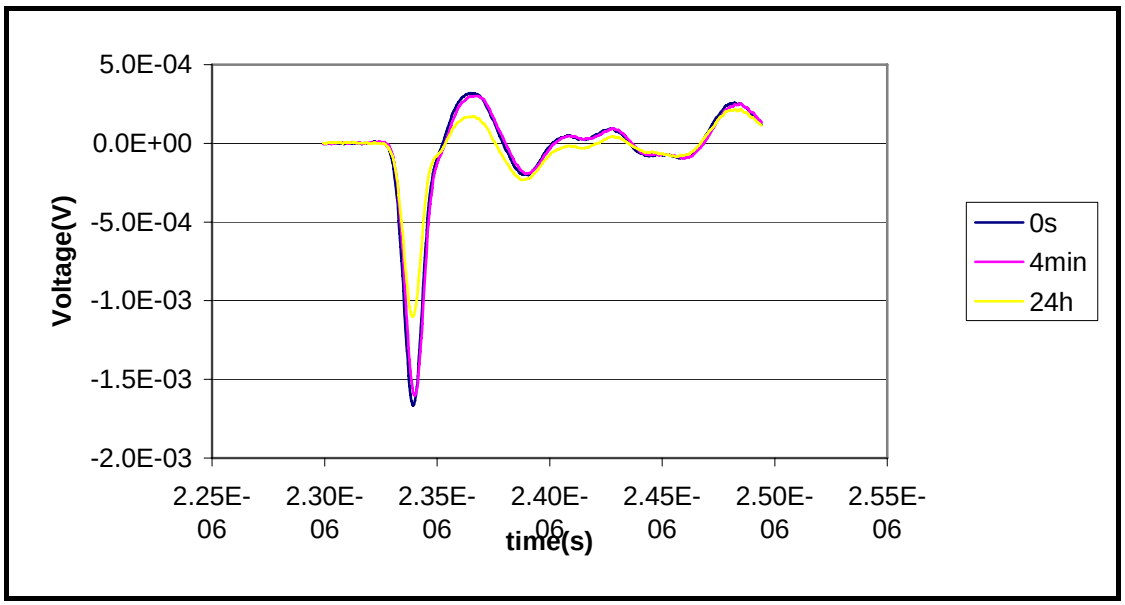

Figure 2.28. *Shows PEA signal measured at E=47.5kV/mm at T = 50ºC. Times of measurements are shown in the inset.*

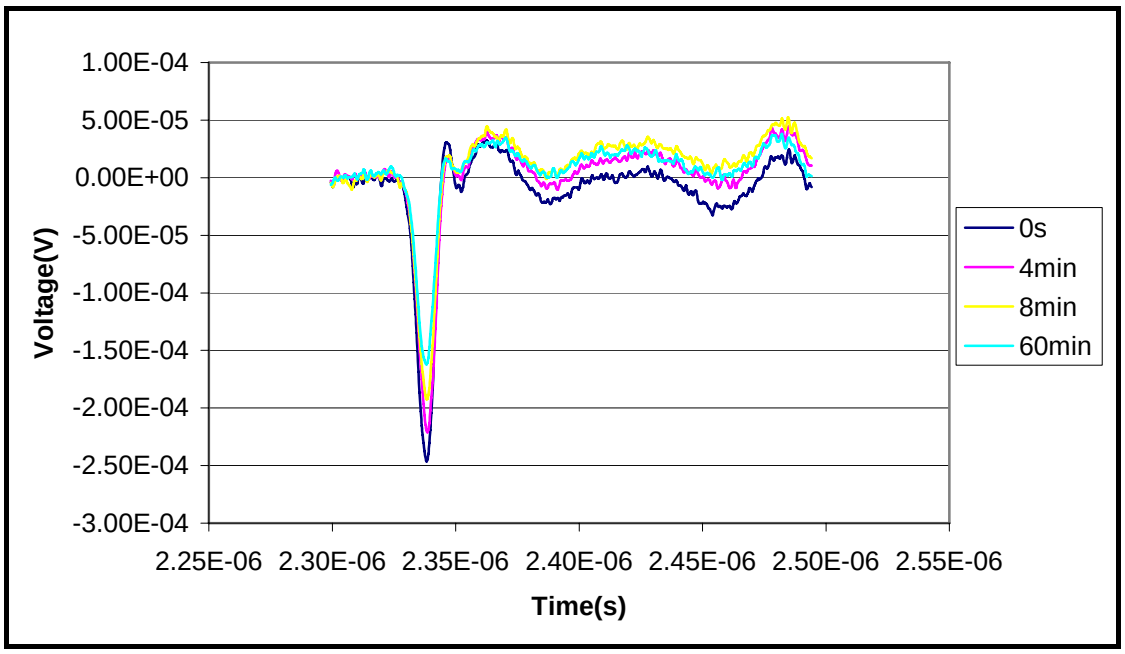

Figure 2.29. *Shows Decay of PEA signal at 50ºC, following voltage removal at 24hours.*

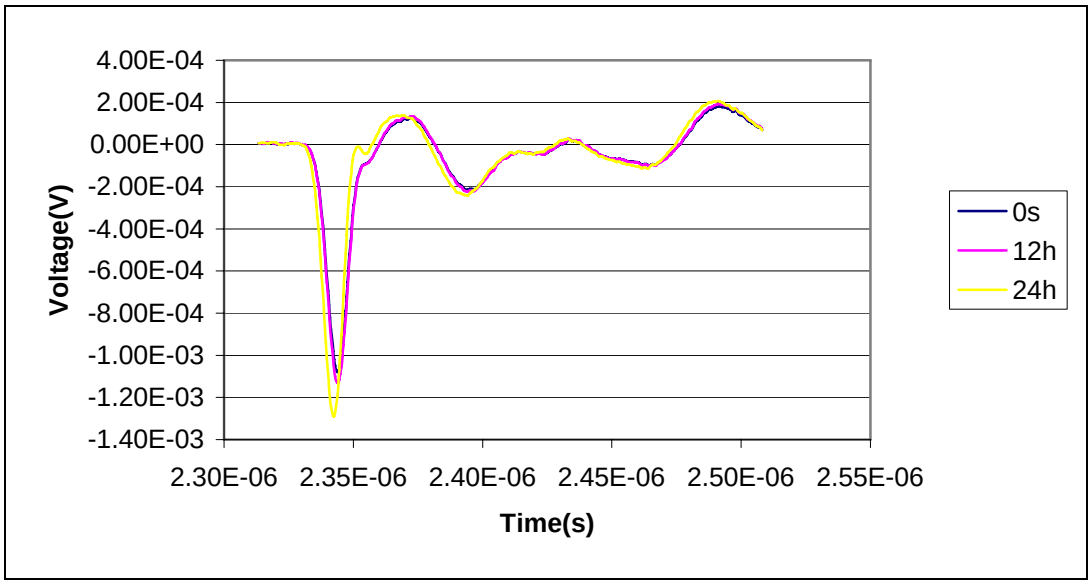

Figure2.30. *PEA signal measured At E=47.5kV/mm and T=60ºC.Times of measurements are shown in the inset.*

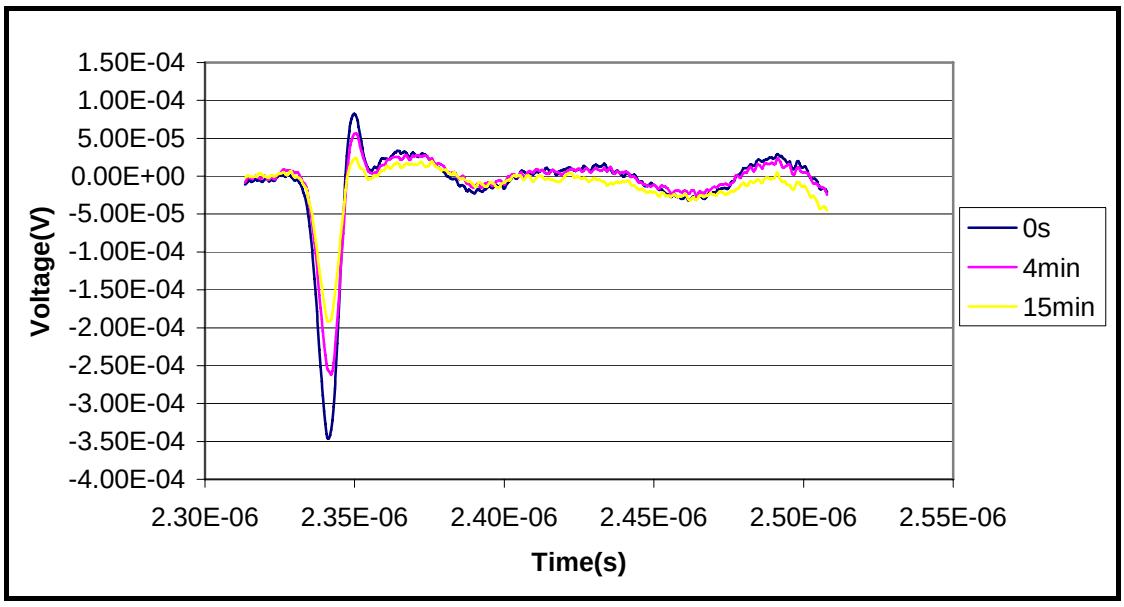

Figure2.31. *Decay of PEA signal at 60ºC following voltage removal at 24hours.*

Considering the Figures 2.22 to 2.31 we can deduce the following general features:

There is a large amount of hetero-charge at both electrodes that can be seen on the first measurement after approximately 1minute of voltage application. This probably originates with the internal frequency dependent transport within the material that would start to build up charge after about 0.1 seconds see section (2.6). The frequency dependent nature of this process means that it builds up capacitive charge by moving charge over long distances in the material; see $C^{//}$ below 0.1 Hz in section 2.6, Figure 2.13

Subsequently homo-charge injection reduces the charge on the electrodes and the heterocharge in the bulk as shown in the plots, except for the experiments at 60C.

At 60˚C Figure 2.30 the charge migration is the more dominant process, charge is migrated from the bulk to the electrodes and hence the charge on the electrodes increases. This may be expected, as at high temperature the charge will be easier to transport as can be seen from the activated nature of the quasi-dc transport process in the composite material.

Below 60˚C charge injection is still taking place after 24 hours. At 60˚C hetero-charge is still building up at 24 hours.

The presence of hetero-charge is revealed in the signals after voltage removal, where it can be seen to induce a charge on the electrodes of the same polarity as that of the applied voltage. The anomaly at 20˚C for the bottom electrode is possibly due to an overlap of the heterocharge peak with a small electrode peak.
The decay process is complex and involves both charge injection to neutralise the heterocharge (predominantly at the anode) and neutralisation by charge transport. The dominant process depends upon the relative time scales involved. In general the process is faster at high temperatures.

The previous results can be summarized in the following tables. The tables show the variation of peaks (magnitude and phase) (1-6), shown in Figure 2.22, with temperature. The applied field is 47.5kV/mm for all temperatures.

Temperature / Peak	Peak magnitude at 20°C	Peak magnitude at 30°C	Peak magnitude at 40°C	Peak magnitude at 50°C	Peak magnitude at 60°C	
1	-2.74	-1.88	-1.58	-1.66	-1.16	$*10^{-3}$V
2	5.77	3.91	2.74	3.01	1.24	$*10^{-4}$ V
3	-4.96	-3.5	-3.26	-2.07	-209	$*10^{-4}$V
4	1.91	1.25	0.68	0.39	0.14	$*10^{-4}$V
5	-1.551	-1.48	-1.33	-0.69	-0.96	$*10^{-4}$V
6	7.93	5.25	3.68	2.48	1.95	$*10^{-4}$V

Table 2.3 *shows the variation of peak magnitude with temperature*

The magnitude of the peaks clearly decreases with increasing temperature. At higher temperature the charge carriers have more energy to move and recombine.

Position of peak at Temperature / Peak	20°C	30°C	40°C	50°C	60°C	
1	2.33	2.33	2.34	2.34	2.34	$*10^{-6}$ s
2	2.35	2.36	2.36	2.37	2.37	$*10^{-6}$ s
3	2.38	2.38	2.39	2.39	2.39	$*10^{-6}$ s
4	2.42	2.42	2.43	2.43	2.43	$*10^{-6}$ s
5	2.45	2.45	2.46	2.46	2.46	$*10^{-6}$ s
6	2.47	2.47	2.48	2.48	2.49	$*10^{-6}$ s

Table 2.4. *Peaks positions for different temperatures*

The peaks positions is almost the same for all temperatures

The following tables summaries the PEA signal features after field removal.

Peak magnitude at Peak / Temperature	20°C	30°C	40°C	50°C	60°C	
1	4.36	-1.29	-2.88	-2.40	-3.41	$*10^{-3}$ V
2	-	0.30	0.83	0.31	0.02	$*10^{-4}$ V
3	-	-0.17	-0.40	-0.15	-0.01	$*10^{-4}$ V
4	-	-	0.40	-	-	$*10^{-4}$ V
5	-	-0.38	-0.31	-0.25	-0.03	$*10^{-4}$ V
6	-	0.08	0.075	0.22	0.24	$*10^{-4}$ V

Table 2.5 *shows the variation of peak magnitude with temperature after voltage removal.*

The magnitude of the peak near the sensor, peak 1, is going down to negative values with increasing temperature. This explains why the value is high at 20 °C. The magnitude of the peaks is decreasing with increasing temperature. Charge decay is faster at higher temperatures.

Peak position at Temperature / Peak	20°C	30°C	40°C	50°C	60°C	
1	2.33	2.33	2.34	2.34	2.34	$*10^{-6}$ s
2	-	2.35	2.36	2.37	2.36	$*10^{-6}$ s
3	-	2.38	2.39	2.39	2.39	$*10^{-6}$ s
4	-	-	2.43	-	-	$*10^{-6}$ s
5	-	2.45	2.46	2.46	2.46	$*10^{-6}$ s
6	-	2.48	2.48	2.48	2.49	$* 10^{-6}$ s

Table 2.6. *Peaks positions for different temperatures after voltage removal.*

2.8. Differential Scanning Calorimetry (DSC).

Differential Scanning Calorimetery is used to determine the enthalpies of a change in the physical state of a material such as melting or transition from one crystalline form to another [25, 26].

DSC is a technique for detecting the temperature difference between the sample and a reference during the process of heating or cooling, which is carried out at a specific rate in identical environments. If a temperature difference develops between the sample and the reference (because of exothermic or endothermic reactions in the sample) the power is adjusted to remove this difference.

DSC measures the difference in heat flow between the sample and the reference. A signal proportional to the difference between the heat input to the sample and that to the reference is fed into a recorder. The recorder also registers the average temperature of the sample and the difference, see Figure 2.32.

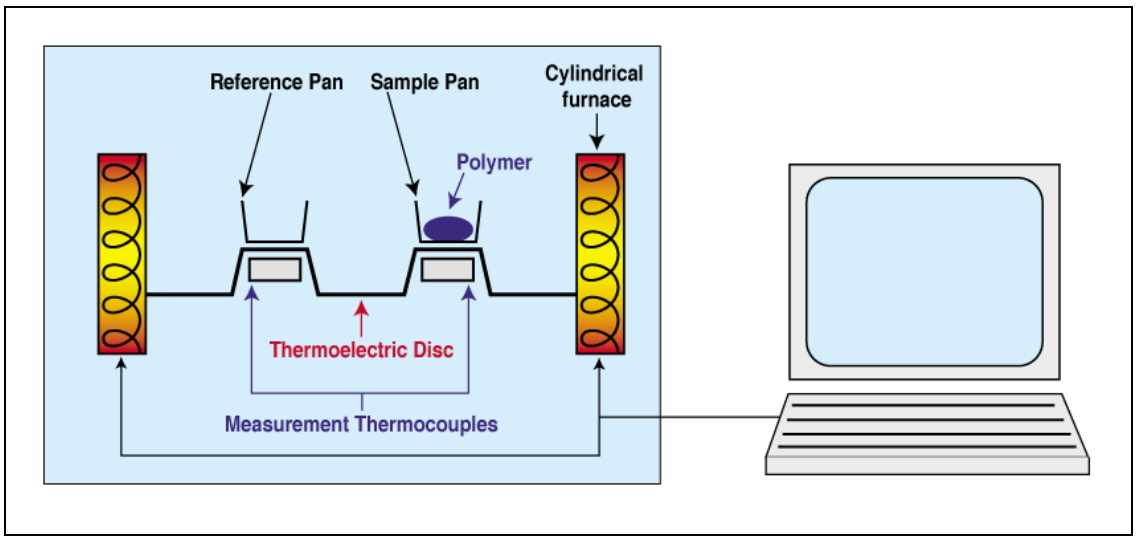

Figure 2.32. *Schematic representation of the DSC thermal analysis system.*

2.8.1 Glass transition temperature.

All amorphous polymers exhibit a glass transition temperature. Tg is the common abbreviation for the glass transition temperature. Amorphous regions in partially crystalline polymers exhibit the characteristic changes associated with the polymer at its Tg. As the polymer is heated, it undergoes a transition. It is characterised by a change in the expansion coefficient and heat capacity. These changes, however, occur over a temperature range. Consequently, Tg is sometimes difficult to detect. Tg is one of the most important parameters that define the properties and behaviour of polymers [27]. Below Tg the polymer is hard and glassy, while above Tg it behaves as a rubber and finally as the temperature increases it behaves as a highly viscous liquid (thermoplastic) or degrades (thermosetting). The glass transition temperature is obtained from a specific volume- temperature plot of observations taken on cooling. This is not the case in DSC measurements. In this research Tg was obtained by DSS. Figure 2.33 illustrates an idealised output (thermogram) from the DSC for Tg determination. The y-axis is heat flow rate in millicalories/second, and the x-axis is the temperature in ˚C. Tg is taken as the midpoint (inflection point) in the thermogram. The Tg value depends slightly on the rate of flow of heat, being lower for lower rates [28].

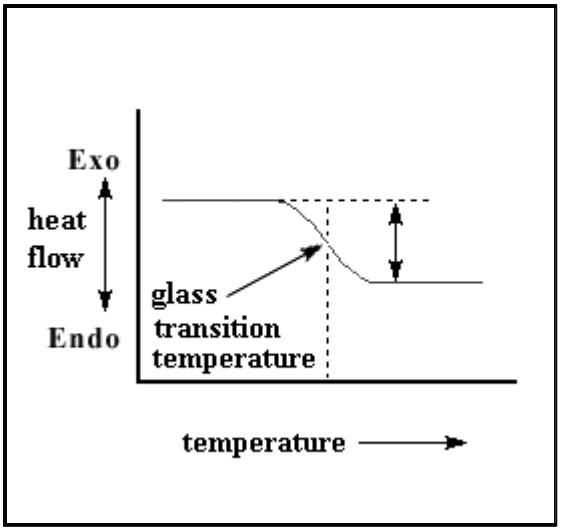

Figure 2.33. *Ideal DSC output*

2.8.2 Tg and degree of cure

Polymeric materials may be broadly divided into two classes, thermoplastics, and thermosets.

In general thermoplastic consist of high molecular weight molecules of more or less linear structure. Thermoplastic polymer molecules have inter-molecular interactions . Because of this, the molecules are relatively free to move with respect to each other like the individual strands in a bowl of spaghetti.

A thermoset material has a molecuular structure, which is cross-linked. The molecules are chemically bound together in a three-dimensional network by a curing reaction. On raising the temperature, the curing (cross- linking) reaction proceeds to form a rigid structure. Thermoset materials are not reformable, because of their rigid three-dimensional structure. When heated they will degrade to lower molecular weight products produced by a random scission of chemical bonds.

The degree of cure, the percentage completion of the curing reaction, is an important parameter in determining the electrical and mechanical properties of the material. The glass transition temperature increases as the curing reaction proceed to completion due to the increase of cross- linking.

DSC can be used to test for the degree of curing. Figure 2.34 shows a typical thermal behaviour of an epoxy resin. On first of heating the glass transition temperature is observed. Upon continued heating, the appearance of the cross-linking exotherm peak indicates that the curing reaction is taking place. The exotherm peak is heat generated by the curing reaction of the non cross-linked portion of the resin. The area under the peak is in units of energy, called the residual energy, proportional to the amount of cross-linking, which is taking place. In theory a zero area means 100% curing.

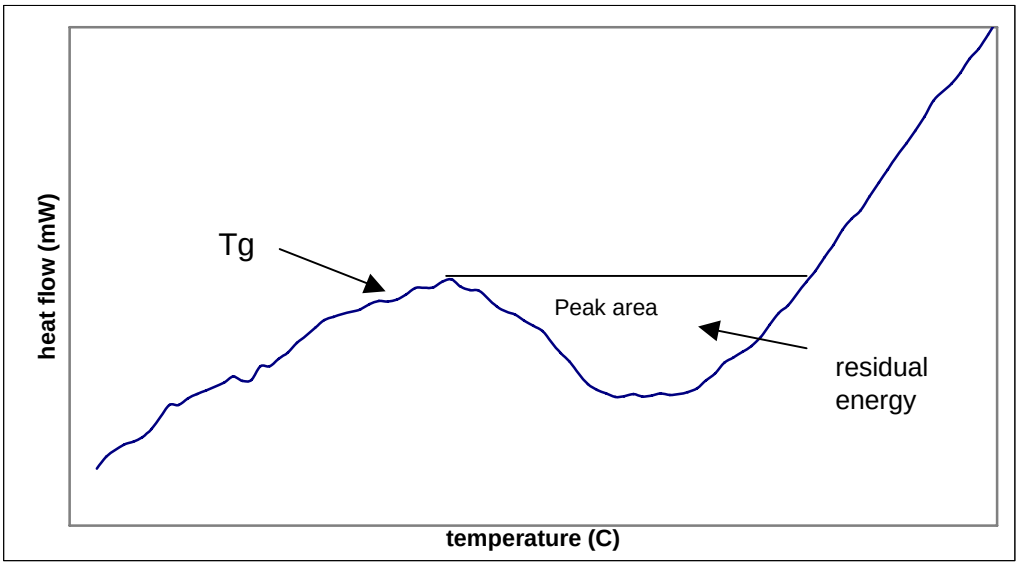

Figure 2.34. *The area under the exothermic peak generated by curing reaction and proportional to the amount of cross-linking.*

2.8.3 Experimental results

DSC was used to determine the glass transition temperature of the composite material, and to check the degree of cure in the pure epoxy resin. The samples were well encapsulated to ensure good thermal contact and prevent volatiles from escaping. The samples weights were around 5mg. The samples were heated from 20°C to 180°C at constant rate of 20 ˚C per minute. The results were obtained via a computer connected to the DSC machine. The results are shown below:

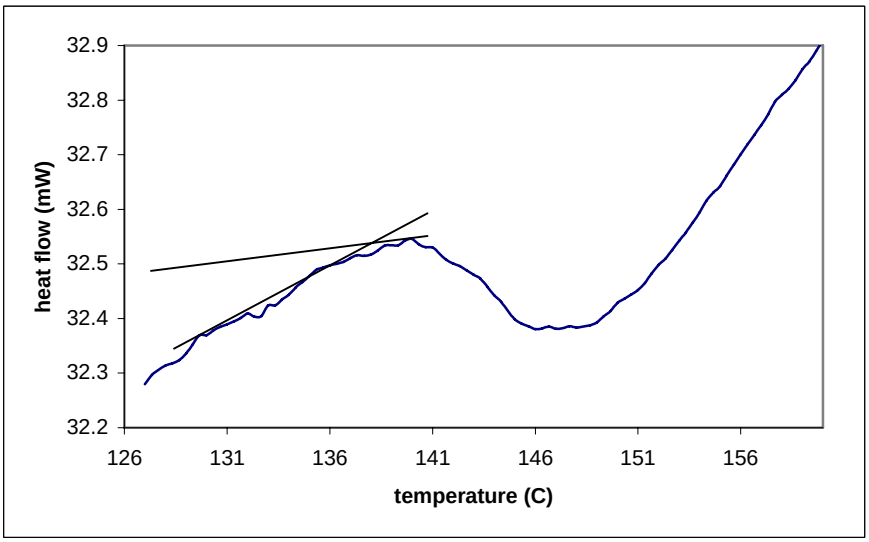

Figure 2.35. *Showing that Tg for the composite is 138.9 ℃.*

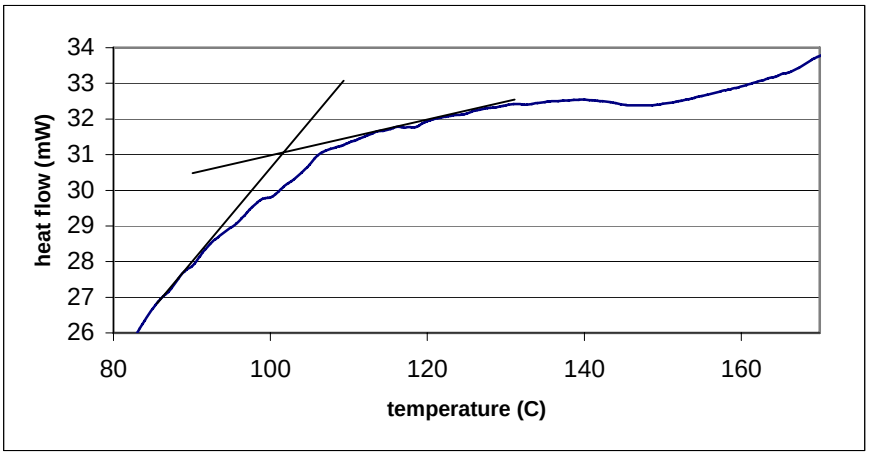

Figure 2.36. *After10 minutes curing Tg is 102℃.*

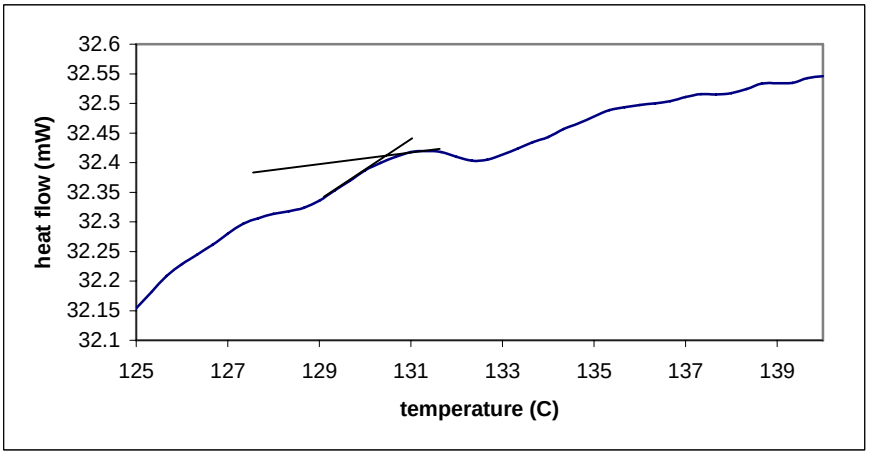

Figure 2.37. *After 1 hour curing Tg is 130℃.*

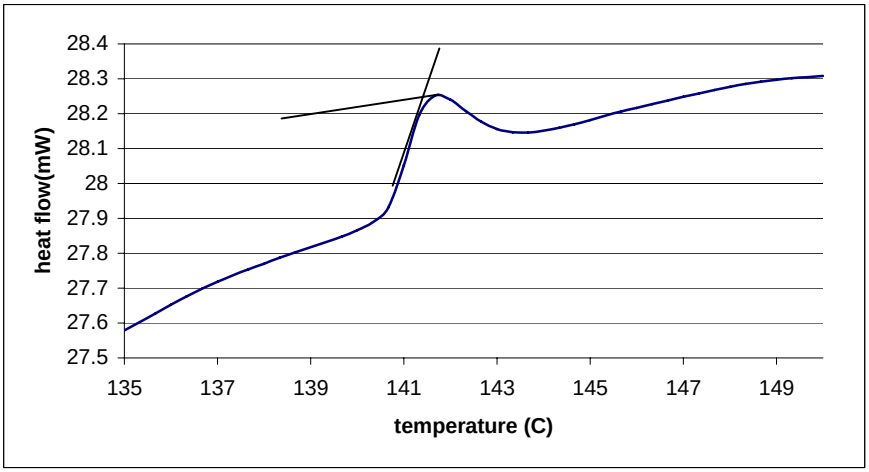

Figure 2.38. *After 6 hours curing Tg is 141℃.*

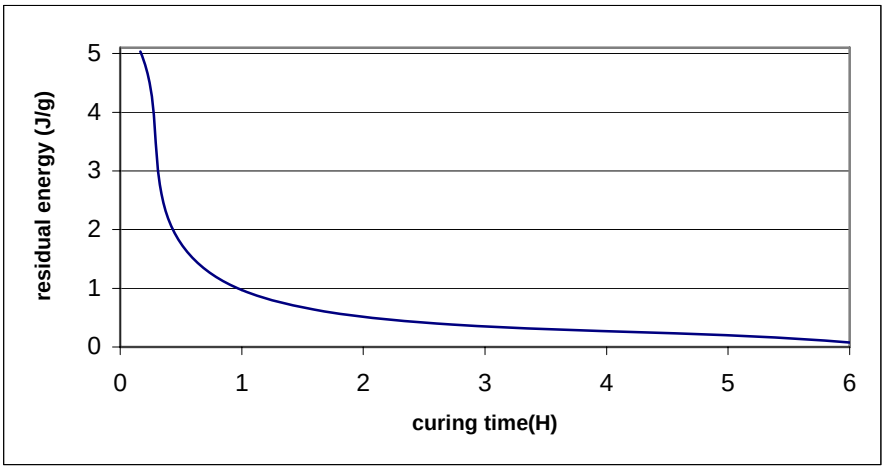

Figure 2.39. *The residual energy against curing time.*

Figure 2.35 shows the thermal behaviour of the composite material, the glass transition temperature is encountered at 138.9 °C, which agrees with the manufacturer specification of 140 °C [29].

Figures 2.35-2.38 show the DSC response for different curing conditions of the pure epoxy, the glass transition temperature is shifted depending on curing time, the area under the peak is in units of energy and directly proportional to the amount of cross-linking which has taking place [30, 31].
The DSC for the composite material shows that there is a residual energy, i.e. the material is not 100% fully cured. This indicates that the epoxy may not have such a strong bond to the fibres as it would when fully cured.

The results can be summarized in the following table.

Curing time	Glass transition °C
10 min	102
1 hour	130
6 hours	141
Manufacturers	138.9

Table 2.7. *Glass transition temperature for different curing time*

The glass transition temperature increase with increasing curing time.

2.9 Dynamic Mechanical Analysis (DMA)

Rheology is the study of materials response to an applied deformation (strain) or stress. Materials will respond to strain by dissipating energy in the form of heat (viscous dissipation), storing the energy elastically, or through a combination of both of these two mechanism [31,33]. DMA makes it possible to measure both of these properties.

Figure 2.40. *Dynamic mechanical analysers measure changes in mechanical behaviour, such as modulus and damping, as a function of temperature, time, frequency, stress or strain or combinations of these parameters*.

Dynamic Mechanical Analysis (DMA) is used to analyse both elastic and viscous material response simultaneously.

A sinusoidal strain is applied to a material via a motor. The resulting stress is measured with a force transducer. The force is then separated into elastic stress and viscous stress. Elastic stress is in phase with applied strain and viscous strain is in phase with the rate of applied strain. The phase lag results from the time necessary for molecular rearrangements.

2.9.1 Experimental results

A torsion rectangular test was performed on a rectangular sample of 16mm length, 7.3mm width and 0.4mm thick, under the following conditions:

Frequency range [0.01 to 100] Hz, a range of temperatures between 40°C and 160°C

Figure 2.41 and 2.44 shows the results in terms of the real and imaginary part of the compliance (J*= 1/G* where G* is the complex modulus) plotted as a function of the frequency.

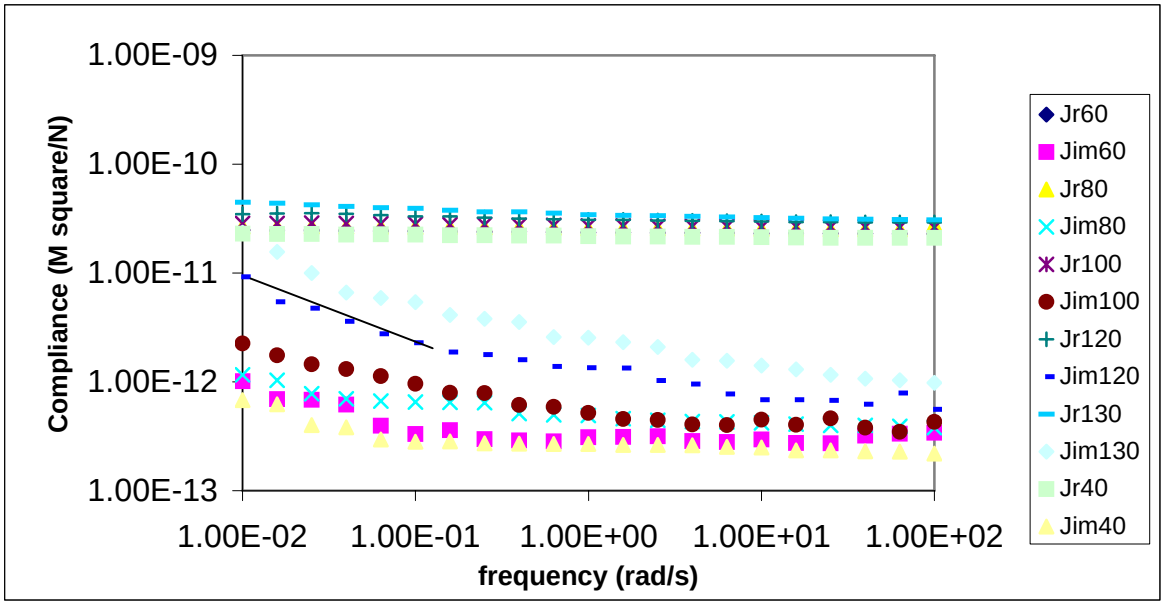

Figure 2.41. *DMA response for the composite material. For real (upper) and imaginary (lower) parts of compliance. For 8 temperatures 60,80,100,120, and130˚C*

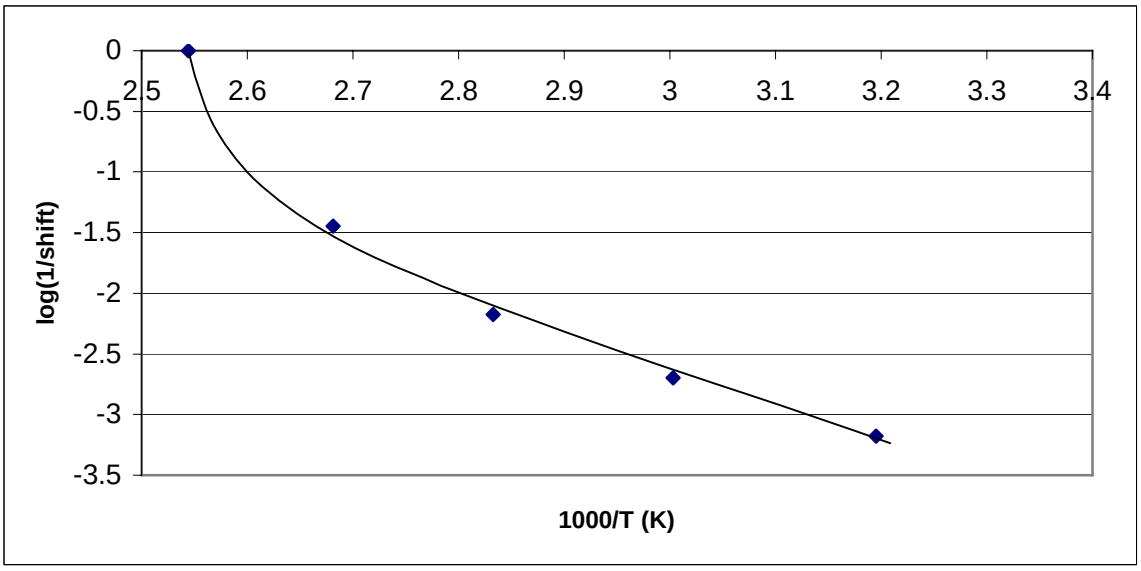

Figure 2.42. *Plot for DMA response for the low frequency process. For the composite material. The shift is in amplitude.*

This is not a straight line, so the process is not an Arrhenius process.

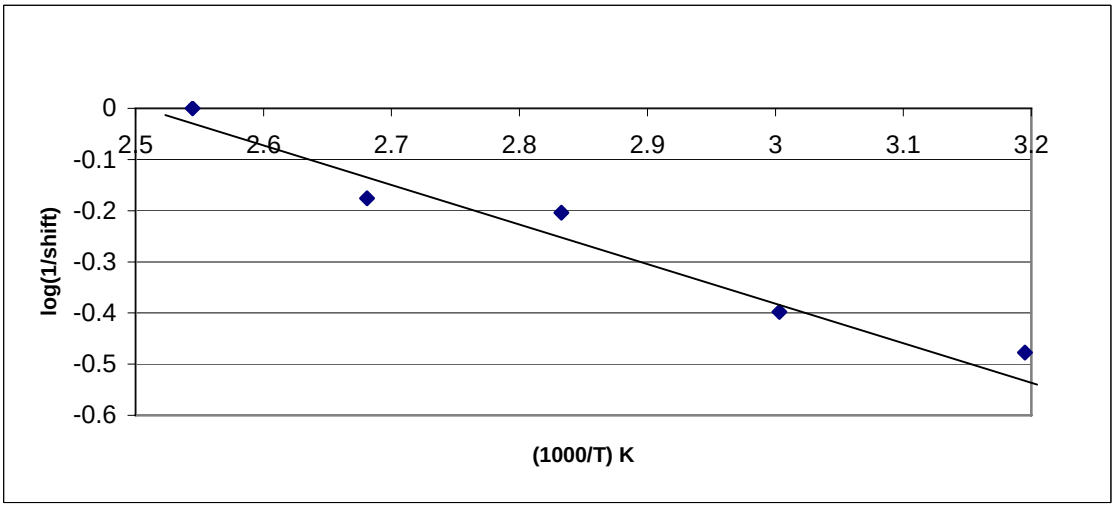

Figure 2.43. *Activation energy plot for DMA for the high frequency process. For the composite material. The shift is in amplitude.*

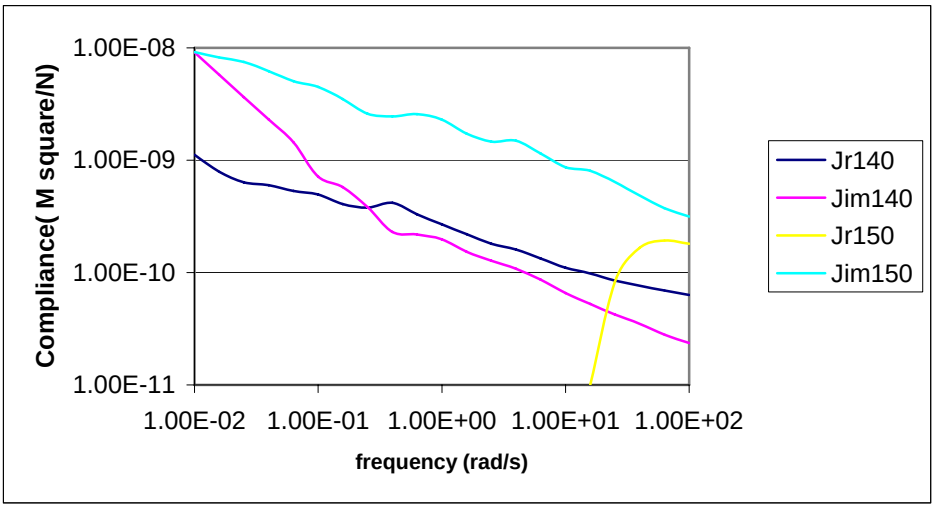

Figure 2.44. *The compliance against frequency for the composite material at 140 and 150˚C.*

From the analogy between the electrical dielectric response and the Dynamic Mechanical response, particularly the compliance and the capacitance we can deduce the following:

At 120˚C and 130˚C the slope of the imaginary compliance is –1 at low frequencies shown in Figure 2.41. This implies the existence of constant viscosity near the glass transition temperature, which is 140˚C.

The complex compliance $J = J' - iJ''$ where J' represents elastic compliance and J'' viscous compliance. Figure 2.44 shows a plot of the complex compliance above the glass transition.

At a temperature 150˚C the results are untrustworthy. At temperatures of 100°C and below a broad loss peak can be observed at around 10rad/s. Another loss process also occurs whose peak would be below 10^{-2} rad/s. The peak at 10 rad/s does not correspond to anything observed dielectrically and so must relate to motions that do not involve dipoles. The lower loss process occurs in the region of the q-dc behaviour (see section2.5.1). An explanation in terms of charge transport cannot be applied to the DMA behaviour unless the charges that move are ionic. Then an equivalent mechanical response may possibly be observed.

An Arrhenius plot is shown in fig 2.43 for the amplitude data peaked around 10rad/s. The frequency shift of this process with temperature could not be discerned because

of its low magnitude and the obscuring effect of the low frequency process. However, an increase in magnitude with temperature is noticeable in Figure 2.41. The magnitude change was found to be activated with activation energy of 0.2eV. This process was not observed in the dielectric response and its temperature dependence indicates the activated displacement of non-polar regions, the concentration of which increases with temperature.

2.10. SEM Analysis

SEM is Scanning Electronic Microscopy. This is used to investigate the microscopic structure of the material and provide an elemental analysis [34].
Figure (2.45) shows an elemental analysis obtained on a sample prior to ageing using an SEM. The carbon peak is quite strong, as are peaks associated with the elemental content of the glass fibres (e.g. Si, Ca, Al).

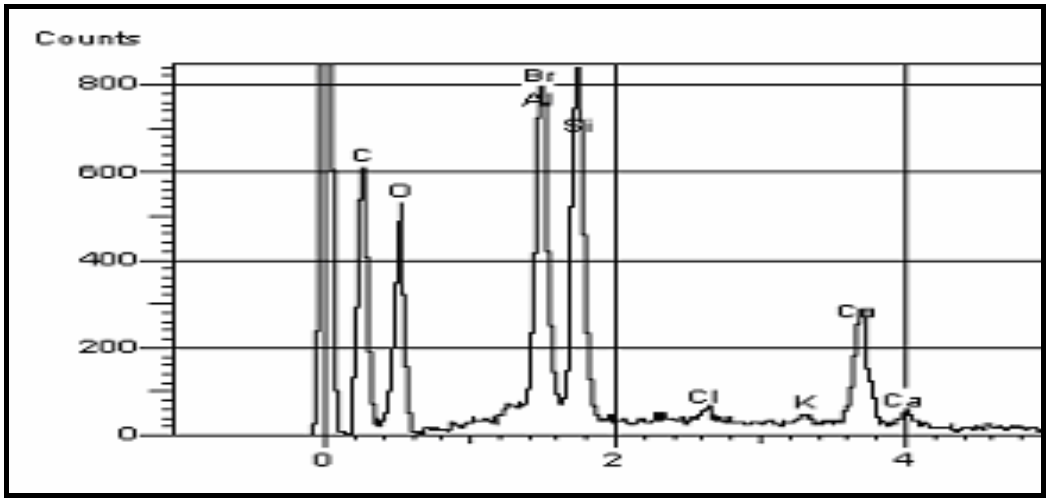

Figure 2.45. *Elemental analysis of composite material.*

2.10.1 Glass fibre composition.

The glass used in the composite is woven E-glass as specified in IPC-4412.

The formula is as follows: [35].

B_2O_3: 5 - 10%
CaO: 16 - 25%
Al_2O_3: 12 - 16%
SiO_2: 52 - 56%
MgO: 0 - 5%
Na_2O and K_2O: 0 - 2%
TiO_2: 0 - 0.8%
Fe_2O_3: 0.05 - 0.4%

F_2: 0 - 1.0%

The aluminium found in the SEM elemental analysis of the glass Figure 2.46 is therefore a constituent of the glass fibres.

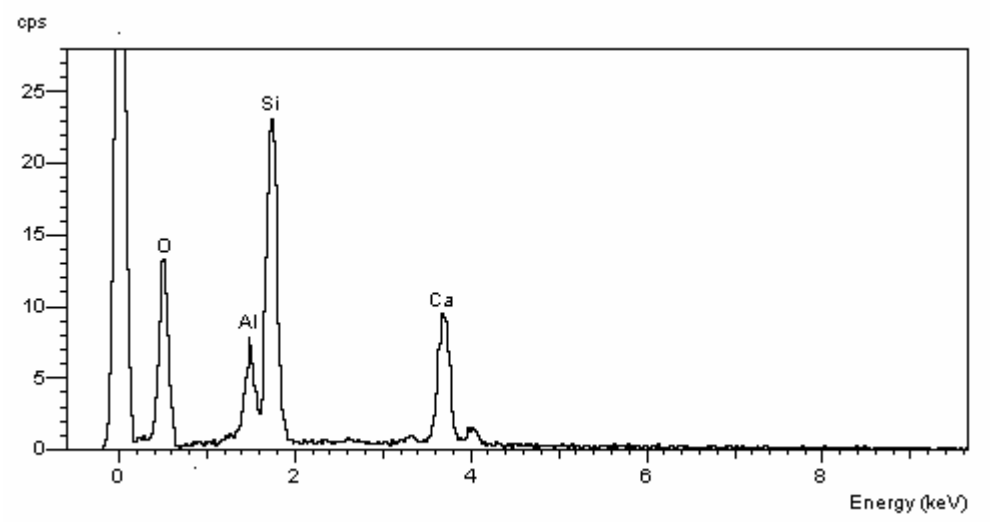

Fig 2.46. *Elemental analysis for the glass fibre mat.*

The bromine found in the elemental analysis of the composite material comes from the flame retardant "tetrabromobisphenolA", as confirmed by the manufacturers, which was reacted with the resin [35].

CHAPTER 3

AGEING

3.1 Introduction:

The Insulation system (epoxy/glass fibre) composite described in this thesis is subjected during operation to combined electrical, thermal, mechanical and environmental stress. During long time in service those stresses may act and interact in a sophisticated way to deteriorate the equipment and possibly lead to degradation and failure [1]. In order to understand and evaluate the way in which the insulation system reacts to stresses mentioned, it is necessary to investigate the characteristic of aged material. The composite material was characterised before ageing with the results presented in Chapter 2. An ageing program was put in place to investigate the effect of ageing on the composite material.

Ageing conditions were more severe than those experienced in normal working conditions. The reason for this is that ageing takes a long time and it is hard to do in the laboratory. Accelerated ageing can give an insight into what happens to the material after years in service [8]. The ageing program includes electrical ageing, thermal ageing, and a combination of both.

In the last thirty years extensive research has been carried out on XLPE cables with regards to electrical treeing, from the start to the final stage [3]. Treeing was found to be involved in the degradation process for most of the ageing mechanisms. Critical ageing processes were found to occur in the bulk structure and the interfaces [(insulation /electrodes), (insulation/fillers) and external interfaces (composite/air or oil)]. So interfaces are very important in the ageing, degradation and breakdown mechanisms.

Ageing leads to degradation and breakdown as mentioned before. Ieda et al. [4,5] investigated the relationship between breakdown and polymers properties such as the

chemistry and the morphology. Defects and impurities were found to play a major role in ageing degradation and breakdown.
In this thesis the interface between epoxy and glass fibre has been shown to be the weak point where ageing is initiated.

3.2 Ageing programme

Several attempts using different methods were made to perform the ageing experiments at {15,20,25)} kV and {90 degrees, room temperature} but were unsuccessful due to a flashover problem. Eventually the problem was overcome by using a silicone rubber encapsulation. The samples were immersed by a thin layer of silicone rubber leaving a region where an electrical connection could be made between the sample and the electrodes.

The following is a table of aged samples:

Sample	Field (kV/mm)	Temperature ºC	Duration (day)	Analysis
1	62.5	90	10 minutes (a)	
2	50	90	50 minutes (b)	
3	37.5	90	3 hours (b)	
4	62.5	15±5	154 (b)	PEA, Dielectric spectroscopy, SEM
5	50	15±5	0 (a)	
6	37.5	15±5	168 (b)	Dielectric spectroscopy. DSC
7	62.5	15±5	7 (a)	
8	62.5	90.	12 (a)	
9	50	15±5	25 (b)	Dielectric spectroscopy, SEM
10	25	90	237 (c)	Dielectric spectroscopy, PEA
11	12.5	90	244 still ageing (c)	
12	25	90	208 (b)	PEA, Dielectric spectroscopy, SEM,DSC
13	12.5	90	227 still ageing (c)	
14	37.5	15±5	68 (b)	
15	37.5	15±5	83 (b)	
16	62.5	15±5	69 (b)	
17	62.5	15±5	40 (b)	
18	0	90	177 (c)	Dielectric Spectroscopy
19	0	90	237 (c)	Dielectric spectroscopy

Table 3.1 *Ageing conditions*

Where

a: is flashover around outside of the sample.

b: breakdown through the volume of the sample.

c: did not breakdown.

Sample 5 broke down immediately. It was a flashover breakdown. This flashover is caused by contamination on the electrode surface and the electrode geometry. This led to a re-design of the electrode geometry.

Sample 1 broke down by flashover after 10min. It broke down in the same way as sample 5, i.e. due to the electrode geometry.

Sample 2 broke down after 50min, and sample 3 after 3 hours. Both sample 2 and 3 had a breakdown through the material at almost the same place, which might represent real breakdown data.

The way in which sample 1 and 5 broke down creates the need for samples with different electrode arrangements.

Sample 8 was made with only one electrode ring on both sides; it is under 62.5kV/mm and 90 degree C.

It seems that this electrode arrangement is not causing any premature breakdown

Sample (9) broke down after 25 days of ageing at 50kV/mm and room temperature, Investigating the breakdown under the microscope shows breakdown all the way through the sample, it also shows very thin black lines near the breakdown but perpendicular to the field direction. Such lines were not observed in the un-aged samples.

Samples 10 and 11 were aged at 90ºC under lower fields than samples (1-3) and sample 8 since the other samples could not withstand the higher fields at 90ºC.
Sample 7 and sample 8 broke down after 7 and 12 days respectively.
Sample 4 lasted for 154 days during which progressive Dielectric measurements were made.
Sample 6 lasted for 168 days.
Samples 10 to 13 were aged under (12.5,25) kV/mm.

3.3 Experimental programme.

The aged material system was characterised by means of dielectric response [6, 7, 8], space charge measurements [9, 10, 11], differential scanning caloromity (DSC) [12,13,14], and scanning electronic microscopy (SEM) . The aim of the experiments is to find out how ageing affects the response of the material and how to characterise ageing in terms of the material response.
The results show significant differences in response between the aged and non-aged material. The following results demonstrate these differences.

3.4 Dielectric Measurements on aged samples

Dielectric measurements made on samples removed temporarily from ageing at one week, five weeks, 87 days, 237 days (at E=62.5 and 25kV/mm DC, T= 90 and 15±5ºC) and on the sample that failed showed the same form of response as for the un-aged composite. However, the q-dc process had moved to higher frequencies.
The results are shown in the following plots 3.1 – 3.21

3.4.1 Room temperature aged sample

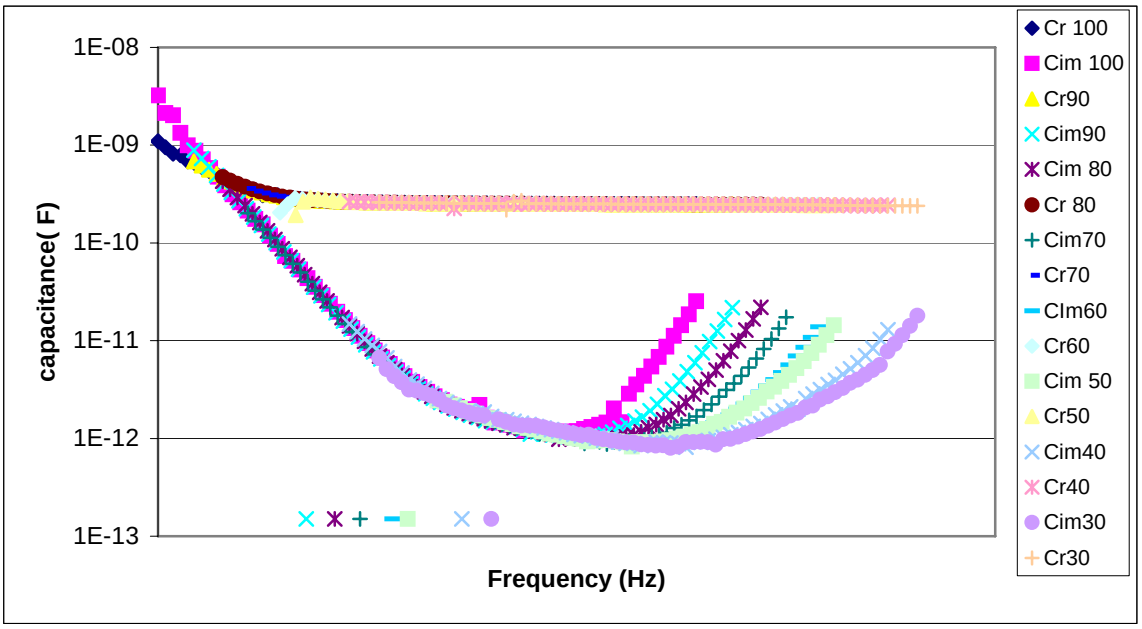

Figure 3.1. *Master plot for composite material for the low frequency process q-dc process. For real (upper) and imaginary (lower) parts of capacitance, for 8 temperatures from 30-100˚ C. This is for sample (4), aged for 35 days (at E=62.5kV/mm DC, T=15±5℃).*

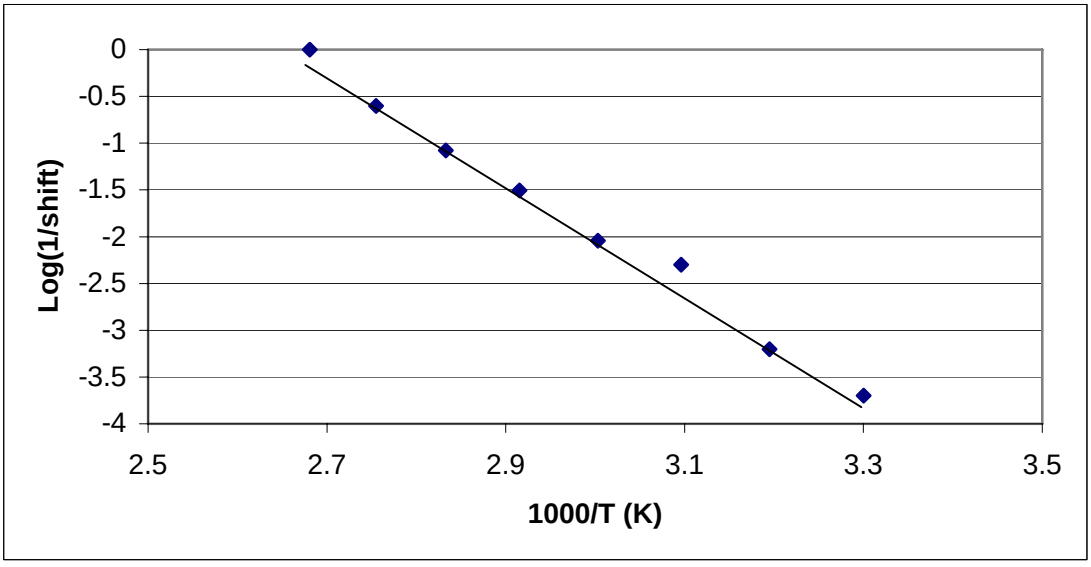

Figure 3.2. *Arrhenius plot for composite material associated with low frequency. process, q-dc. This is for sample (4), aged for 35 days (at E=62.5kV/mm DC, T=15±5℃).*

The activation energy was calculated to be 1.1±0.05eV. The activation energy did not change after 35 days ageing compared with un-aged sample, which is given in Figure 2.11, 1.1± 0.02eV.

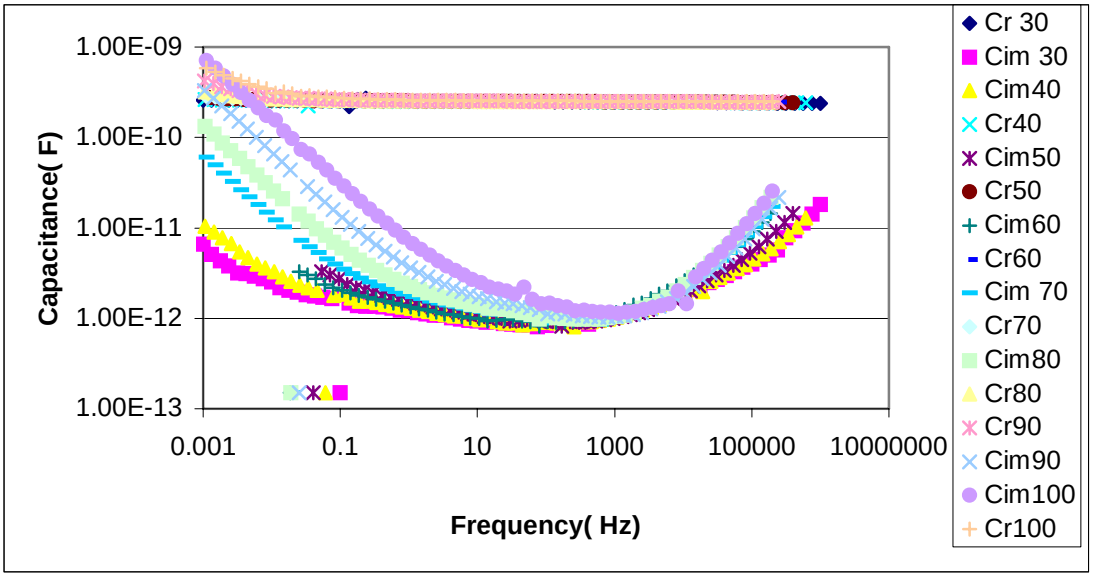

Figure 3.3. *Master plot for the composite material for the high frequency process, the β process. For real (upper) and imaginary (lower) parts of capacitance, for 8 temperatures from 30-100˚ C. This is for sample (4), aged for 35 day (at E=62.5kV/mm DC, T=15±5℃).*

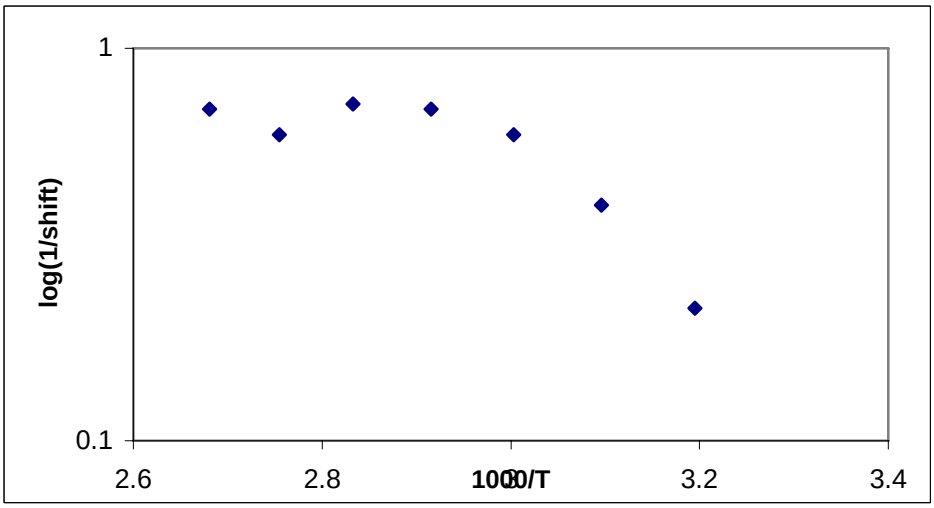

Figure 3.4 *plot for composite material plot associated with the high frequency β process. This for the sample (4), aged for 35 days (at E=62.5kV/mm DC, T=15±5℃). The activation energy is 0.3±0.05eV*

This is not a straight line so the process is not an Arrhenius process. This is could be due to a curing reaction while the sample under measurements due to high temperatures.

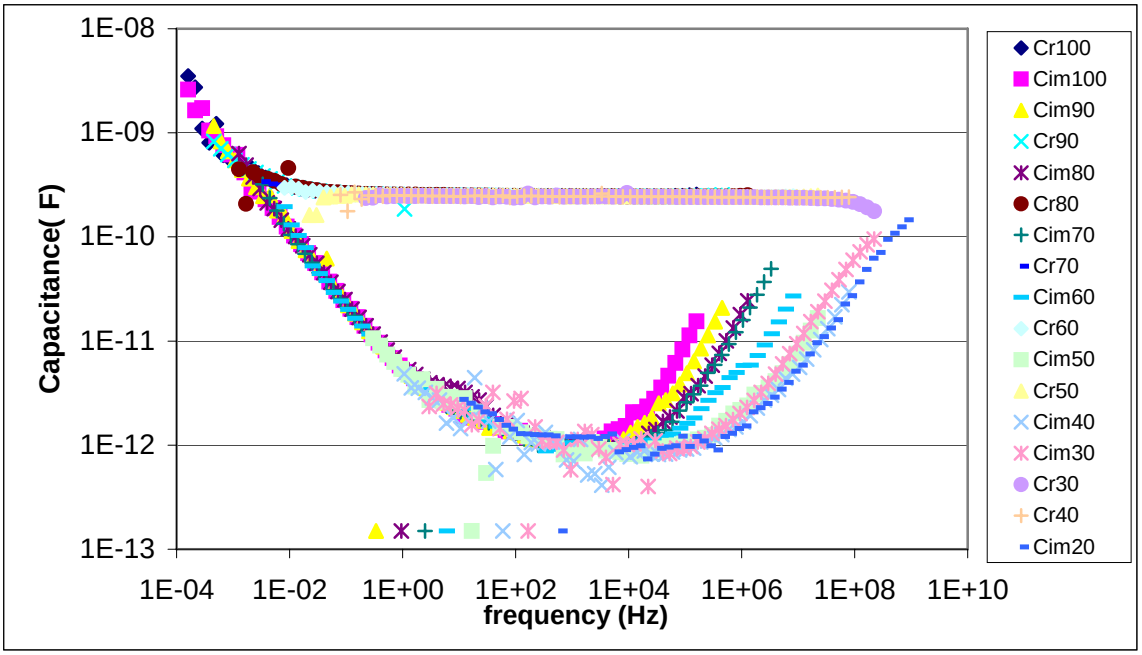

Figure 3.5. *Master plot for composite material for the low frequency process q-dc process. For real (upper) and imaginary (lower) parts of capacitance, for 9 temperatures from 20-100˚ C. This is for sample (4), aged for 87 days (at E=62.5kV/mm DC, T=15±5℃).*

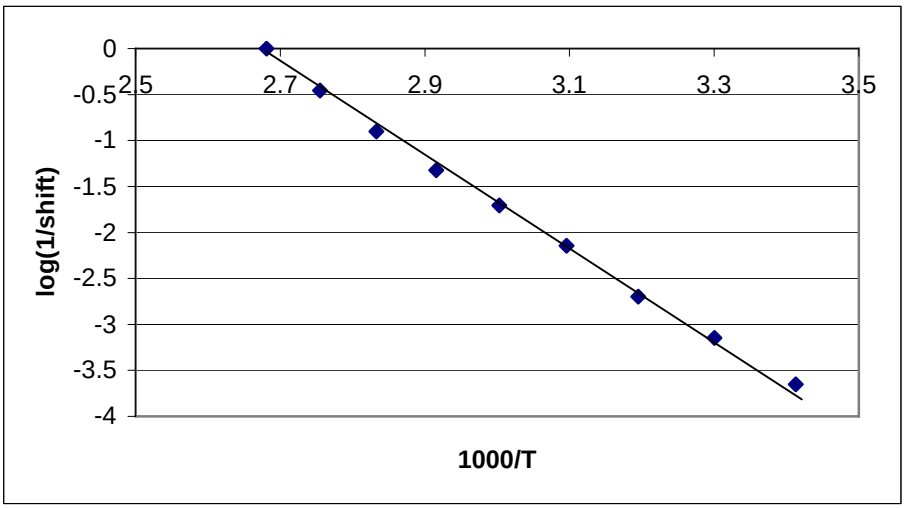

Figure 3.6. *Arrhenius plot for composite material plot associated with low frequency process, q-dc. This for the sample (4), aged for 87 (at E=62.5kV/mm DC, T=15±5ºC). The activation energy was calculated to be 1 ±0.05eV. The activation energy has not changed after 87 days ageing.*

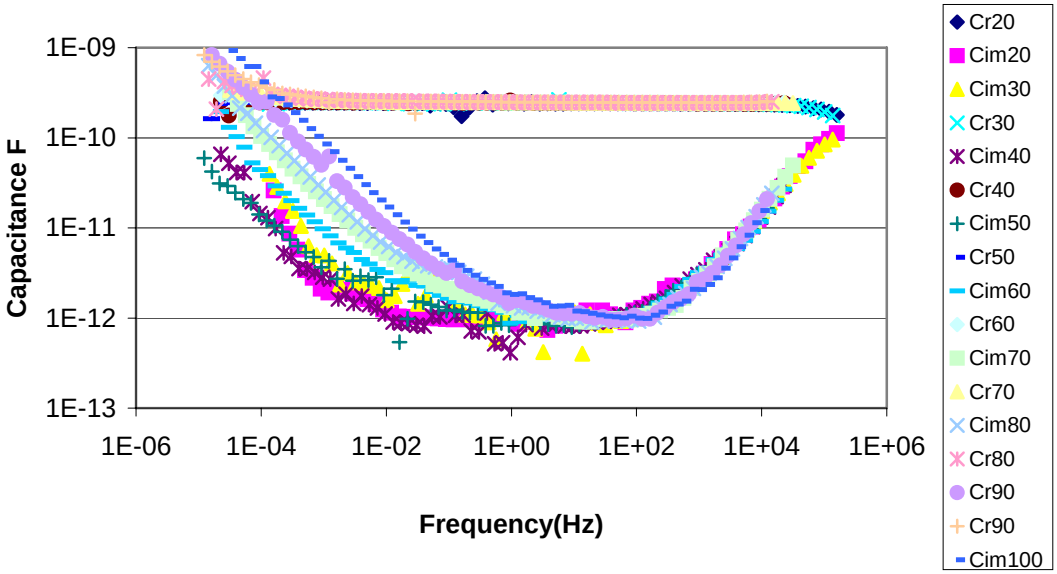

Figure 3.7. *Master plot for composite material for the high frequency β process. For real (upper) and imaginary (lower) parts of capacitance, for 9 temperatures from 20-100˚C. This is for sample (4), aged for 87 days (at E=62.5kV/mm DC, T=15±5ºC).*

The Arrhenius plot for β response above was found to be unreliable because it was not a straight line. The shape of the response was different to that observed in the un-aged samples and indicated an instrument problem in the high frequency range.

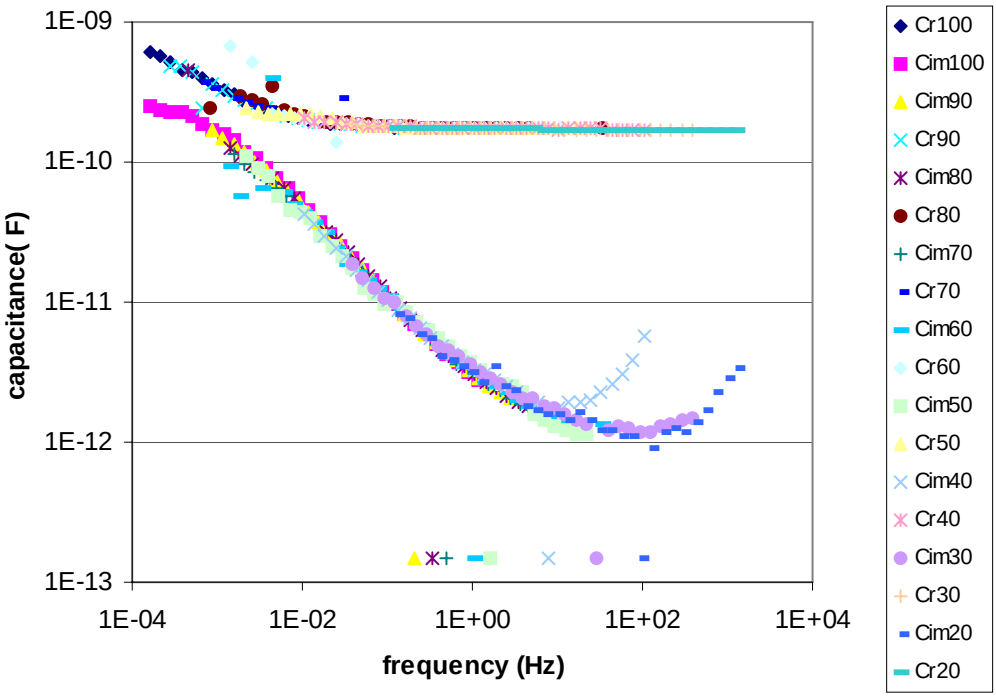

.

Figure 3.8 *Master plot for composite material for the low frequency process q-dc process. For real (upper) and imaginary (lower) parts of capacitance, for 9 temperatures from 20-100˚C. For failed sample (9) after 25 days (at E=50kV/mm DC, T=15±5℃).*

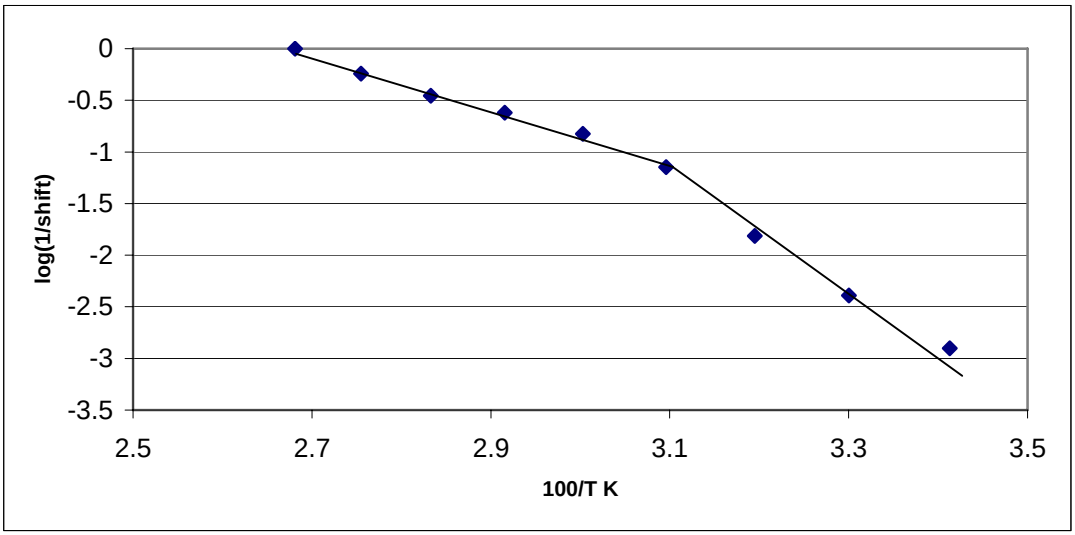

Figure 3.9 *Arrhenius plot for the composite material associated with low frequency process, q-dc. This is for failed sample (9) after 25 days (at E=50kV/mm DC, T=15±5℃).*

The results show there are two activation energies. One for low temperatures (below 50ºC) of 1.1±0.02 eV and one for high temperature (higher than 50ºC) of 0.53±0.02eV.

3.4.1.1 Overall comments on room temperature ageing results.

The response at low frequencies for different ageing periods shows a quasi –dc conductance see Figures (3.1,3.5,3.8,3.14,3.17). The activation energy of this process was calculated to be approximately 1.1eV see Figures (3.2,3.6,3.9,3.12,3.15,3.18). Figure 3.3 shows the master plot for the β peak with an activation energy of 0.3eV. The ageing has, therefore, not produced a change in the activation energy of the q-dc but increased the β process activation energy a little. The normalisation for the β process for the samples shown in Figure 3.7 was found to be unreliable. Figure 3.10, and Figure 3.11 show the results after ageing superimposed on those before ageing at (T=80,30 °C). The reason for choosing these temperatures is to see both processes (q-dc and β). There is a clear difference Between the two results, even though the activation energy is the same for the q-dc. The q-dc process has moved to higher frequencies indicating that the pre-exponential factor has increased, possibly because there are more carriers moving. In the case of the β-response the process has shifted to lower frequencies, see Figure (3.3).

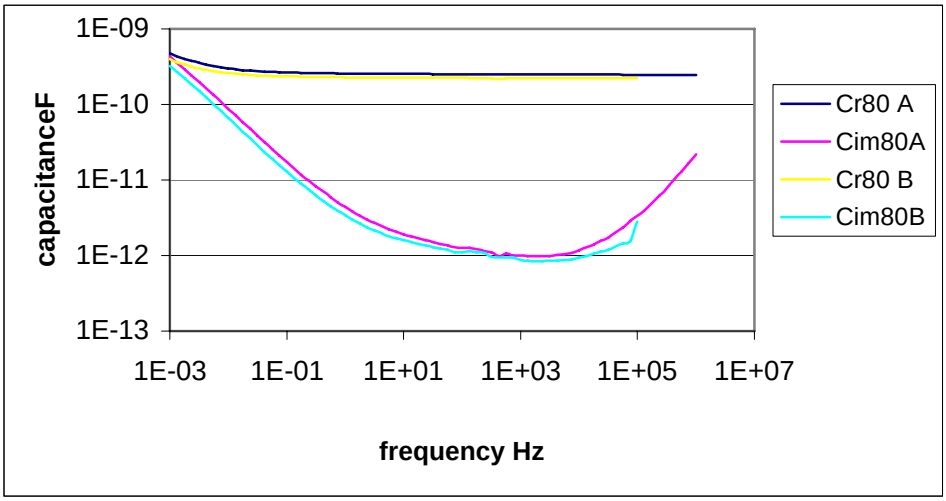

Figure 3.*10* *The real and imaginary capacitance at 80°C. (A stands for after ageing, and B for before Ageing).*

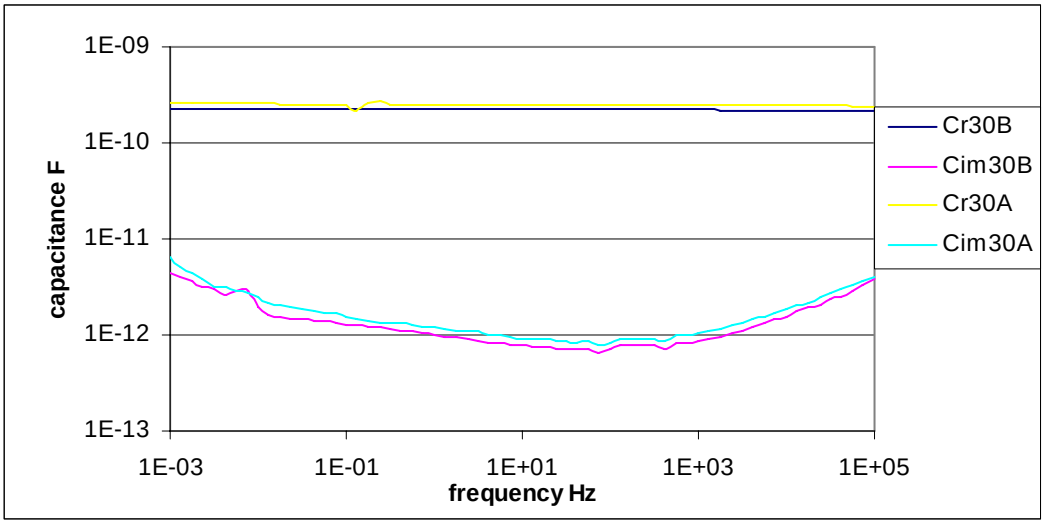

Figure 3.*11* *The real and imaginary capacitance at 30°C. A stands for after ageing, and B for before Ageing.*

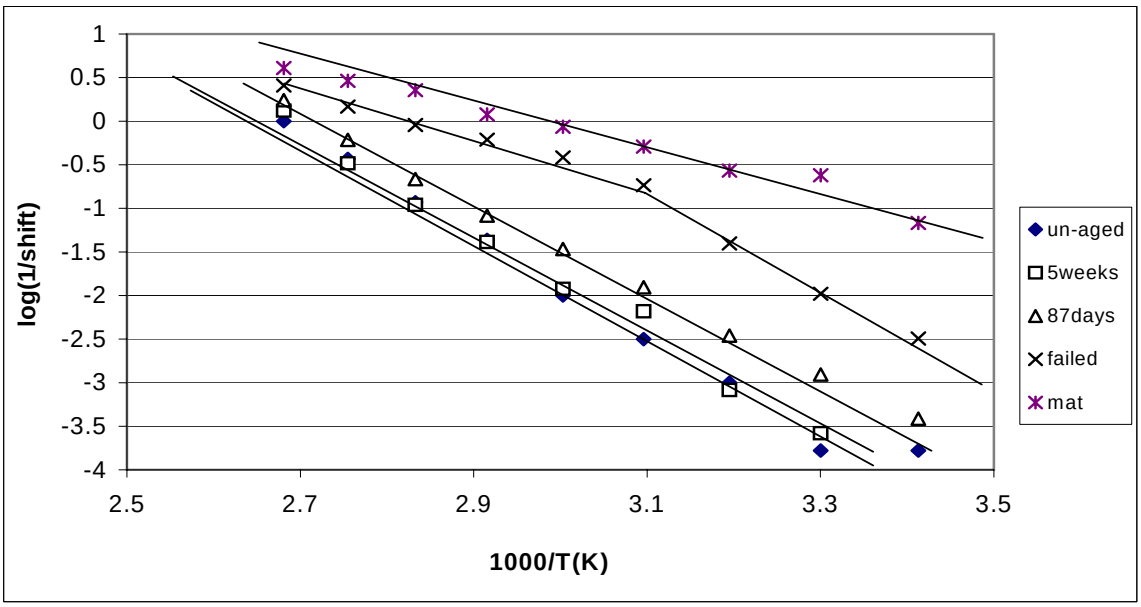

Figure 3.12. *Arrhenius plots of dielectric q-dc response in a range of samples as shown .See key for notation. This data was located by choosing a temperature and a frequency and referenced the q-dc of each sample to one another at that temperature and frequency.*

It can be seen from Figure 3.12 that except for the high temperature region of the failed sample, the activation energy has not changed with ageing. There is, however, a displacement towards higher frequencies, i.e. the process moves towards the behaviour observed on the fibre mat alone. This is even more marked in the failed sample where the activation energy changes at high temperatures to a value (0.53eV) close to that of the mat.

3.4.2 Results for samples aged at 90˚C.

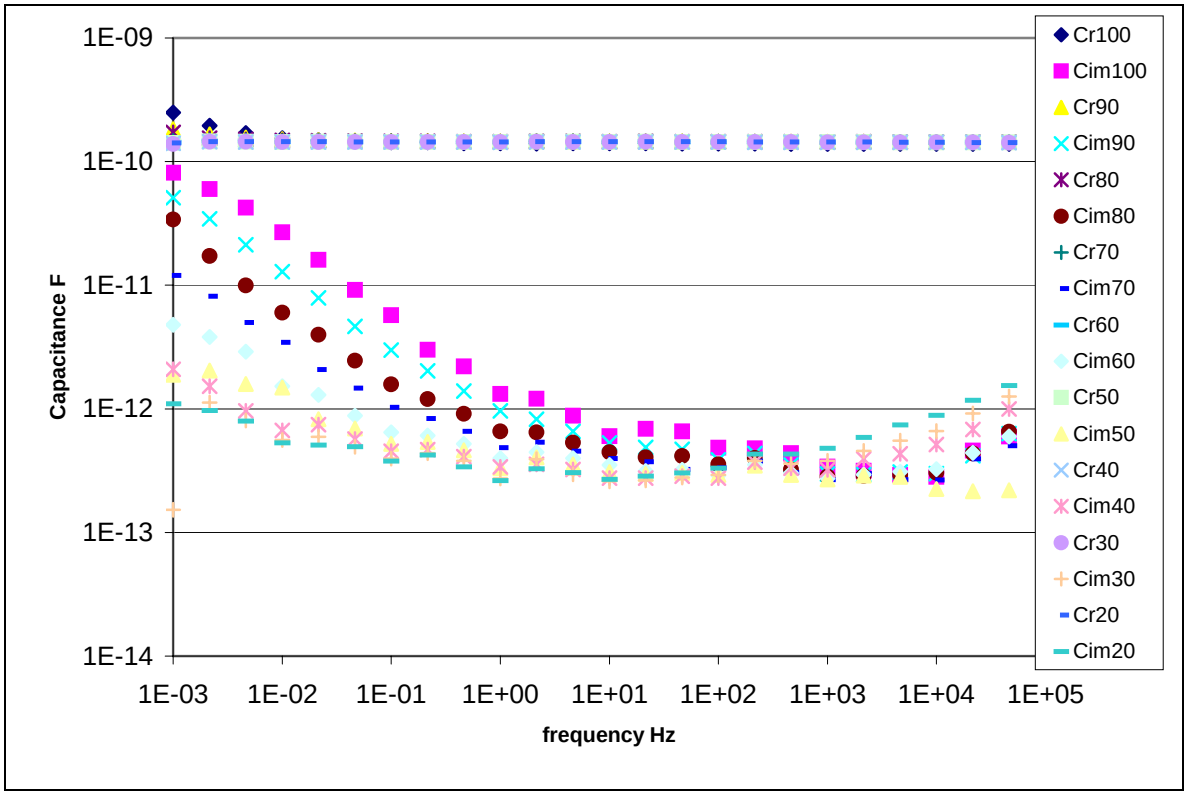

Figure 3.13. *The real and imaginary part of the capacitance against frequency for the composite material for the low frequency process, q-dc process. For real (upper) and imaginary (lower) parts of capacitance, for 9 temperatures from 20-100˚C. This is for sample (10) that was aged for 237 days (at T = 90˚C and E=25kV/mm).*

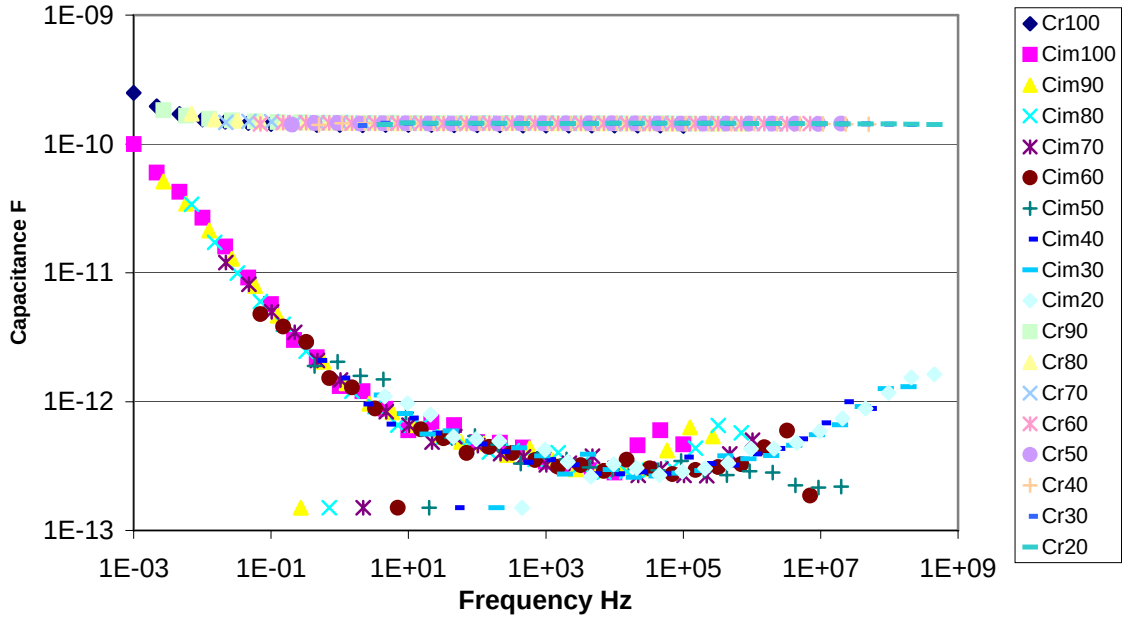

Figure 3.14. *Master plot of the low frequency process q-dc for the composite material. For real (upper) and imaginary (lower) parts of capacitance, for 9 temperatures from 20-100˚C. This is for sample (10) that was aged for 237 days (at T = 90˚C and E=25kV/mm).*

The β process for this sample could not be normalised.

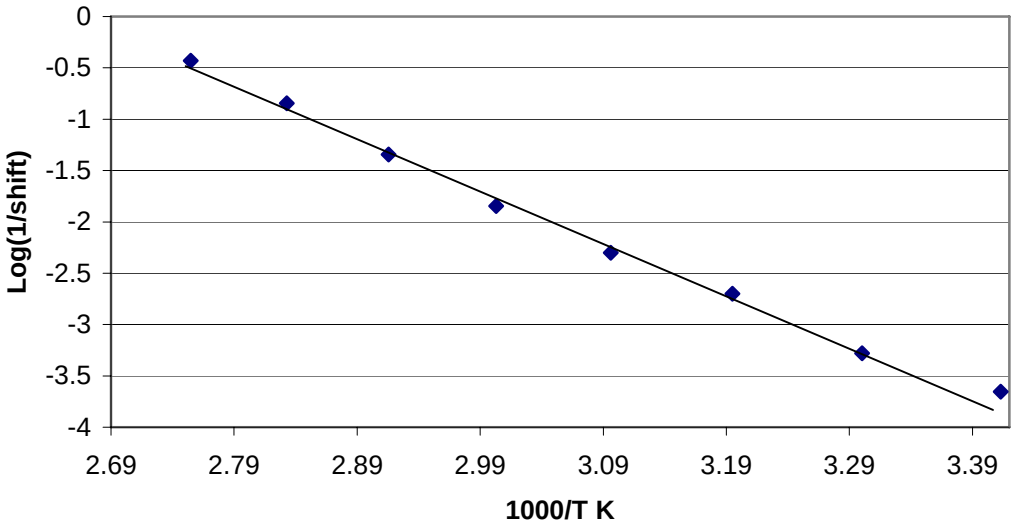

Figure 3.15. *Arrhenius plot for composite material plot associated with low frequency process. This is for sample (10) that was aged for 237 days (at T = 90˚C and E=25kV/mm). The activation energy is 1.05±0.03 eV.*

There is a small decrease in the activation energy compare to the un-aged sample, 1.1±0.02 eV.

3.4.3 Thermal Ageing

The results in the previous section show the effect of ageing on the dielectric response on samples that were aged electrically at room temperature and electro-thermally at 90˚C. It was necessary to investigate the effect of thermal ageing alone on the dielectric response. Two samples were aged in the oven at 90˚C for 237 days. The dielectric results are shown in Figure 3.16.

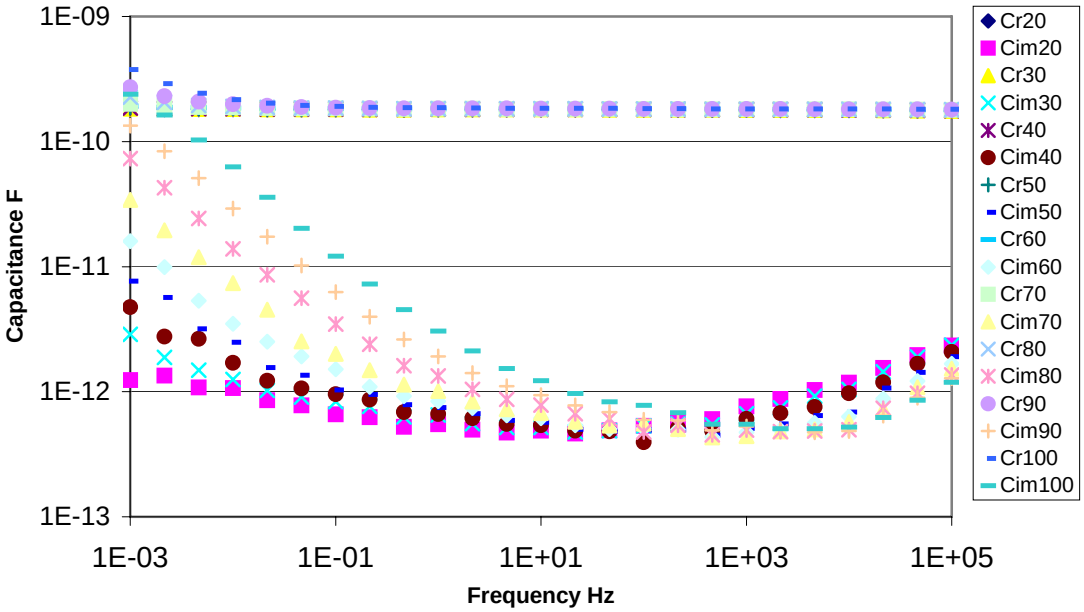

Figure 3.16. *The real and imaginary part of the capacitance against frequency for the composite material for the low frequency process, q-dc process. For real (upper) and imaginary (lower) parts of capacitance, for 9 temperatures from 20℃ -100℃. This is for sample (19) that was aged for 237 days (at T = 90˚C and E= 0kV/mm).*

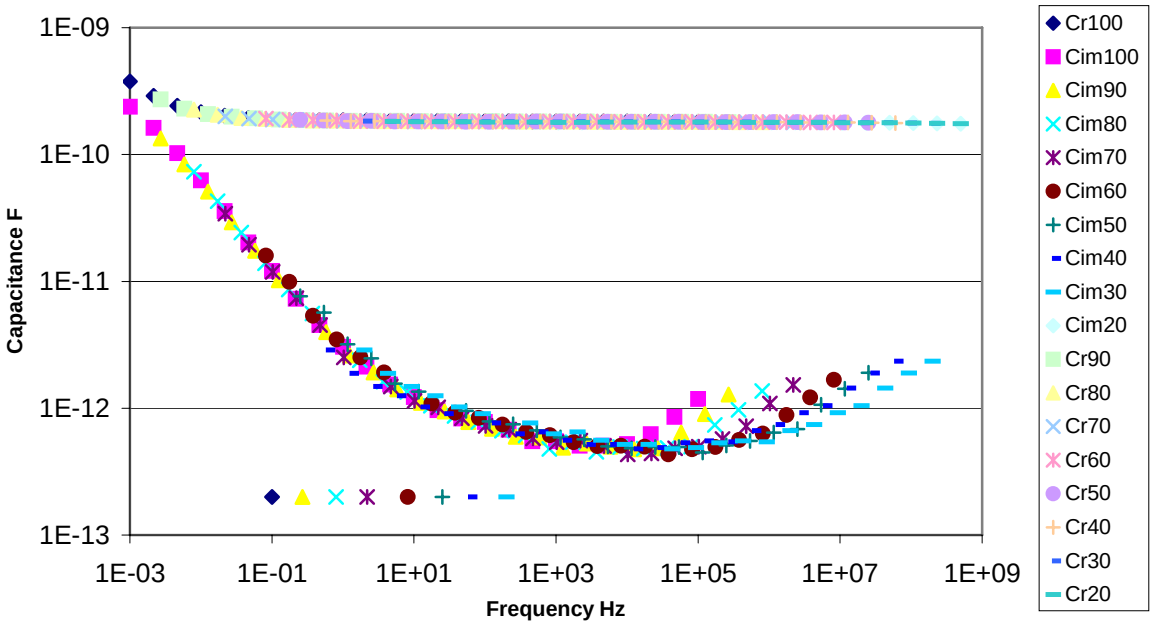

Figure 3.17 *Master plot of the low frequency process q-dc for the composite material. For real (upper) and imaginary (lower) parts of capacitance, for 9 temperatures from 20-100˚ C. This is for sample (19) that was aged for 237 days (at T = 90˚C and E= 0kV/mm).*

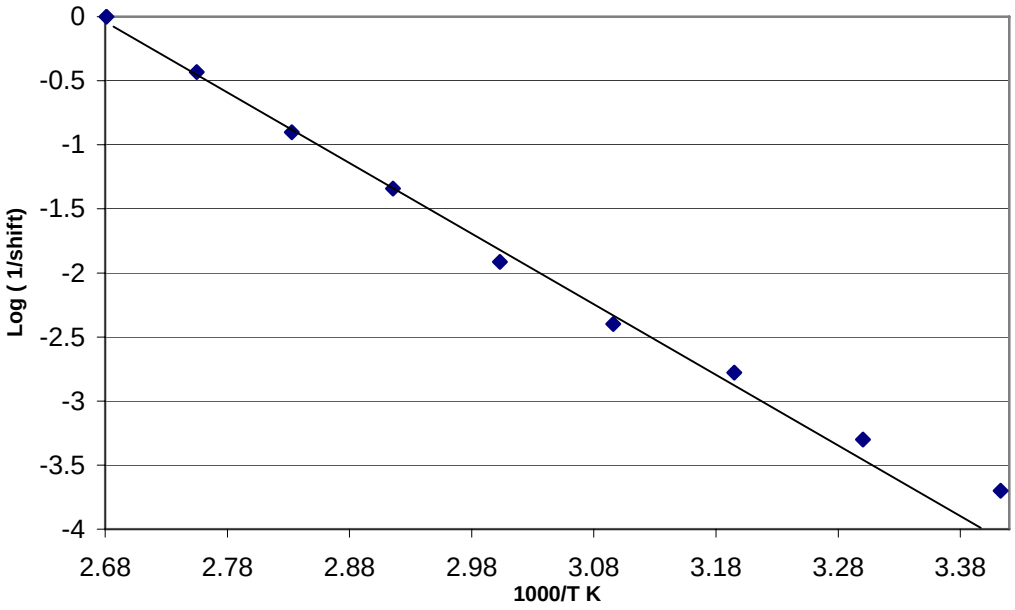

Figure 3.18 *Arrhenius plot for composite material plot associated with low frequency process. This is for sample (19) that was aged for 237 days (at T = 90˚C and E= 0kV/mm). The activation energy is 1.1±0.02eV*

The activation energy is exactly the same as that of the un-aged sample.

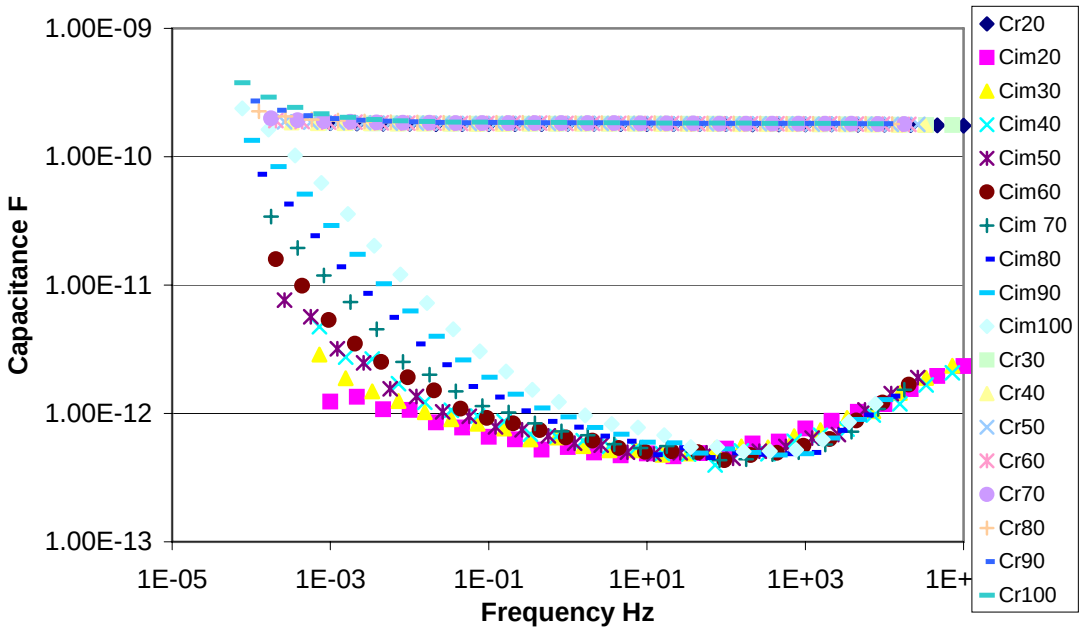

Figure 3.19. *Master plot for composite material for the high frequency β process. For real (upper) and imaginary (lower) parts of capacitance, for 9 temperatures from 20-100˚ C. This is for sample (19) thermally aged for 237 days (at E= 0 DC, T= 90ºC).*

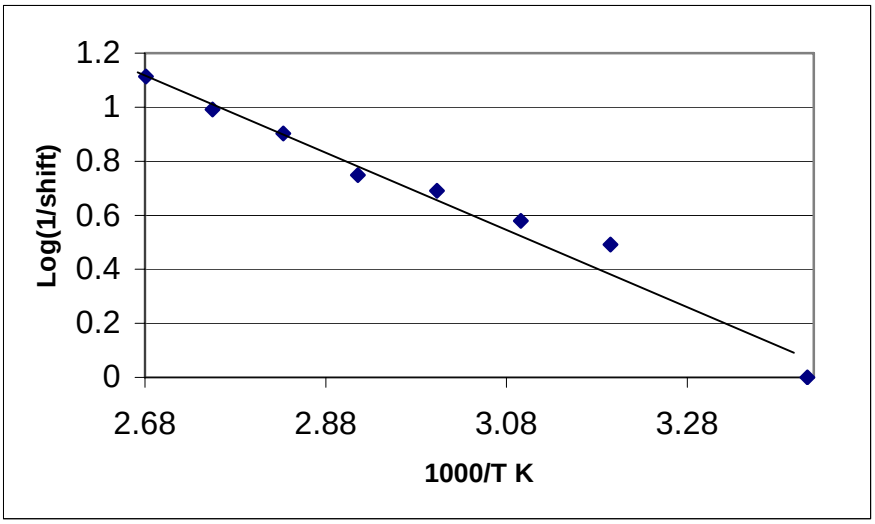

Figure 3.20. *Arrhenius plot for composite material plot associated with high frequency process. This is for sample (19) that was thermally aged for 237 days (at T = 90˚C and E= 0kV/mm). The activation energy is 0.31eV. This is the same as the unaged material.*

The activation energy is bigger than that observed in the un-aged material of 0.3±0.03 eV.

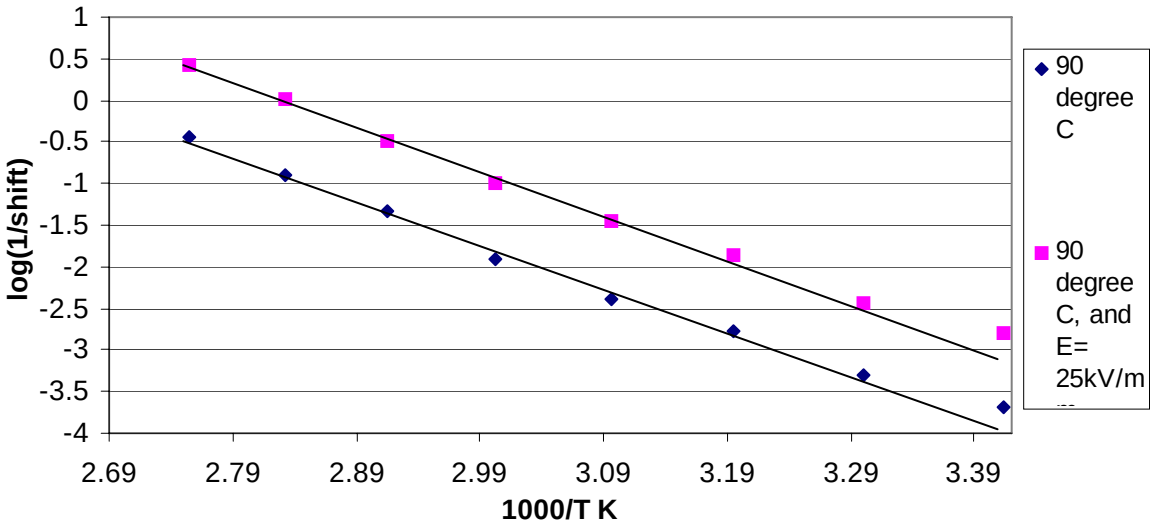

Figure 3.21. *Activation energy of dielectric q-dc response for two aged samples as shown. See key for notation. The two samples were aged under identical thermal conditions. One sample was subjected to 25kV/mm and the other 0kV/mm.*

It can be seen from this plot that, the activation energy has not changed with ageing for either sample. There is, however, a displacement towards higher frequencies in the electrically aged sample compared with the only thermally aged sample.

The results can be summarised in the following table.

	A	B	C
q-dc activation energy eV	1.05±0.03	1.1 ±0.02	1.1 ±0.02
β- process activation energy	Could not be normalised	0.31 ±0.04	0.28±0.03
Shift in frequency Compare to un-aged sample.	Shifted to higher frequency	Did not shift	-

Table 3.2

A: Sample aged for 237 days at 25kV/mm and 90 °C
B: Sample aged for 237 days only thermally at 90 °C
C: Un-aged Sample

3.5 SEM Analysis:

One sample (sample number 9) shows a breakdown in the sample volume. Investigating the breakdown under the optical microscope shows breakdown all the way through the sample, it also shows very thin black lines near the breakdown but perpendicular to the field direction. Such lines were not observed in the unaged samples. SEM was used to investigate the nature of these black lines since we could not focus on them by the optical microscope

Figure 3.22 shows a view of a black line from above and there is little to see. Figure 3.23 shows a clearer view of such a line. The line can be seen to be a 2.5μm void running alongside the glass fibre for millimetres. Figure 3.24 shows an elemental analysis obtained on a sample prior to ageing using an SEM. The carbon peak is quite strong, as are peaks associated with the elemental content of the glass fibres (e.g. Si, Ca, Al). The same analysis taken around the 'black line' in the failed sample, Figure 3.25, shows a strong reduction of the carbon peak with respect to the aluminium peak. This indicates that the black lines are <u>not</u> carbonised tracks such as may be produced by partial discharges.

Figure 3.26 and Figure 3.27 show the elemental analysis of glass and pure epoxy respictivly.

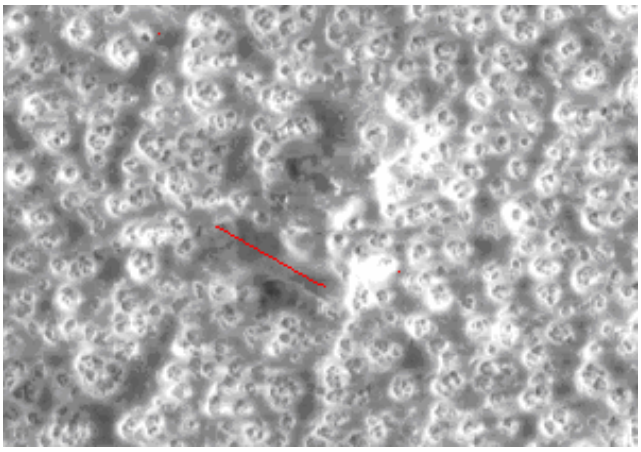

Figure 3.22. *Shows the area near a black line that is indicated by the bar.*

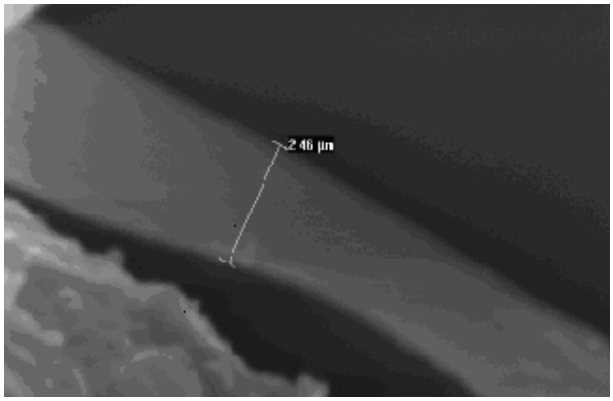

Figure 3.23 *Shows the voids (black lines) between the fibres and epoxy. The white line is 2.46 µm long*

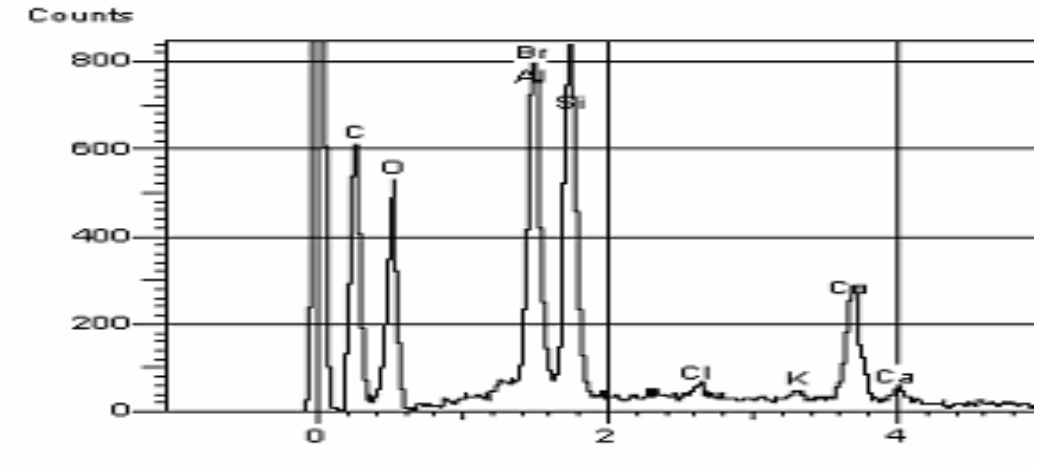

Figure 3.24. *Elemental analysis of un-aged composite material (cps vs. keV).*

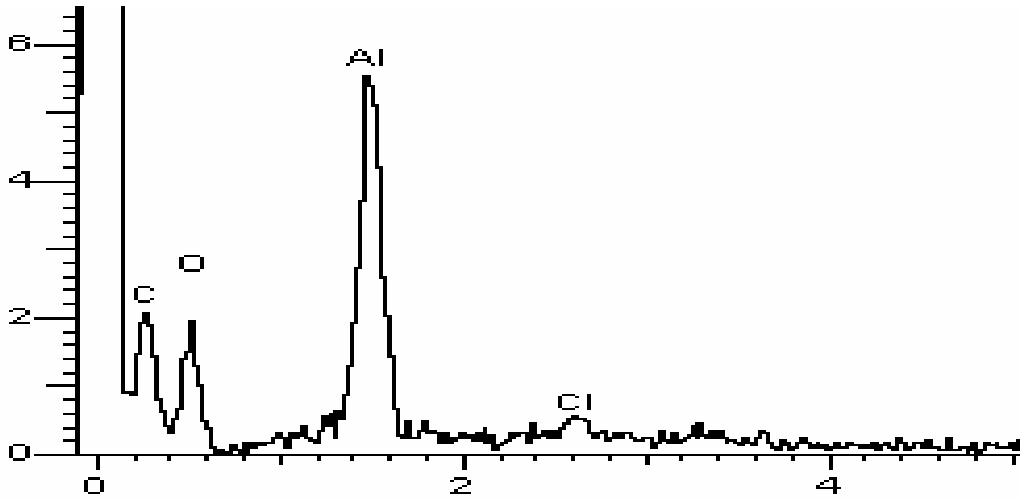

Figure 3.25. *Elemental analysis of black line region (cps vs keV).*

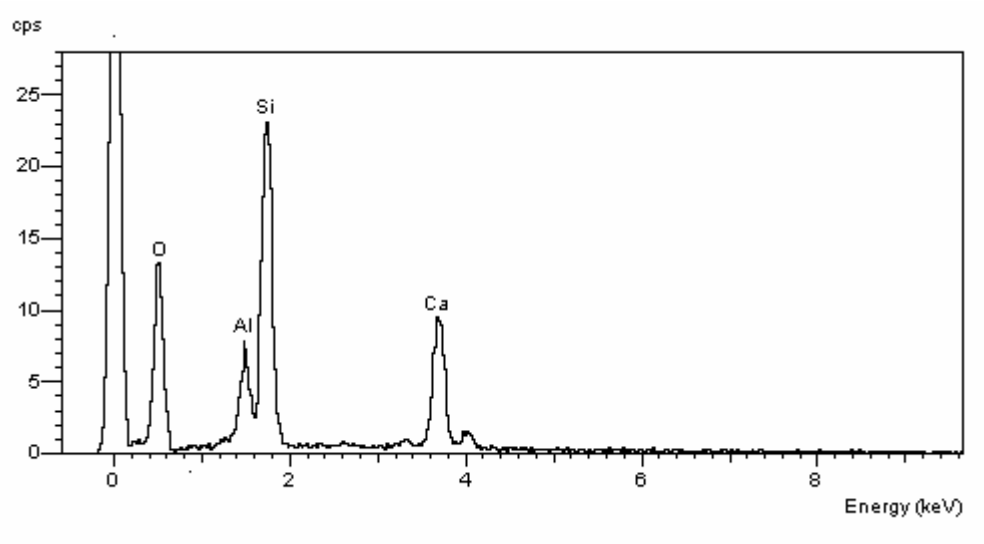

Figure 3.26. *Shows elemental analysis of glass.*

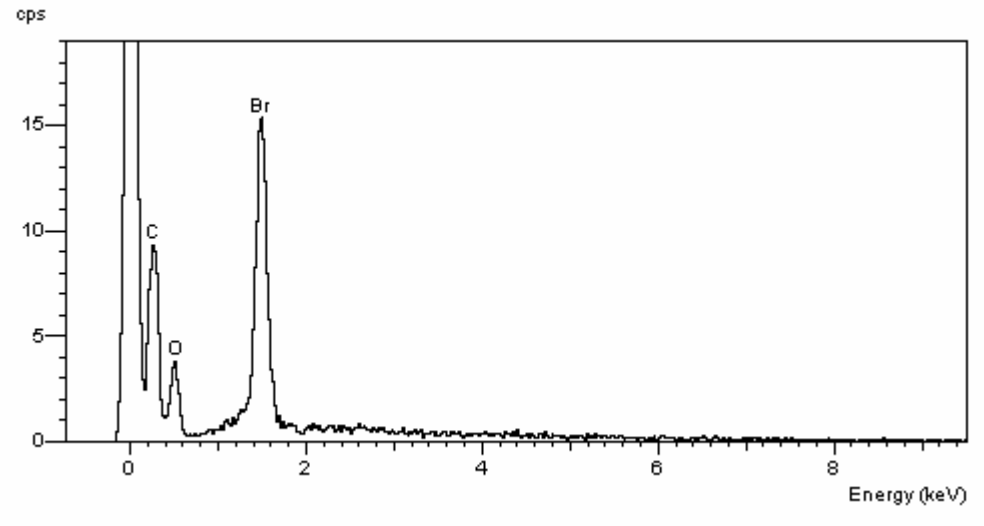

Figure 3.27. *Shows elemental analysis of pure epoxy*.

3.6 Space Charge Experiment Using PEA

PEA experiments were carried out on the aged composite material samples at (20 and 30) kV/mm and temperatures [40 and 60]ºC. The sample was subjected to the field for 3 hours at each temperature with the signal being measured at a number of selected times.

The purpose of the experiment is to investigate the existence of space charge in the material under high DC fields, and to characterise its high field behaviour after ageing.

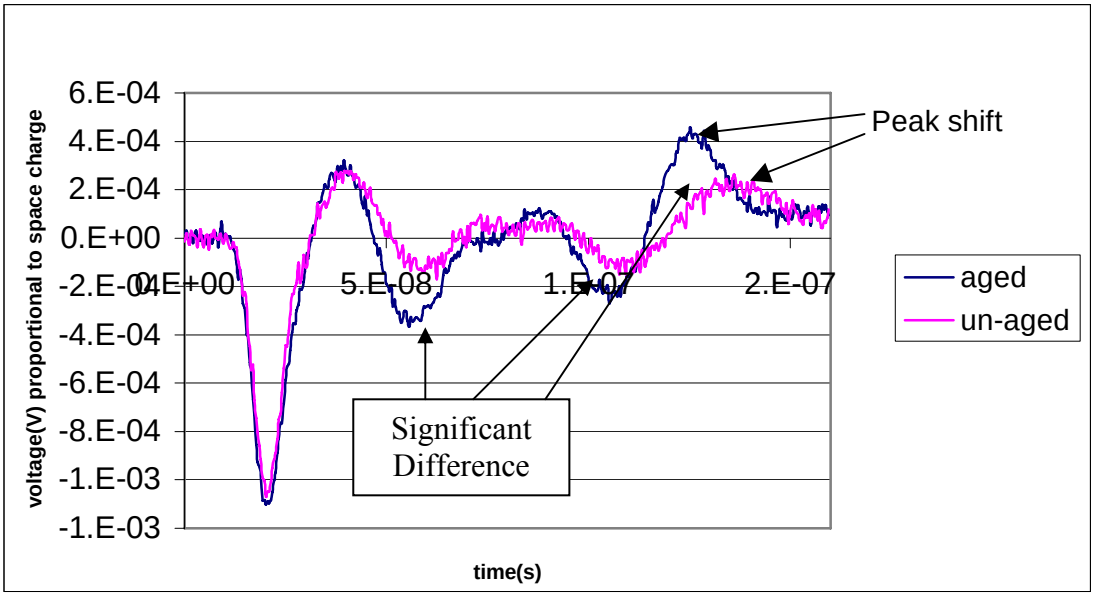

Fig 3.28. *It shows a comparison between PEA for aged and non-aged material for E=30kV/mm and T= 60ºC for 140 minutes. The measurements were taken under identical conditions.*

The results show a very significant difference from that of the un-aged material. There is more charge (space charge) on the interface between the glass and the epoxy. Fig 3.28 shows the difference very clearly. There is a clear shift of the bottom electrode peak of 11ns.

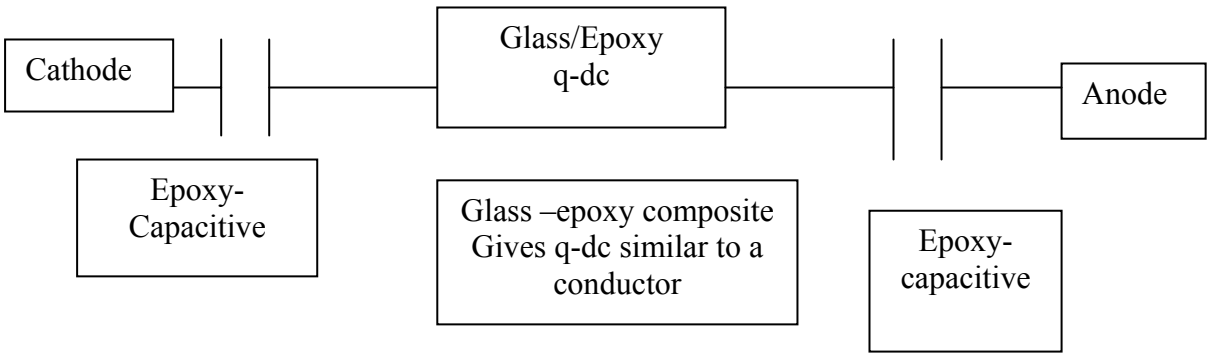

Figure 3.29. *The aged material thought of as two capacitor with a resistor in between in a series configuration*.

On ageing the q-dc gets faster, consequently the charge separation in the glass region gets bigger at a given time. The PEA for the aged sample shows an increase in the space charge.

Figures 3.30 to 3.37 shows results from sample (10) aged at (T =90 ºC, E =25kV/mm) for 87 days

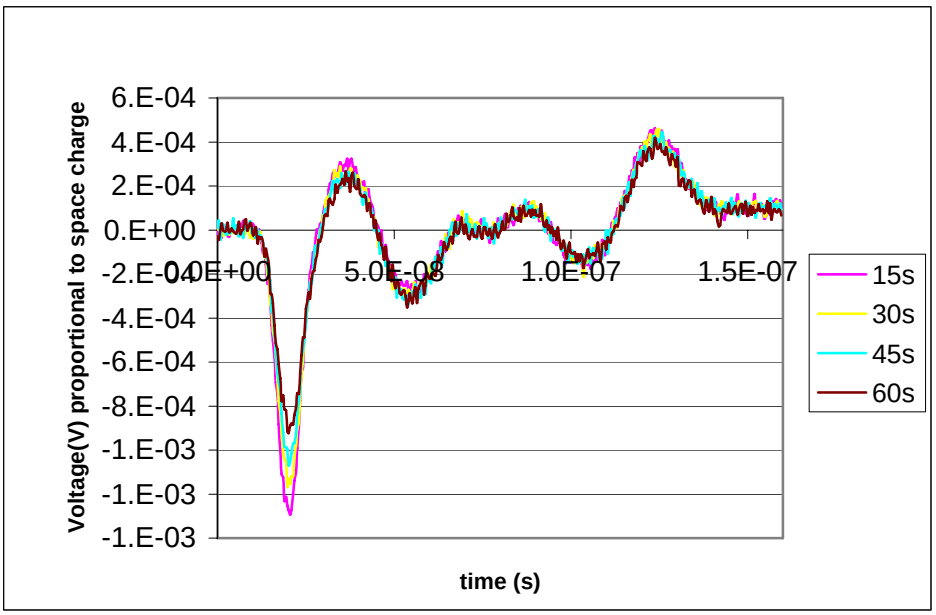

Figure 3.30. *Space charge measurements for 60s, at E=20kV/mm and T=40˚C .*

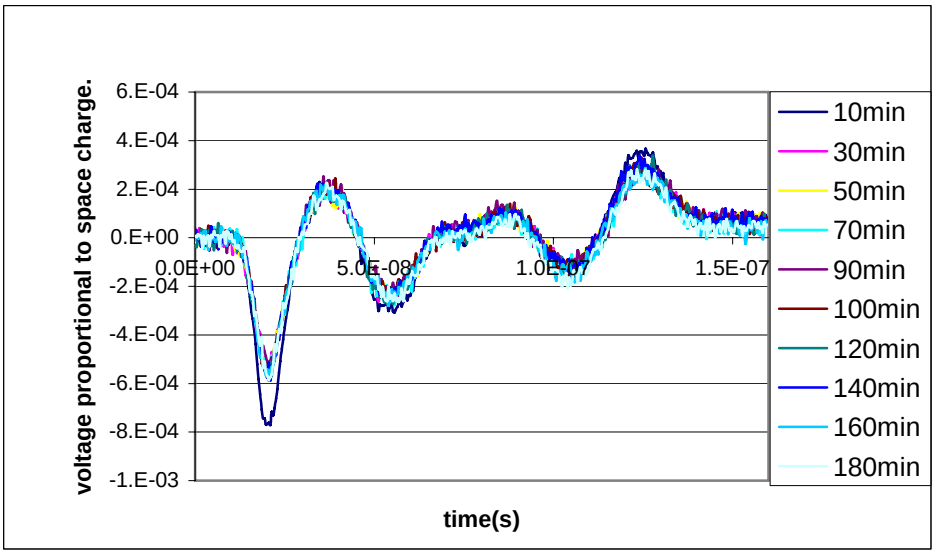

Figure 3.31. *Space charge measurements for180min, at E=20kV/mm and T=40˚C.*

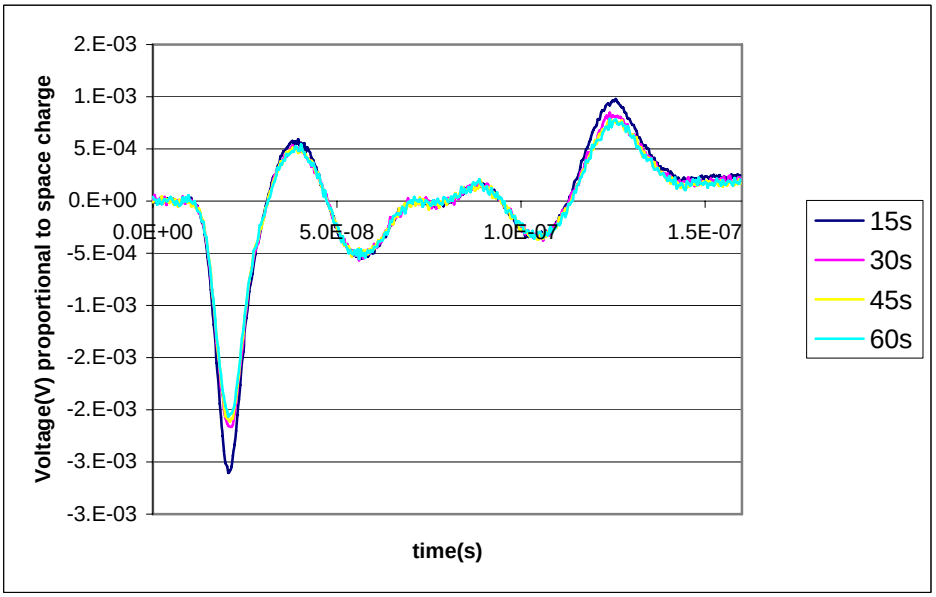

Figure 3.32. *Space charge measurements for 60s, at E=30kV/mm and T=40˚C.*

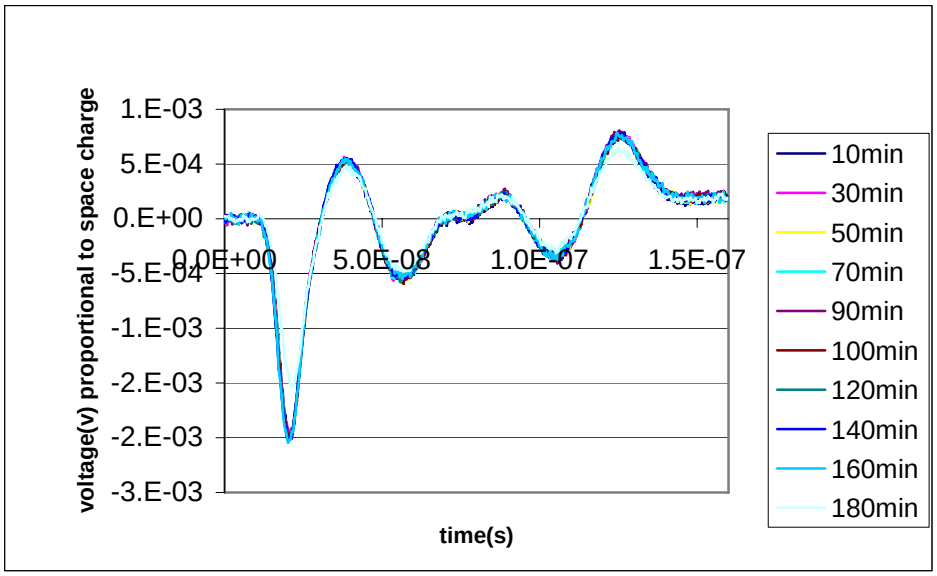

Figure 3.33. *Space charge measurements for 180min, at E=30kV/mm and T=40˚C.*

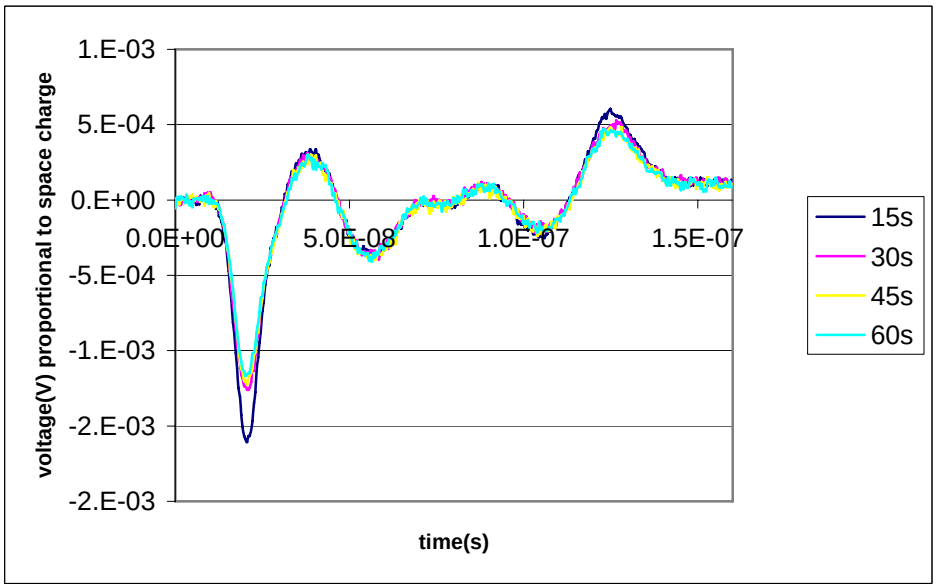

Figure 3.34. *Space charge measurements for 60s, at E=30kV/mm and T=60˚C.*

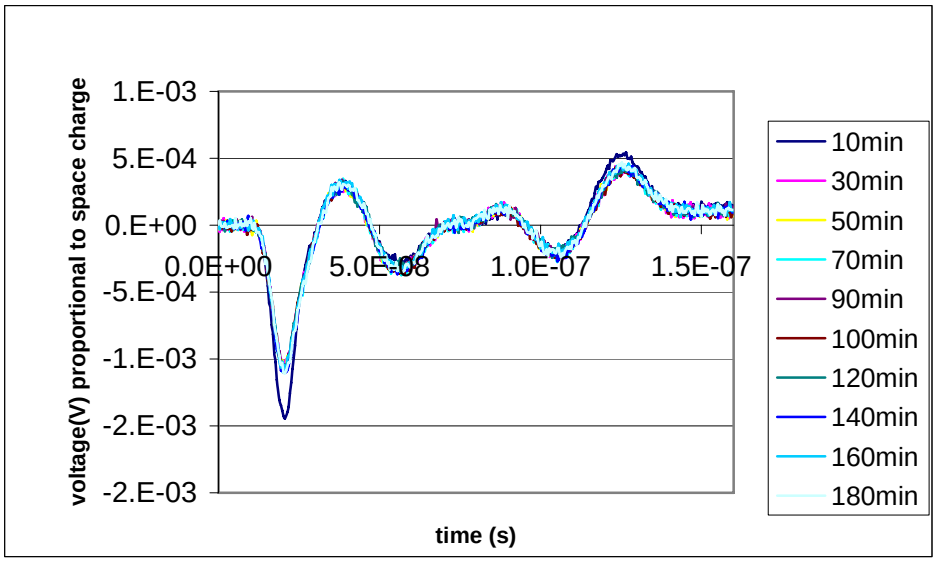

Figure 3.35. *Space charge measurements for 180min, at E=30kV/mm and T=60˚C.*

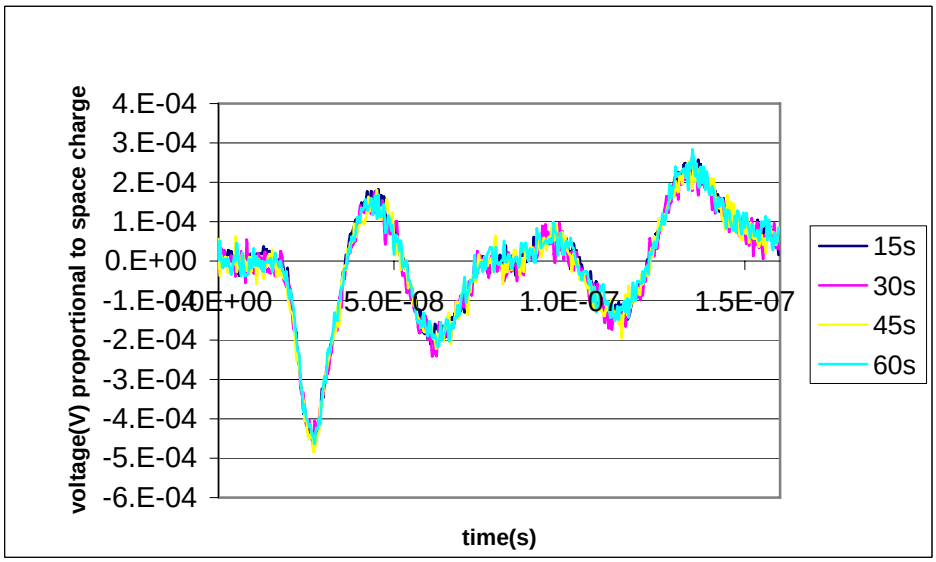

Figure 3.36. *Space charge measurements for 60s, at E=20kV/mm and T=60˚C.*

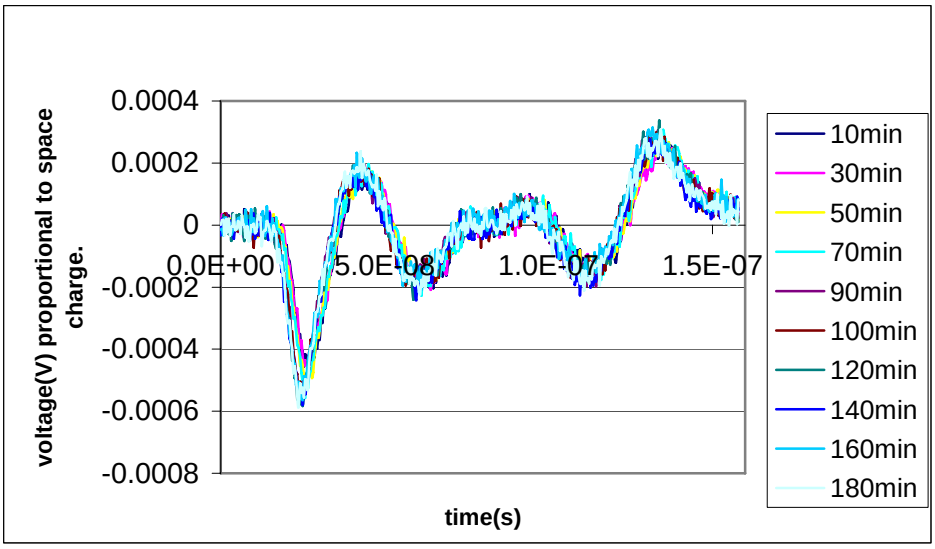

Figure 3.37. *Space charge measurements for 180, at E=20kV/mm and T=60˚C.*

The results show that there is a large amount of hetero-charge at both electrodes that can be seen on the first measurement after voltage application. This is similar to the results obtained for the unaged material in 2.5.2.

The difference is that in this case the hump corresponding to space charge is bigger.

PEA signal features of the aged samples at 40 °C and 60°C and at fields of 20kV/mm and 30kV/mm are summarized in the following tables.

Peak magnitude at field / Peak	20kV/mm	30 kV/mm	
1	-1.27	-2.1	$*10^{-3}$
2	3.23	4.7	$* 10^{-4}$
3	-2.83	-4.5	$* 10^{-4}$
4	0.93	1.9	$* 10^{-4}$
5	-1.19	-3.7	$* 10^{-4}$
6	3.82	7.3	$* 10^{-4}$

Table 3.3

The peaks clearly increased with increasing the applied field. The magnitude of the peak before reflection, peak 1 and peak 2 directly proportional to the field. The field at 20kV/mm is 2/3 of that at 30kV/mm

Peak position at field / Peak	20kV/mm	30kV/mm	
1	20.09	20.09	* 10^{-9}
2	30.70	39.8	* 10^{-9}
3	50.52	57.2	*10^{-9}
4	80.66	89.8	*10^{-9}
5	100.24	100.5	* 10^{-9}
6	120.24	127	*10^{-9}

Table 3.4

The peaks position did vary a little. The PEA system was serviced after the measurements on the un-aged sample. This is could explain this slight variation in the peak position.

PEA signal features at 60 °C

Peak magnitude at field / Peak	20 kV/mm	30kV/mm	
1	-5.5	-13.5	*10^{-4}
2	2.3	2.9	*10^{-4}
3	-2.2	-3.	*10^{-4}
4	0.91	1.2	*10^{-4}
5	-1.8	-1.9	*10^{-4}
6	3.1	5.0	*10^{-4}

Table 3.5

Peak position at field / Peak	20kV/mm	30kV/mm	
1 in 10^{-9}	25.0	22	* 10^{-9}
2 in 10^{-9}	42.7	40	*10^{-9}
3 in 10^{-9}	60.0	58	* 10^{-9}
4 in 10^{-9}	93.60	89.8	* 10^{-9}
5 in 10^{-9}	112.0	107	* 10^{-9}
6 in 10^{-9}	130.21	127	* 10^{-9}

Table 3.6

Comparing the results for 40 °C and 60 °C for constant field, it is clear the magnitude of the peaks decreases with increasing temperature. At higher temperature the charge carriers have more energy to move and recombine.

3.7 Differential Scanning Calorimetry (DSC):

Differential Scanning Calorimetery was used to investigate the effect of ageing on glass transition temperature.

The samples were aged at (room temperature, 37.5kV/mm) for 168 days and (90ºC, 25kV/mm) for 208 days.

The results are shown in Figure 3.38 to 3.42

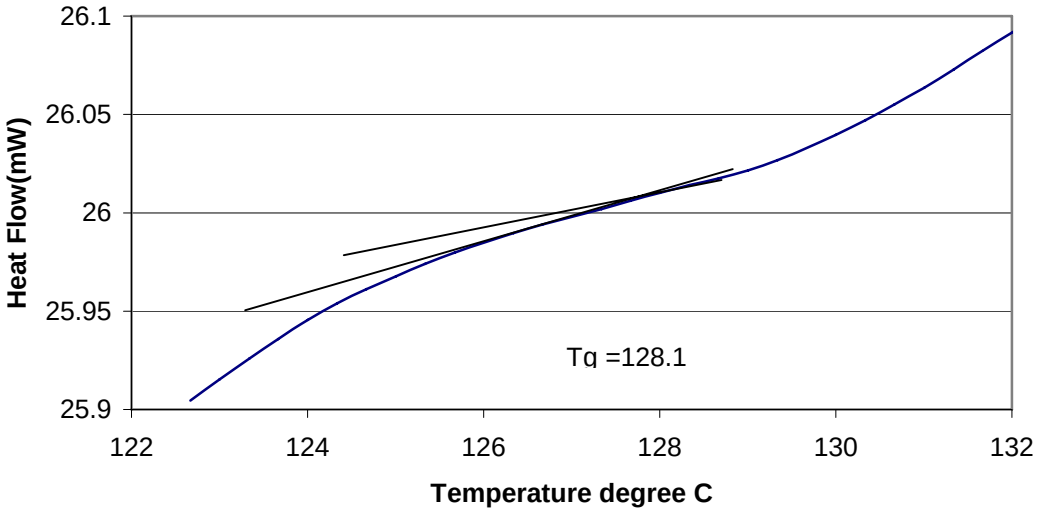

Figure 3.38. *A temperature scan of sample (6) aged at (room temperature, 37.5kV/mm) for 168 days. Glass transition temperature is 128.1˚C.*

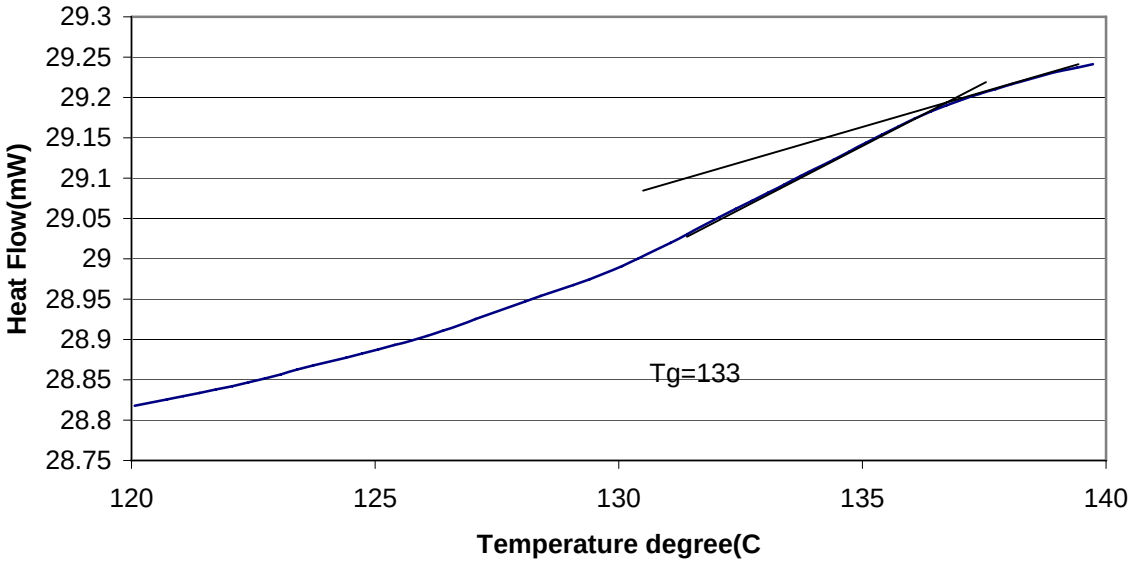

Figure 3.39. *A temperature scan of sample (6) aged at (room temperature, 37.5kV/mm) for 168 days. Glass transition temperature is 133˚C.*

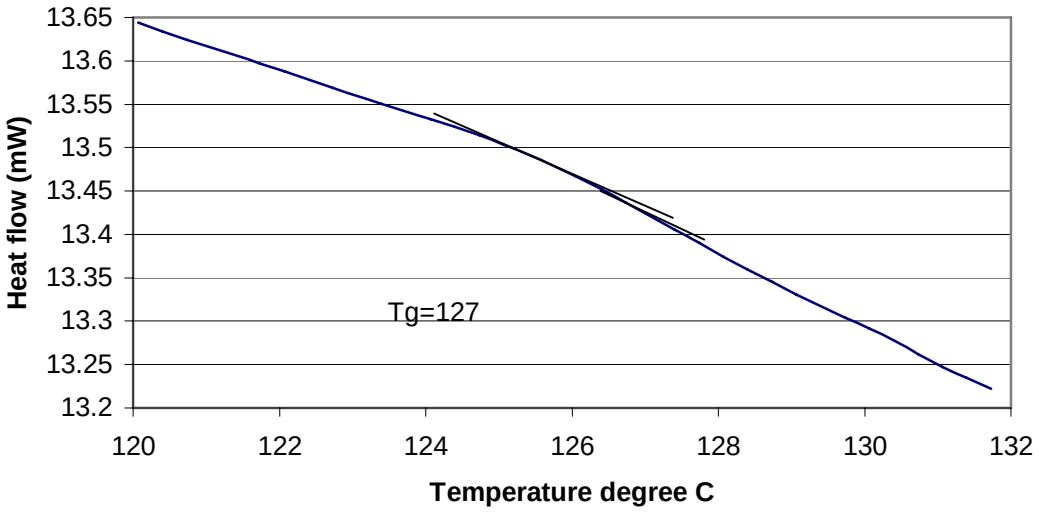

Figure 3.40. *A temperature scan of sample (12) aged (at 90˚C, 25kV/mm) for 208 days. Glass transition temperature is 127˚C.*

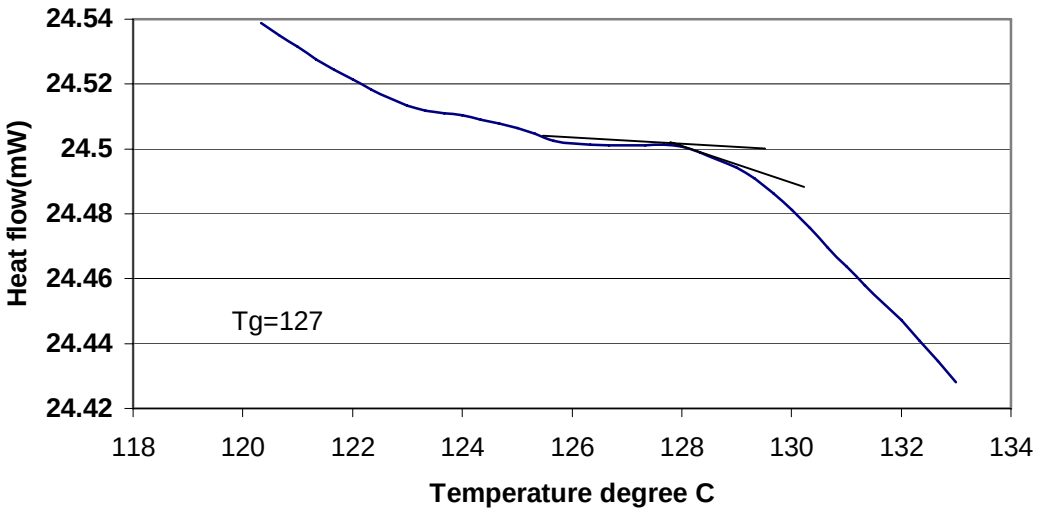

Figure 3.41. *A temperature scan of sample (12) aged (at 90˚C, 25kV/mm) for 208 days. Glass transition temperature is 127˚C.*

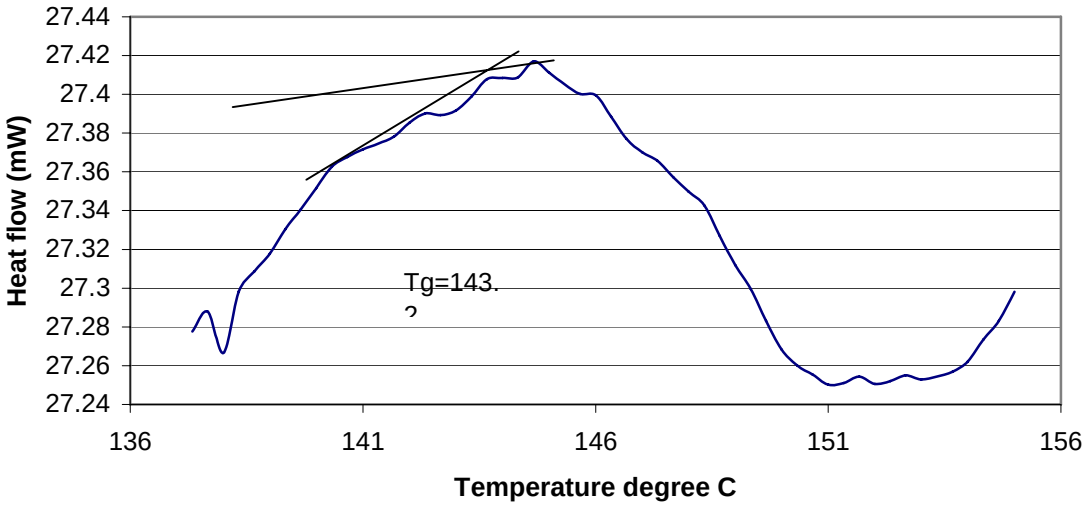

Figure 3.42. *A temperature scan of sample (19) aged (at 90˚C, E=0kV/mm) for 237days. Glass transition temperature is 143.2˚C*

The results show very clearly that the glass transition temperature has moved down with electrical ageing. This is a clear indication that electrical ageing is changing the morphology of the material. Thermal ageing has increased the glass transition temperature. This may be due to the effect of post curing.

A: Sample (6) aged at room temperature for 168 days at 37.5kV/mm
B: Sample (12) aged at 90°C, and 25kV/mm for 208days.
C: Sample (19) aged at 90°C, and 0kV/mm for 237 days
D: un-aged sample.

	A	B	C	D
Glass transition Tg °C	128.1	127	143.2	138.1

Table 3.3

CHAPTER 4
DISCUSSION

A wide range of experiments has been performed to characterise the material before and progressively through ageing as reported in chapter 2 and chapter 3. In this discussion, an attempt will be made to analyse these experimental results so that valid deductions can be made concerning the effect of high electric field on epoxy /glass fibre composite material. The evidence relating to the processes that go on inside the material will be examined in order to fundamentally understand the cause and effect of these processes. The dielectric response obtained for the system will be represented by the Dissado and Hill model [1]. The effect of ageing on space charge were determined. The change in dielectric, mechanical, and thermal response will be determined as a function of ageing. The main contention in this thesis is that ageing causes delamination between the glass fibre and epoxy resin. Throughout this discussion evidence from dielectric, space charge, DSC, DMA, and SEM will be used to deduce facts concerning the system that will be used to support this contention.

4.1 Dielectric Response

The relative permittivity of the composite material ε_r was calculated to be 4.8 in frequency range (10-100)Hz, the manufacturing specification is 4.4 at 1MHz.The difference between the calculated value and the manufacturing specification value is due to the fact that both measurements were taken at different frequencies. The relative permittivity goes down as the frequency goes up. This is due to the fact that at higher frequencies it is not possible for the polarised molecule to make their full contribution to the total polarisation, which reduces the permittivity [2].

The dielectric response of the composite material has shown a q-dc process in the low frequency region. The process follows the constant angle phase (CPA) behaviour where $C'(\omega) \propto C''(\omega) \propto \omega^{-p}$ [1,2,3]. A similar process was found on single and double glass fibre mat, see section 2.6. Comparing the single and double glass fibre

mats the only difference is the thickness, so in principle the real and imaginary parts of the capacitance (C' , and C'') of the single mat should be double that of the double mat. The real and imaginary parts of the double glass fibre mat were therefore multiplied by two and plotted together with the response of the single mat as shown in Figure 2.14 page 2-56.

In the frequency range 1Hz to 100kHz, the real part of the capacitance is almost the same for the single mat and 2x the double mat, and shows no real temperature dependence. This means that in this region the permittivity of the glass fibres contributes to the capacitance in accordance with the sample thickness. The small deviations from exact equality that are observed are probably the result of variations in the surface area of the fibres for the single and double mat cases.

At frequencies below 1Hz there is a frequency dependent transport process (C'' proportional to f^p and C' increasing with decreasing frequency) such as that observed in the composite. It is therefore likely that the same process is involved in the two cases. However, unlike the case of the composite the transport process is observed in this frequency range at room temperature. The charge transport involved is therefore easier in the mats than in the composite.

In Figure2.14 it can be seen that C'' for the charge transport process is dependent on sample thickness. Therefore it is not a process limited to the electrode. However, C'' does not come into co-incidence when the mat thickness is allowed for, i.e. doubling the C'' for the double-mat sample does not bring the two C'' curves into equality. This means that the charge transport does not contribute in accordance with the thickness of the sample. The most probable origin of this process is therefore charge transport around the surfaces of the fibres. These paths are tortuous and will not scale in length with the sample thickness. The variation in the power exponent p would also suggest such an origin, since this exponent should depend upon the tortuousity of the transport path [3,4], which will be different for the single and double mat cases. Such an origin would be in agreement with the greater ease of the process in the mats compared to the composite, since in the composite the charges must move along the interface between epoxy and glass and in the mats the interface is air and glass. If the transport process were to be due to conduction within the fibres and inter-fibre transmission at

contact points it is extremely unlikely that the replacement of air by epoxy resin would reduce the facility of the process to the extent observed in the composite sample where transport is only present above 30° C in the frequency range of the measurement. Furthermore it is highly unlikely that the fibres have very good contacts to allow for the charge transport to be within the fibre.

There is a general trend of an increase in $C^{//}$ with temperature such as found in the composite. This indicates that the charges may be moving on the fibre surface by an activated hopping. The nature of the charges is not known, but they may be associated with adsorbed water vapour. The elemental analysis of the pure epoxy shows that it contains Bromine Br. It is also possible that Br^- is the ion whose transport provides the q-dc in the composite. To investigate the nature of this charge, dielectric experiment was performed on samples for various humidity levels. The results are shown in Figure 4.1. It can be seen that the q-dc was decreased for the dry sample, and increased for the more humid samples. This is suggesting that water molecules are involved in the q-dc process. In the glass fibre mat there is no bromine available for transport so the charge is most probably water molecules on the surface of the mat. Furthermore the activation energies for this process are 1.1eV in the composite and 0.46eV in the glass fibre mat. This is further evidence that it is much easier for the charge transport to occur in the mat than the composite.

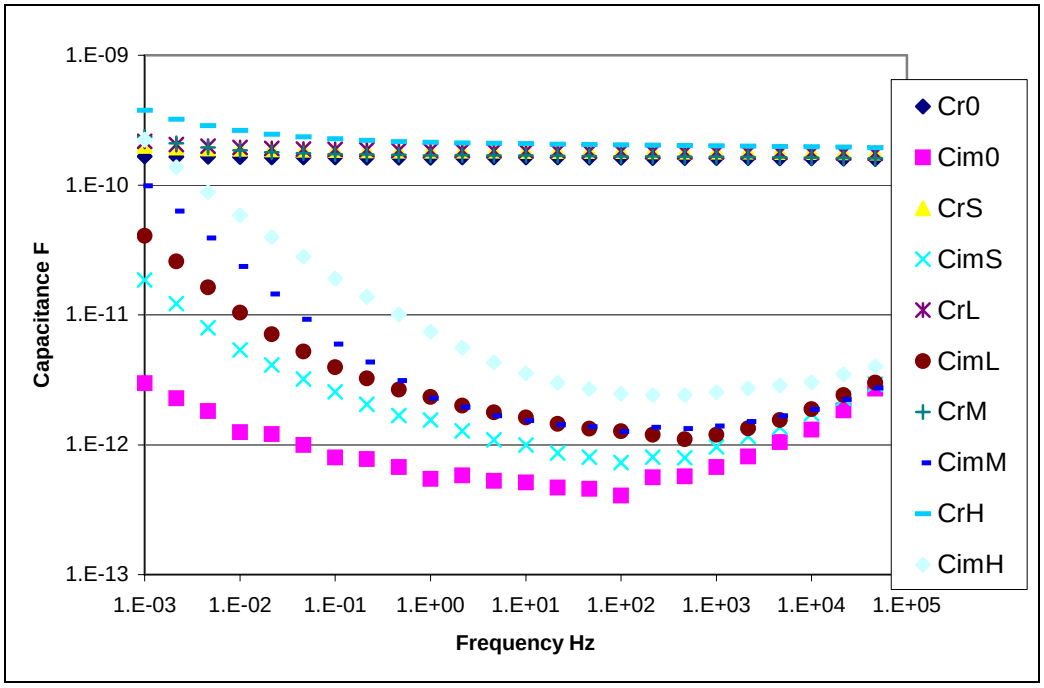

Figure 4.1: *Shows the real and imaginary part of the capacitance against frequency for the composite material for various levels of humidity. The symbols in the inset are defined as follow:*

0 means sample has 0% relatively humidity, the sample was left for 72 h in a vacuum oven at 50˚C.

S means the standard humidity, which existed in the sample at room temperature (15±5)°C.

L sample was left in water for 12h.

M means sample was left in water for 24h.

H sample was left in water for 72h.

All measurements were made at 20˚C.

This form of dielectric response has been associated with equivalent circuits that exhibit self-similarity, i.e possess a scaling relationship between sub-circuits of different size [1,3]. Percolation systems lie in this class and a model for them has been developed [1] in the form of a scaled circuit hierarchy, Figure 4.2. Repeated embeddings of the generator circuit, as shown in Figure 4.2 gives the macroscopic system. The derived response [1] has a CPA form with an exponent p whose value is determined by the arrangement of capacitors and resistors in the generator circuit, i.e. the system geometry. The CPA behaviour corresponds to the increasingly tortuous paths needed to achieve transport over ever-longer distances. At very low frequencies

the conducting paths that cross the sample yield a limiting dc conductance. The capacitance and conductance contributions to the system response are inversely dependent upon a power of the sample thickness. These results can be interpreted on the basis of this model if we assume that charge transport takes place on the surface of the glass fibres, with contacts between fibres acting as blocking capacitors. In the case of the fibre mats a direct contact to the electrode occurs and so the limiting dc-conductance is observed. The fractional power low (FPL) response given in Figure 4.2 of [1] is very close to the dielectric response observed throughout this thesis, see chapter 2 .The fibres will perform the same function in the composite, but now the epoxy on their surfaces increases the activation energy for charge transport.

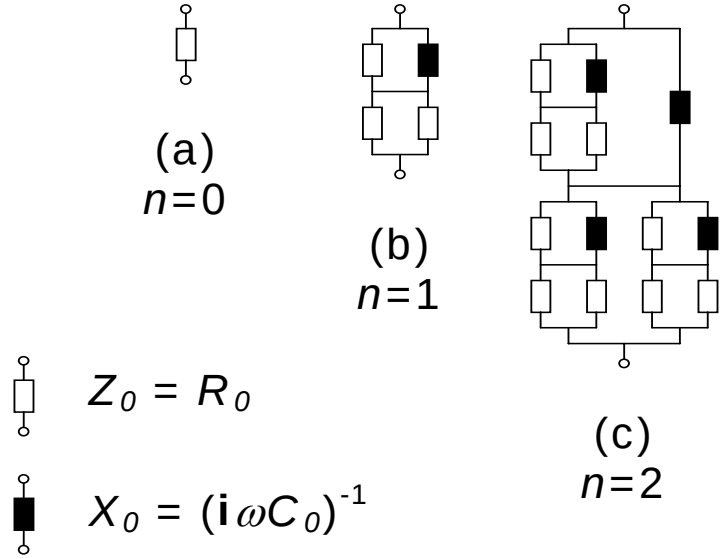

Figure 4.2. *Three embeddings of a simple scaled circuit representation of a percolation system. Taken from [1].*

A layer of epoxy resin will also block access to the electrode, preventing the observation of a limiting dc-conductance. It is probable that the charge carriers involved in the transport are supplied by water molecules adsorbed on the fibre surfaces [5], though other ionisable molecular species produced during the curing procedure may also be involved.

4.1.1 The effect of ageing on the dielectric response

The above picture allows an interpretation of the changes in dielectric response measurements in terms of the physical changes introduced by thermo-electric ageing.

The results from the aged samples show a consistent trend towards a bigger and/or faster response without any significant change in activation energy, or exponent p. This implies that the circuit geometry remains the same, but that the resistance and/or the capacitances of the components have reduced. The time scale of the response is scaled to that of the elemental system, i.e. $\tau_0 = C_0 R_0 \equiv (\omega_0)^{-1}$, so smaller R_0 and C_0 leads to a shift of the response to higher frequencies This would be achieved if some portion of the capacitive areas were to become conducting. This is just what would happen if the epoxy became de-bonded from the fibres in some places. The SEM analysis of the failed sample, see Figure 3.23 and 3.25, suggests that this in fact has taken place during ageing.

The dielectric response of the failed sample showed other features in addition to the q-dc behaviour. In part this may be due to the presence of the bored-out breakdown channel. The activation energy plot shows two regions of behaviour: one at low temperatures that paralleled that of the composite and one at higher temperatures that followed the fibre mat behaviour. A possible explanation is that this response is contributed by two systems in series. In this case the one with the largest impedance will dominate. Thus the one with the smallest activation energy will dominate at high temperatures, and vice-versa, the one with the largest activation energy will dominate at low temperatures. Figure 4.3 shows an interpretation for such behaviour

The total impedance is

$$Z_t = Z_1 + Z_2$$

assume $Z_1 \propto \exp(\frac{\Delta_1}{kT})$, $Z_2 \propto \exp(\frac{\Delta_2}{kT})$

Δ_2 is bigger than Δ_1

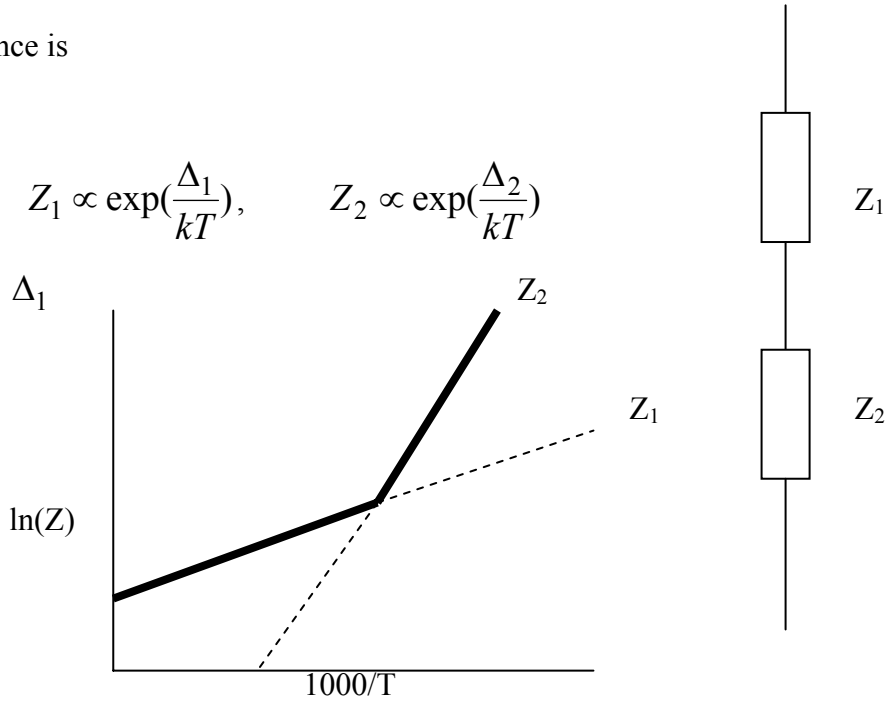

Figure 4.3. *A model for the behaviour of a failed sample*

The values of the activation energies obtained indicate that the two systems correspond to regions where the fibre mat has become substantially de-bonded and regions where the fibre mat is still mainly bonded to the epoxy. During the period of stress progressive development of de-bonding between the epoxy and the fibres has been shown to occur. Since the epoxy-fibre interface is the region where the percolative charge transport takes place it is possible that the heating effects of local currents may have caused the de-bonding. However, there is no sign of carbonisation in the de-bonded regions investigated via SEM. It is possible therefore that the de-bonding may have occurred as a result of mechanical stresses produced by interface fields [6]; see sections 4.6 and 4.7. Alternatively the de-bonding may be the result of differential thermal expansions of fibres and epoxy under the local temperature rise caused by Joule heating, see section 4.8.

4.2 Dynamic Mechanical Analysis.

The activation energy obtained from DMA is for the amplitude, while that from dielectric spectroscopy is for the frequency. The activation energy in the DMA case refers to the concentration of the entities that can move under mechanical stress. The charge transport is nearly dc (q-dc) involving an activation energy of 1eV. The DMA is similar in form, i.e. a near viscous flow. Consider a situation with fibre- epoxy barrier (bottleneck). An ion can move from one side of the barrier to the other via a state with 1eV of thermal energy. The number of moving segments can also be increased under a mechanical. What might be happening is the following. Giving 1eV of thermal energy to the material of the epoxy-fibre bottleneck allows it to move, this would contribute to the DMA, but when it moves the ion can travel through where the barrier was. This allows the ion to contribute to the q-dc.

The relationship would be that freeing of the bottlenecks does not allow more ions to move, it just allow the same number of ions to move more easily. The barriers to movement are the bottlenecks in both cases.
The DMA Technique was found to be not useful, as the machine was not working. Consequently, it was not possible to measure the aged sample.

4.3 Space charge profile

The interpretation of the PEA signal is not simple because the material is a composite. The mismatch between the acoustic impedances of the epoxy and glass fibre components will give rise to reflections that may reach the detector at the same time as other direct signals. Since the time delay is used to identify the position of the charge in the material, some portion of the charge at a given position will be identified as originating from deeper within the material or even as fake peaks further away than the upper electrode.

In the PEA experiment the composite material sample is bound and held between plane parallel electrodes [9]. The sample consist of three layers as shown in Figure 4.4

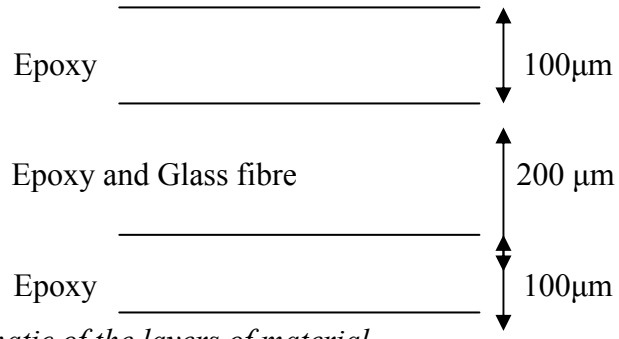

Figure 4.4. *Schematic of the layers of material.*

Consider a space charge in the epoxy layer as shown in Figure 4.5.

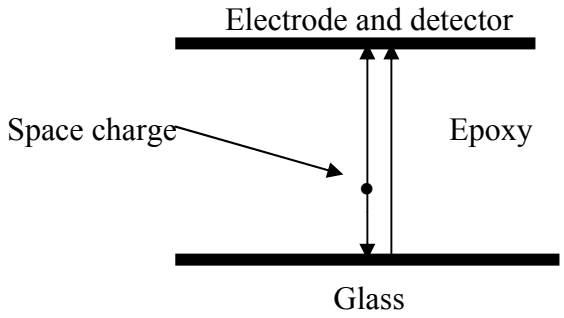

Figur4.5. *Shows direct (in compression) and reflected (in rarefaction) of the acoustic wave generated by hitting the space charge with the pulse.*

The acoustic plane wave propagating away from the detector in the epoxy is reflected and transmitted at the epoxy/ glass interface with wave amplitude components in accordance with the reflection coefficient ρ

$$\rho = \frac{\frac{\eta_2}{\eta_1} - 1}{\frac{\eta_2}{\eta_1} + 1} \qquad 4.1$$

This is from epoxy to glass

η_1 is the acoustic impedance of epoxy; η_2 is the acoustic impedance of glass.

$$\eta_1 = D_1 c_1 \qquad 4.2$$

$$\eta_2 = D_2 c_2 \qquad 4.3$$

D_1, and D_2 are the densities of epoxy and glass respectively, c_1, c_2 are the velocities of epoxy and glass respectively,

Assume the transmitted signal has a magnitude E_t; the reflected signal at epoxy glass interface would be E_r, where

$$E_r = \rho E_t \qquad 4.4$$

Substituting the values from table1 and table2 from chapter2 gives

$$E_r = 0.6 E_t$$

The reflected signal travels in the opposite direction to the incident wave and the total signal is the victor sum of the direct and the reflected signals.

The wave length λ is of the acoustic wave is given by

$$c = \lambda f \qquad 4.5$$

and since the pulse is 5ns long so the fundamental frequency Fourier transform is 0.2 $*10^9$ Hz and hence λ=13μm in the epoxy.

The behaviour of the acoustic signal is dependent on the dimension of the glass fibre and the glass fibre spacing in the material. If the glass fibre separation is large compared with the signal wavelength, then the signal may not experience a change in acoustic impedance on its way to the detector. If the glass fibre spacing dimensions are small compared with the signal wavelength the signal will be refracted, reflected and scattered by the glass fibres. The spacing between the fibres is about 6 μm. The spacing dimensions are smaller than the wavelength, so that some of the signal will be reflected by the glass fibres as calculated above. Some of the signal will be diffracted and scattered. The signal wavelength needs to be smaller than 100 μm, for the signal to be able to propagate through the material.

The PEA signal profile observed is a combination of reflected and transmitted signal and so it is complicated.

The scattering of the reflected signal off the glass can be seen in Figure 4.6.

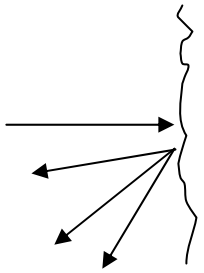

Figure 4.6. *Scattering of the glass fibre surface.*

4.3.1 Dispersion calculation

Dispersion is the difference in time taken between the fastest and slowest signal to reach the detector. The difference in time taken is due to the difference in the length or in the nature of the paths taken. The PEA signal will suffer from dispersion. To calculate dispersion, consider Figure 4.4. The slowest time is when the signal travels all the way in the epoxy and the fastest is when it travels half of the distance in the glass.

The maximum time taken for the signal is:

$$t_{\max} = \frac{400 * 10^{-6}}{2600} = 154ns$$

The minimum time taken is

$$t_{\min} = \frac{200 * 10^{-6}}{2600} + \frac{200 * 10^{-6}}{5100} = 116ns$$

The dispersion $\Delta t = t_{\max} - t_{\min} = 38ns$ 4.6

The effect of dispersion on the signal is shown in Figure 4.7

The dispersion broadens the signal observed, i.e. it progressively increases the width of the peaks originating at greater distance from the detector.

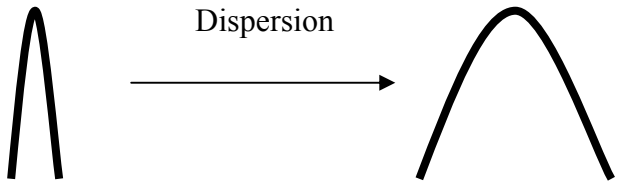

Figure 4.7. *It shows the effect of dispersion on the signal*

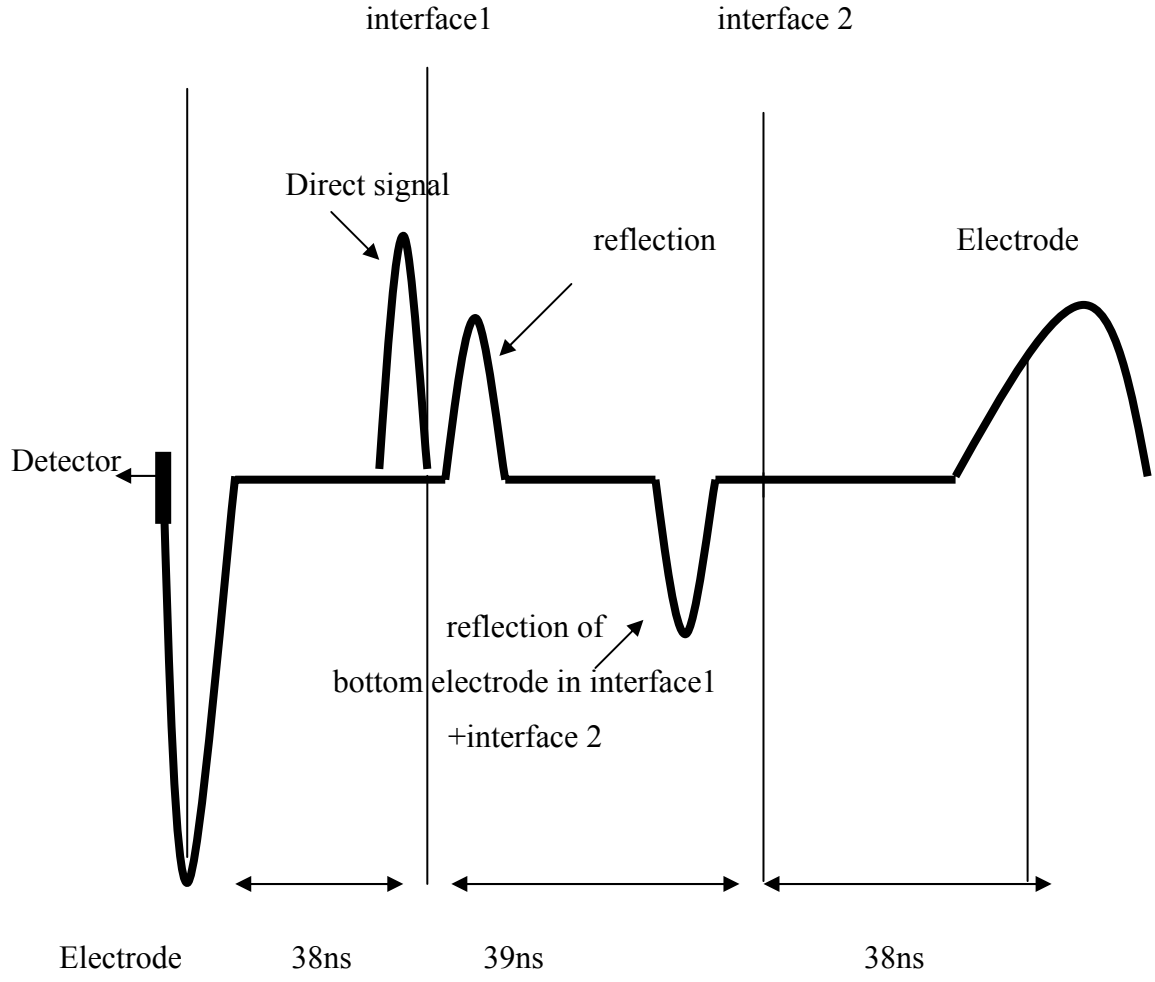

Figure 4.8 *Basic PEA signal*

The method of Images for sound waves can be used to analyse the PEA signal [10]. A source of sound on one side of the plane boundary between two extended media may be regarded as having an image at a distance on the other side of the boundary. The resultant effect at any point in the first medium will then be made up of the sum of the effects due to the source and its image. The phase of the reflected wave will depend

on the values of the acoustic impedances of the two media. Thus if a sound wave in the epoxy is reflected from the glass as shown in Figure 4.5, the image will be exactly similar to the source.

Consider space charge near the epoxy glass interface. The pulse acts on the space charge producing a mechanical stress with an amplitude proportional to the density of the space charge. In response to this, two stress waves, one in compression, and one in rarefaction are generated in accordance with reflection coefficient as shown in Figure 4.5. The rarefaction wave will be reflected by the glass fibre and change phase and become in compression. The time taken for the signal to reach the detector is equal to the distance travelled divided by the speed of sound in the medium. The repetition frequency of the pulse can go up to 1kHz .The signal to noise ratio of the measurements was improved by taken repeated measurements. 1024 measurements were recorded and the average taken. Consider Figure 4.8 the signal can be explained from the calculation of the time taken for direct and reflected signals to b received at the detector. The detector is near the bottom (negative) electrode so the pulse from the electrode does not travel far and a sharp peak is observed. For the top electrode (positive) the signal travels through the glass and epoxy and suffers from attenuation, reflection and dispersion. The time taken for this signal to reach the detector is $t = \frac{200}{2600} + \frac{200}{5100} = 116ns$. Other signals will be hidden underneath this signal, such as reflection from interface 1 charge, and charge from interface 2. Signals may be out of phase, which lead to a further decrease in the signal amplitude. The signal near interface 1 is a direct signal. The signal near interface 2 a reflection of the bottom electrode in the first interface plus maybe some direct signal.

This is the picture in the PEA signal obtained. In Figure 2.21 in Chapter 2. The width of electrode peak is increased due to dispersion, the signal magnitude is decreased due to attenuation, and the extra part of the signal is due some space charge, reflection and scattering. It is very complicated to compute the values for the signal. However the signal shows some space charge accumulated near the epoxy glass interface, see Figure 2.21.

The composite material can be modelled by a combination of resistors and capacitors as shown Figure 4.9.

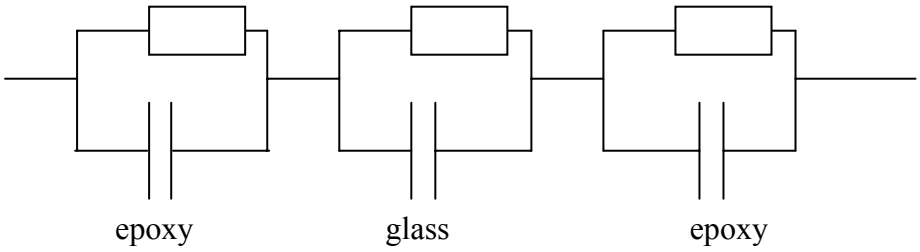

Figure 4.9. *A circuit model for the composite material, combinations of resistors and capacitors.*

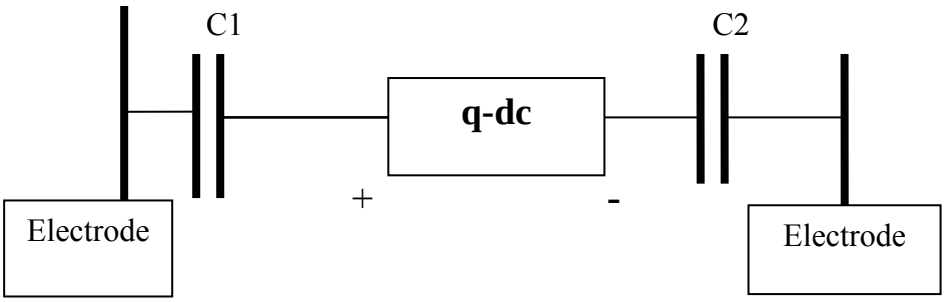

Figure 4.10. *An approximate model for the PEA response*

The q-dc process charging the capacitors (the epoxy fibre bottleneck). The charge in the material is accumulated by the charge transport process q-dc.

4.3.2 The effect of ageing on space charge

The pulsed electro-acoustic (PEA) space charge measurements show a very clear difference between the aged and non-aged composite material, see Figure 3.28. There is more space charge in the aged material. It could be due to chemical traps [11] and free volume created by bond breaking due to ageing. Considering the model in Figure 4.1. ageing may increase the speed of q-dc by reducing the time constant for charging the capacitors. This will lead to more interface charge at the edge of the fibre layers. The effect of this is bigger fields in the epoxy layer and lower fields in the glass fibre layer. The space charge will enhance the electric field at the epoxy- glass fibre interface. This is will lead to more mechanical stress leading to delamination.

4.4 DSC

The DSC results from the un-aged samples show clearly that the composite material is not fully cured. The glass transition temperature goes up as the amount of curing time goes up. Electrical ageing was found to decrease the glass transition temperature. This may be due to an increase of the free volume due to bonds breaking. A glass is formed by the loss of bulk viscosity, caused by the structure becoming rigid. Lowering the glass transition temperature means that it is easier to reduce the rigidity. Since in epoxy the rigidity is produce by cross-linking, lowering the glass transition temperature implies that some of the cross-links have been broken. The effect of thermal ageing on the glass transition temperature is quite the opposite. The glass transition temperature was found to increase as a result of thermal ageing. This could be due to the effect of post curing, producing more cross-linking. This is a very significant finding, as only electrical ageing seems to create the delamination. The delamination causes the voids that lead to partial discharge and hence electrical breakdown and failure.

4.5 General Discussion

The generation of the interface voids and delamination is likely to be the cause of dielectric breakdown [7] as long as they are aligned with their long axis in the direction of the electric field [8]. Because of the weave of the mat most such voids will be aligned perpendicular to the field direction with a width of around 2-3μm, which is insufficient to support discharges at the fields applied [8]. At some stage, however, such voids can be expected to join together to provide a gap in the field direction long enough to support discharges. Once discharges can occur failure will follow rapidly.

The thermal ageing alone did not produce the same effect on the dielectric response, see section 3.4. The activation energy was the same as that for un-aged and for the electrically aged. The response did not move to higher frequency as in the aged samples. This is indicating that only electrical ageing causes the effect discussed above.
The space charge increases the field in the epoxy this will lead to bond breaking between the epoxy and the glass fibre creating small voids. With time this will lead to delamination. The voids will enhance the field further and break more bonds and create more voids. This is a positive feedback mechanism and at some stage the voids will be coalescence and lead to partial discharge and failure.
The decrease of glass transition with ageing indicates an increase of the free volume of the material.

4.6 Strain and expansion calculations.

To further support the argument presented here, mechanical strain and thermal expansion calculations are presented here.
These calculations are to find approximate values for the mechanical strain resulting from electric field E at the interface between the epoxy and the glass fibre [15,16].
The electrostatic compressive mechanical stress σ is

$$\sigma = 1/2\varepsilon_0 \varepsilon_r E^2 \qquad 4.7$$

where ε_0 is the permittivity of free space and equal to $8.854*10^{-12}\ Fm^{-1}$ ($C^2N^{-1}m^{-2}$)

ε_r is the relative permittivity and E is the electric Field.

The relative permittivity for the epoxy is 2.9, and 6.7 [17] for the glass at 1MHz.

There are two boundary conditions; the composite can be thought of as two materials in series or in parallel. In reality the material system will be somewhere in between.

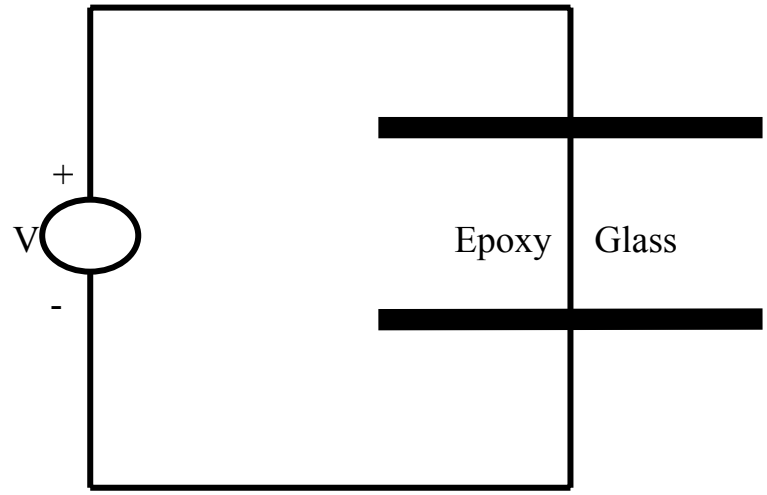

Figure 4.10. *The epoxy and glass fibre represented by two capacitors in parallel. The electric field is equal in both materials but the flux density will be different*.

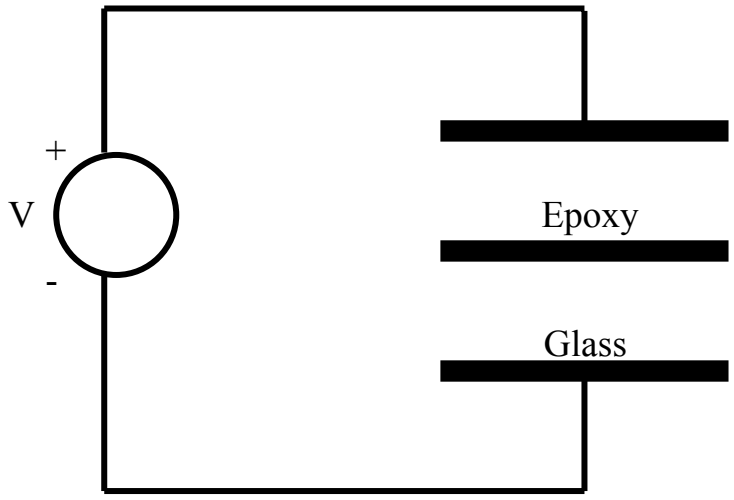

Figure 4.11. *The epoxy and glass fibre represented by two capacitors in series. The flux density is the same in both material, but the electric field will be different.*

Consider the system arrangement shown in Figure 4.10. the capacitors are in parallel. The electric field E will be the same in each material, but the flux density D will be different.

If the field is the same then, from equation 4.7

σ (glass)/ σ (epoxy) = ε_r (glass)/ ε_r (epoxy) = 6.7/2.9 = 2.31. The strain in both materials will be different according to Young's modulus Y

Y = Stress/strain 4.8

Young's modulus for the epoxy is approximately 3GPa. Young's modulus for the glass is approximately 80GPa , from table 2.1 page 2-33

Y (epoxy) = stress (epoxy)/strain (epoxy).

Y (glass) = stress (glass)/strain (glass).

If we divide Young's modulus of glass by Young's modulus of epoxy

Y (glass)/Y (epoxy) = [stress (glass)*strain (epoxy)]/[strain (glass)*stress (epoxy)]

Substituting the values above, we have:

Strain (epoxy) = 11.5 Strain (glass).

This means the electrostatic compressive stress produces twelve times as much strain in epoxy as in glass. This could lead to delamination in the composite. This is very much in agreement with previous argument.

Now let us consider the system arrangement shown in Figure 4.11 in which the electric flux is the same in both materials, but the electric field is different.

Following a similar argument.

$$D = \varepsilon_0 \varepsilon_{glass} E_{glass} \qquad 4.9$$

$$D = \varepsilon_0 \varepsilon_{epoxy} E_{epoxy} \qquad 4.10$$

$$\varepsilon_{glass} E_{glass} = \varepsilon_{epoxy} E_{epoxy}$$

$$\frac{E_{epoxy}}{E_{glass}} = 2.31 \rightarrow E_{epoxy} = 2.31 E_{glass} \qquad 4.11$$

$$\sigma = \frac{1}{2} \varepsilon_0 \varepsilon_r E^2$$

$$\sigma_{glass} = \frac{1}{2} \varepsilon_0 \varepsilon_{glass} E_{glass}^2$$

$$\sigma_{epoxy} = \frac{1}{2} \varepsilon_0 \varepsilon_{epoxy} E_{epoxy}^2$$

substituting the values

$\sigma_{glass} = 0.42\sigma_{epoxy}$

using Young modulus equation

Y (glass)/Y (epoxy) = [stress (glass)*strain (epoxy)]/[strain (glass)*stress (epoxy)]

Substituting the values above, we have:

Strain (epoxy)= 63.5 Strain (glass).

The stress and strain considered so far are perpendicular to the glass fibre mat direction. A strain in the vertical direction will produce a strain in the other horizontal direction in accordance with Poisson ratio ν.

Strain (horizontal)= ν*Strain (vertical) 4.12

Poisson ratio is 0.4 for epoxy and 0.3 for glass.

In the horizontal direction for the case considered in Figure 4.10

Strain (epoxy)=0.4/0.3*11.5=15.3 (strain glass).

In the horizontal direction in for the case considered in Figure 4.11.

Strain (epoxy)=0.4/0.3*63.5=84.5strain glass.

If we consider shear modulus, G

Shear modulus is sheer stress/ shear strain

$$G = \frac{E}{2(1+\nu)} \qquad 4.13$$

$$G_{(glass)} = \frac{80*10^9}{2(1+0.3)} = 30.76*10^9 \text{ Pa}$$

$$G_{epoxy} = \frac{3*10^9}{2(1+0.4)} = 1.07*10^9 \text{ Pa}$$

Assuming a tangential electric field using the same analysis as above

For case in Figure 4.10 the, strain epoxy=12.44 strain glass, and for the case in Figure 4.11, strain epoxy =68.5 strain glass.

It can be seen that either boundary condition results in very different strains existing in the materials. The strain is mainly in the epoxy. One would therefore expect strong mechanical forces in the interfacial regions producing different strains in the two

materials. This is the type of strain that would produce mechanical failure of the interface if it is big enough.

4.7 Electric stress calculations in gaseous cavities.

The electric stress is enhanced in voids delaminations and cavities within the dielectric as mentioned in chapter1 [12, 13, 14].

The field enhancement in cavities is highly dependent on the shape of the cavity and its axis of orientation with respect to the applied electric field [13]. A cavity with its axis parallel to the direction of the applied electric field produces the highest stress enhancement.

The shape of the voids created by the mechanical stress is not known. A typical applied voltage is 10kV, the sample thickness is 400μm so the average applied field is 25kV/mm, and a field enhancement of 1 to 100 was considered. However, the difference in permittivity between the epoxy and the glass means that the field in the epoxy is larger than the average value.

If the applied field is 25kV/mm, how much the field inside the epoxy

To calculate that consider Figure 4.4.

$$Vtotal = Vglass + Vepoxy \qquad 4.14$$

$$Vtotal = Eglass * Lglass + Eepoxy * Lepoxy$$

substituting the value for Eglass from equation 4.11

gives $Eepoxy = 1.4 Eapplied$ 4.15

Field in the epoxy V/m	Enhancement	Enhanced field V/m	Stress N/square m	Strain	Energy per unit volume Joule/cubic meter
3.5E+07	1	3.5E+07	1.57E+04	5.24E-06	4.12E-02
3.5E+07	1.5	5.3E+07	3.54E+04	1.18E-05	2.09E-01
3.5E+07	2	7.0E+07	6.29E+04	2.10E-05	6.60E-01
3.5E+07	3	1.1E+08	1.42E+05	4.72E-05	3.34E+00
3.5E+07	5	1.8E+08	3.93E+05	1.31E-04	2.58E+01
3.5E+07	7	2.5E+08	7.71E+05	2.57E-04	9.90E+01
3.5E+07	10	3.5E+08	1.57E+06	5.24E-04	4.12E+02
3.5E+07	15	5.3E+08	3.54E+06	1.18E-03	2.09E+03
3.5E+07	20	7.0E+08	6.29E+06	2.10E-03	6.60E+03
3.5E+07	30	1.1E+09	1.42E+07	4.72E-03	3.34E+04
3.5E+07	50	1.8E+09	3.93E+07	1.31E-02	2.58E+05

Table 4.1. *Stress strain and stored energy calculations for the epoxy.*

The mechanical strain is plotted against enhancement in a log-log scale as shown in Figure 4.13.

The electromechanical stress will create very small voids as shown in Figure 4.12, with time these voids maybe will coalescence and align themselves in the field direction and cause partial discharge and hence failure.

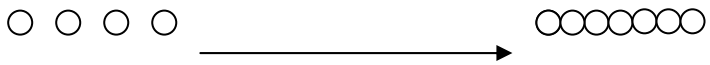

Figure 4.12. *The small voids with time they form a bigger void as shown.*

The energy per unit volume produced by the electromechanical force is calculated in table 4.1.

$$Energy = \frac{1}{2} stress * strain \qquad 4.16$$

The bond agent used to bind the glass to the epoxy is Amino- and epoxy- silanes, a typical bond length is 200pm.

Consider the bond volume, to calculate the energy per bond volume, assume bond volume is $20*10^{-30}$ m^3.

Consider, as an example, a field enhancement of 5, from table 4.1 the energy per unit volume stored in the material is $25.8Jm^{-3}$. The energy per bond is $3.22*10^{-9}$ eV; the energy required to break a bond is 3.5eV. The energy stored per bond is very small compared with the energy required to break the bond. If the energy stored per bond were to be comparable with energy required to break a bond the material will fail

instantly. The question is how does the bond break if the calculations show that energy available is much smaller than the energy required to break a bond. The points to consider are: The time scale, ageing is a progressive process, the q-dc shift to higher frequency is a function of ageing time the longer the sample aged the more the dielectric response shift to higher frequency. With time some bonds will acquire enough energy to break, which in turn will reduce the modulus and increase stored energy and with time more and more bonds will break causing voids and delamination between the epoxy and the glass fibre.

If the q-dc is in the middle layer, which is, there will be little field there. Most of the field will be in the epoxy glass interface. This will lead to a higher concentration of energy near the epoxy-glass fibre interface causing bonds to break.

Only energy to break a few bonds is required so progressive build-up q-dc causing more stress reducing the yield strength of the epoxy. This will lead to a non-linear stress strain relationship causing plastic deformation hence voids and delamination.

There could be a statistical distribution of energy in the material causing some bonds to have much more energy than the average energy per bond. The points mentioned supports delmination occurrence between the epoxy and glass.

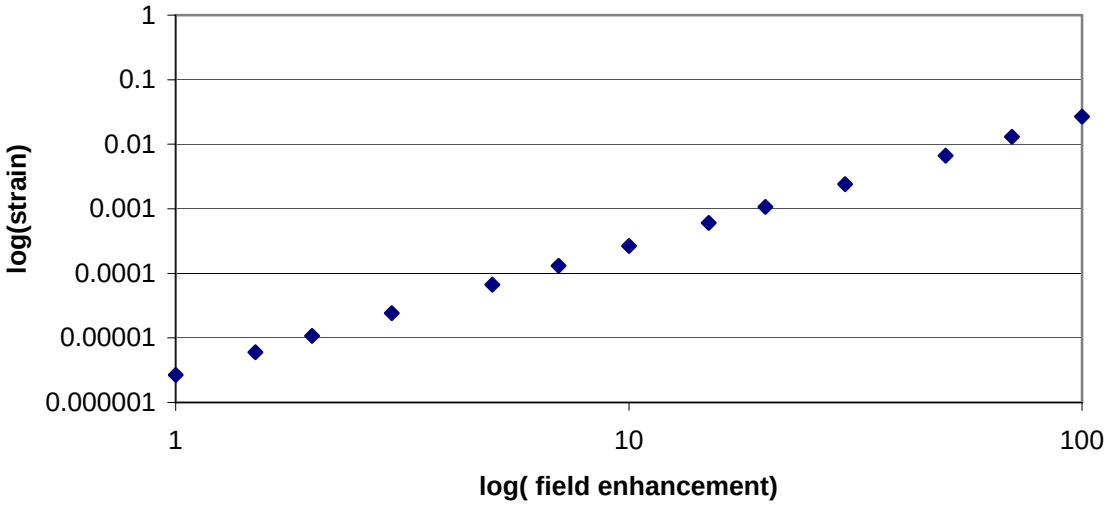

Figure 4.13. *The log of mechanical strain against the log of field enhancement in the epoxy.*

4.8 Thermal expansion calculations.

Now let us consider the thermal expansion effect.
The coefficient of thermal expansion for the glass is $5*10^{-6}$m/m/°C at [20 –100] °C.
The coefficient of thermal expansion for epoxy is $70*10^{-6}$m/m/°C at [20 –100] °C.
If the temperature goes up from 20°C to 100°C, the glass will expand by $400*10^{-6}$m /m, while the epoxy will expand by $5600*10^{-6}$m/m.
The difference between the two expansions $5600*10^{-6}$-$400*10^{-6}$m =$5100*10^{-6}$m. This difference in expansion is likely to create delamination.
The samples that were thermally aged at did not show the same response as the sample that were electrically aged even though this calculation suggests that it should. This could be due to two reasons. The thermal-only ageing produces more cross-linking eliminating any effect caused by thermal expansion. Maybe that is why there was little change in the thermal aged samples.

4.9 Binding Agents

The research program has shown ageing causes a debonding between fibre and epoxy. This debonding creates voids and can lead to electrical breakdown.
Stronger bonding is therefore required.

The manufacturers were contacted regarding the binding agents they used. The silane-binding agent is applied by glass supplier and the exact formulation is proprietary to them.

The silane formulation has a large effect on the finished laminates and
for this reason, glass suppliers like to keep it secret.
Parcnelco (epoxy manufacturer) imply that Amino- and epoxy- silanes were used.

The most effective binding agent will be a silane that contained a group similar to the hardener for the epoxy impregnate. Since this is dicyandiamide then a silane containing amino groups can be expected to give the best bond. However a mixture of amino and epoxy silanes may be the best solution. In this case composition could be varied to try to achieve the best bond.

Other points to consider

Rough glass surface gives more contact surface area, which leads to better bonding.

To try to choose material with combination of permittivity and Young's modulus that results in a similar strain (may depend on frequency).

Choose material in which thermal expansion are similar.

Longer and better curing.

CHAPTER 5

CONCLUSIONS

The work carried out during the course of this study sought to accomplish a fundamental understanding of the electrical ageng mechanism of the insulating material, and its electrical performance as printed circuit board material. In this chapter the main finding of this research work is reported and some recommendations are made to the manufacturers. Some future work is also recommended.

- A q-dc transport process at low frequencies was shown to occur on glass fibre as well as in the composite material. This charge transport process was shown to occur on the surface of the fibre along the epoxy- glass fibre interface.
- Electrical ageing was found to cause de-bonding of the epoxy and fibre resulting in interface voids. Progressive changes in the dielectric response were observed that could be attributed to the increase in de-bonding, and therefore provide a measure of the extent of the ageing that has occurred.
- Ultimate failure is expected to be caused by discharges when voids aligned with the field are formed by coalescence.
- The main finding of the space charge measurements is that, under the same measurements conditions, more space charge accumulated near the epoxy glass fibre interface in the aged samples than in the un-aged. The space charge can be trapped in traps caused by bond breaking due to ageing. The main conclusion is that space charge measurements can be used as a diagnostic technique to check for ageing.
- The main findings of the DSC results are: the glass transition temperature goes down with electrical ageing, the glass transition temperature goes up with thermal ageing, and the composite material is not fully cured. The conclusions that can be drawn out of these are: the composite material needs more curing to increase the bonding between the glass fibre and the epoxy, electrical ageing created free volume that causes the glass transition temperature to go down. DSC can be used as a diagnostic technique to check for ageing.

- Electrical ageing causes delamination that can cause voids that lead to partial discharge, which could lead to failure. Thermal ageing at the temperatures used (less than glass transition temperature) had little effect by itself, doe not have the same effect.

Recommendations

To improve the performance of the composite material the following maybe recommended.

1. A rough glass surface will give more contact surface area, which will lead to better bonding.

2. If materials are chosen with combinations of permittivity and Young's modulus that results in a similar strain (may depend on frequency). This would reduce the interfacial delaminatiom force.

3 Similarly materials in which thermal expansion are similar would reduce interfacial forces.

4. Longer and better curing may be advantageous.

Recommendations for assessing new composite materials

- Strain calculations.
- Ageing conditions, choice (strain, working conditions).
- Diagnostic tests (dielectric response, space charge, DSC).

Chapter 1 References

1 M. Ieda, M. Nagao, M.Hikita, "High-field conduction and Breakdown in Insulating Polymers Present Situation and Future Prospects", IEEE Tran. DEI, Vol. 1, No.5, pp 934-945, 1994

2 Clyde F. Coombs, JR, "Printed Circuits Handbook", New York; London: McGraw-Hill, 2001 Fifth Edition 2001.ISBN: 0071350160.

3 Okamoto,Kenji; Fukunaga,Kaori; Maeno,Takashi; Tsukui,Tsutomu, "Observation of copper ionic migration in insulation layer by pulsed electroacoustic method", IEEE Transaction on Components and Packing Technologies, v25,n 2, p239-243, 2002

4 Helgeson. Anders, Uno. Gafvert, Dielectric Response During Curing of Resin-Rich Insulation System for Rotating Machines, IEE Conference on Electrical Insulation and Dielectric Phenomena., pp 289-292,1999

5 Y. Yamano , T.Tsukui, "Increase of Capacitance and tanδ Between Conductors on Printed Circuit Boards at Low Frequency Due to Ionic Migration", IEE Transactions On Dielectrics and Electrical Insulation, Vol.7, No 3, pp366-373, 2000

6 Hitachi-shi, Ibaraki-Ken, "Breakdown Strength of Various Epoxy Resins for Resin Molded Coils under High Temperatures", Asian International Conference on Dielectric and Electrical Insulation, pp 49-52, 1996

7 Y. Sheiretov and M. Zahn, "Dielectrometry Measurements of Moister Dynamic in Oil-impregnated Pressboard", IEEE Transactions on Dielectrics and Insulations, Vol.2, No.3, pp329-351, 1995.

8 S. Grzybowski, E.A. Feilat, P. Knight, " Accelerated Ageing of High Voltage Encapsulated Transformer for Electronic Applications", The 6th International Conference on Properties and Applications of Dielectric Materials, pp 209-212, 2000.

9 Walter Sikonowiz, "Designing and creating printed circuits". Rochelle Park, N.J: Hayden Book Co, c1981. ISBN: 081040964x.

10 L.A.Dissado, and J.C.Fothergill, "Electrical degradation and breakdown in polymers". Published by P.Peregrinus for IEE,London 1992.ISBN:086341 1967.

11 J.R Fried, "Polymer science and technology", London, Prentice-Hall International Editions ISBN 013685561x, 1995.

12 J.C Anderson , K.D Leaver , R.D Rawlings , J.M. Alexander , "Material Science", Third Edition, Chapman and Hall, ISBN 0442306261,1985.

13 J.Muccigrosso, P.J. Phillips, "The Morphology of Cross-Linked PE", IEEE Transactions on Electrical Insulation. Vol.EI-13, pp.172-178, 1978.

14 W.Tillar Shugg, "Handbook of electrical and electronic insulating Materials", second edition, New York: IEEE Press, 1995**.** ISBN: 0780310306, 1995.

15 Parknelco product specifications, Electrochemical Corporation, 5 Dakota DriveLake Success, NY11042, see internet page www.parknelco.com

16 Malcolm P.Stevens, "Polymer Chemistry an introduction, Reading, Mass". ; London : Addison-Wesley, 1975 , ISBN: 0201073129

17 D.K Das-Gupta, K. Doughty, " Dielectric and Conduction processes in Polyetherether Ketone (PEEK)" , Trans E.I., Vol.EI-22 ,pp. 1-7, 1987

18 D.M. Taylor, T.J.Lewis, "Electrical conduction in polyethylene terephthalate and polyethylene films" J.Phys D: Appl.Phys, Vol.4, pp.1346-1357, 1971

19 T.J.Lewis " The micro-physics of charge in solid dielectrics ".. Published in ' Space Charge in Solid Dielectrics' by the Dielectric Society Edited by J.C. Fothergill and L.A.Dissado.ISBN:0-9533538-0-X, pp1-16, 1998.

20 K. Kojima, Y. Takai, M. Ieda, " Electronic Conduction in Polyethylene Naphthalate at High Electric Fields", J. Appl. Phys., Vol .59, pp. 2655-2659,1986

21 M. Ieda,"Electrical Conduction and Carrier Traps in Polymeric Materials", IEEE Trans .EI., Vol. EI-19, pp 162-178,1984.

22 T.J Lewis," Electrical Effect at Interfaces and Surfaces", IEEE Transactions on Electrical Insulation., EI-21(3), pp.289-295. 1986

23 T.J.Lewis "Ageing A Perspective", IEEE Electrical Insulation Magazine, Vol.17, No.4, July/August 2001.

24 V.A Brzhezitsy, O.S Il'enko, A.V. Mamihev, B.D Russel, S.A Sokolovsky," Partial Empirical Model of the Multifactor Ageing of High Voltage Insulation", Annual Report CEIDP, 94CH3456-1,pp367-372, 1994.

25 J. C, Fothergill.; G. C Montanari,.; G. C Stevens,.; C Laurent.;Electrical, Microstructural, Physical and Chemical Characterization of HV XLPE Cable

Peeling for an Electrical Aging Diagnostic Data BaseTeyssedre, G.; Dissado, L. A.; Nilsson, U. H.; and Platbrood, G., IEEE Transactions on Dielectrics and Electrical Insulation, v 10, n 3, p 514-527, 2003

26 L.A. Dissado, G. Mazzanti, G.C Montanari. " The Incorporation of Space Charge Degradation in the Life Model for Electrical Insulating Materials", IEEE Transactions on Dielectrics and Insulation. Vol.2, No 6.pp1147-1158, 1995

27 L.A.Dissado, G. Mazzanti, G.C. Montanari," A space charge Life Model for AC Electrical Ageing of Polymers " IEEE Transactions on Dielectric and Electrical Insulation Vol.6, No 6, pp864-875, 1999.

28 L.A.Dissado, G. Mazzanti, G.C. Montanari," Discussion of Space Charge Life Model featured in dc and ac Electrical Ageing of Polymeric Materials". IEEE Annual Report CEIDP, Pp36-40, 1997

29 P Cooner, J.P. Jones , J.P Llewellyn and T.J.Lewis " Electric Field induced Viscoelastic Changes In Insulating Polymer films".IEEE CEIDP, pp 27-30, 1998.

30 T.J.Lewis, J.P, Llwellyn, M.J. vander Sluij, J.N. Hampton." A new Model of Electrical Ageing and Breakdown in Dielectrics", IEEE. DMMA.pp.220-224. 1996.

31 Jean- Pierre Crine," A Molecular Model to Evaluate the Impact of Ageing on Space Charge in Polymer Dielectrics, IEEE Transaction on Dielectrics and Electrical Insulation, Vol.4, No 5, pp487-495, 1997.

32 Jean-Luc Parpal, . Jean- Pierre Crine, Chinh Dang,"Electrical Ageing of Extruded Dielectric Cables A Physical Model, IEEE Transaction on Dielectrics and Electrical Insulation, Vol.4, No 2,pp197-209 1997.

33 E. Cooper, "Application of polymer ageing models to cable geometry and time-to-failure distributions", PhD Thesis, University of Leicester, 2002.

34 PWC SAYERS, "Investigation of the Structural Changes in LDPE and XLPE induced by High Electrical Stress", PhD thesis, University of Wales, Banger 2001.

35 M.T Shaw, and S.H Shaw, "Water Treeing in Solid Dielectrics", IEEE Transactions. Electrical Insulation, EI-19, pp419-452, 1984.

36 C.H.Park, T.Kaneko, M.Hara, M. Akazaki, "The Effect of Mechanical Stress in The Dielectric Breakdown Strength of PET and FRP"IEEE Transaction on Electrical Insulation, Vol. EI-17, No.3, pp 234-240, 1982.

37 C.H.Park, T.Kaneko, M.Hara, M. Akazaki, "The Effect of Temperature and Voltage on Dielectric Breakdown Strengths of PET and FRP Under Mechanical Stress"IEEE Transaction on Electrical Insulation, Vol. EI-17, No.3, pp 546-553, 1982.

38 B .Salvage.” Electric Stress in Gaseous Cavities in Solid Dielectrics”PROC. IEE, Vol 11, No 6, pp 1162-1172, 1964.

39 D.D Chng., T.S Sudarshan., and J.E Thompson.” Analysis of Electric Stress Distribution in Cavities Embedded Within Dielectric Structures” IEE Transaction on Electrical Insulation, Vol. E-21, No 2, pp 213219, 1986.

40 P.Connor, J.P Jones, J.P Llewellyn. And T.J Lewis.” A Mechanical Origin For Electrical Ageing And Breakdown In Polymeric Insulation.” IEEE International Conference on Conduction and Breakdown in Solid Dielectrics, pp 434-438, 1997

Chapter 2 References

1. A.K Jonscher, “Dielectric relaxation in solids”, Chelsea Dielectric Press 1983, ISBN:0950871109.

2. L.A. Dissado and R.M. Hill., “Non-Exponential decay in Dielectrics and Dynamics of Correlated Systems”., Nature, 279, pp685-689, 1979.

3. L.A. Dissado and R.M. Hill, “A New Approach to the Structure of Imperfect Materials and their Relaxation Spectroscopy”., Proceedings of the Royal Society .London .A, 390, pp131-180, 1983.

4. L.A. Dissado and R.M. Hill, “Anomalous Low -frequency Dispersion”, J. chemical Society, Faraday Transactions. 2, Vol 80,291-319, 1984.

5. L.A. Dissado and R.M. Hill., Invariant behaviour for the response of simple fractal circuits. J. Physics :Condense Matter 3, pp 9773-9790, 1991.

6. Dissado L.A and Hill R.M, “Constant Phase Angle Response With Fractal Electrodes”, Solid State Ionics 26, pp 295-297, 1988.

7. L.A. Dissado and R.M. Hill., “Constant- Phase Angle and Power Law Regimes in the Frequency Response of A General Determinate Fractal Circuit”, The American Physical Society, Physical Review B, Vol 37, No7, pp3434-3439, 1988.

8. Van Valack, Lawrence.H, “Materials science for engineers”., Reading, Mass. : Addison-Wesley, 1970.

9. Fröhlich, H. “Theory of dielectrics: dielectrics constant and dielectric loss”, Oxford: Clarendon Press, 1986, c1958, 2end edition, ISBN: 0198513798(pbk). Book,

10. A. R. von .Hippel, ,” Dielectric materials and applications”, New York; London: Technology Press of M.I.T. : Wiley, c1954 book.

11. A. R .Von Hippel,.” Dielectrics and waves”, New York : Wiley, 1954 (1959 printing) .

12. B.V.Hamon” An approximate Method for Deducing Dielectric Loss Factor From Direct Current Measurement”, Proc IEE, Vol.99, pp 151-155,1952.

13. 1255 H.F, Frequency Response Analyser, Operating Manual, Solarton Instruments, Issue 2a, Part No 12550006, 1987.

14. J.Pugh, " Dielectric Spectrometer- User Guide" Private issue provide with the system measurements.

15. M. Abramowitz. .I Stegun," Handbook of Mathematical functions" 9th edition, Dover publications, Inc., New York, 1970

16. L.A.Dissado, and J.C.Fothergill, "Electrical degradation and breakdown in polymers". Published by P.Peregrinus for IEE,London 1992.ISBN:086341 1967.

17. J.J . O'Dwyer., "IEEE transactions Electrical Insulation". Vol 21, pp121-127, 1986.

18. K Fukunaga.. " Industrial application of space charge measurements in Japan", IEEE Electrical Insulation. Magazine, Vol. 15, pp.6-18 1999.

19. K Fukunaga., V Griseri." Space charge and external current measurements of filler-free epoxy resin", IEEE Transaction on Electrical Insulation, Vol 15. No 5, 1999.

20. T. Takada " Acoustic and Optical Methods for Measuring Electric Charge Distribution in Dielectrics", IEEE Trans. On DEI, Vol .6 No.5, pp 519-547, 1999.

21. N.H. Ahmed and N.N Srinivas, " Review of Space Charge Measurements in Dielectrics", IEEE Transactions on Dielectrics, Vol.4, No.5 pp.644-656, 1997.

22. J.M.Alison, "A high field pulsed electro-acoustic apparatus for space charge and external circuit current measurements within solid insulators", J.Meas.Sci and Technol. Vol.9, No. 10, pp1737-1750, 1998.

23. A. See, J.C. Fothergill, L.A. Dissado, J.M Alison, " Measurements of space charge distribution in solid insulators under rapidly varying voltage using high voltage high speed pulsed electro-acoustic (PEA) apparatus", J.Meas.Sci and Technol. Vol.12 , No. 8, pp. 1227-1234, 2001

24. A.See "High field space charge measurements in XLPE using a novel pulsed electro-acoustic system" PhD Thesis, University of Leicester, 2001.

25. C.Goupil. P. Norman," The use of Differential Scanning Calorimetry(DSC) in the prediction of metal composition and polymer characterisation, Ref. ITS/Gw-96.007. 1996.

26. McNaughton. J, Mortimer.C " Differential Scanning Calorimetry". Printed from IRS Physical Chemistry Series 2, Perkin-Elmer Corporation, Norwalk, Connecticut 068556.

27. J.R Fried, Polymer science and technology, London, Prentice-Hall International Editions ISBN 013685561x, 1995.
28. J.C Anderson, K.D Leaver, R.D Rawlings, J.M. Alexander, Material Science, Third Edition, Chapman and Hall, ISBN 0442306261,1985

29. Parknelco product specifications, Electrochemical Corporation, 5 Dakota DriveLake Success, NY11042, see internet page www.parknelco.com

30. B Cassel., PH.D. Perkin-Elmer Corporation, Characterisation of thermosets, the 28th Pittsburgh Conference in Cleveland, Ohio, March 1977.

31. R Bruce. " Differential Scanning Calorimetry of the epoxy Cure reaction" Polymer engineering and Science, Vol.13, No.5, pp 365-371 , 1973.

32. L.E Nielsen., Mechanical properties of polymer and composite, Volume1, Marcel Dekker, INC.Nework 1970.

33. N McCrum., B. Read., Williams.G," Anelastic and Dielectric Effects in polymeric Solids", London, John Wiley and Sons Ltd, ISBN:0-486-66752-9, 1991.

34. FEI and Philips, XL30 ESME TMP, Scanning Electron Microscope, Issue 2.64, 4022 280 00110, 1999.

35. Mboardman@parknelco.com. RFC 822. the contact at parknelco who supplied the information.

Chapter 3 References

1 M. Ieda, M. Nagao, M.Hikita, "High-field conduction and Breakdown in Insulating Polymers Present Situation and Future Prospects", IEEE Tran. DEI, Vol. 1, No.5, pp 934-945, 1994

2 S. Grzybowski, E.A. Feilat, P. Knight, " Accelerated Ageing of High Voltage Encapsulated Transformer for Electronic Applications", The 6th International Conference on Properties and Applications of Dielectric Materials, pp 209-212, 2000.

3 T.Tanaka, T.Okamato, K. Nakanishi, T. Miyamoto, " Review: Ageing and related phenomena in Modern Electric Power Systems", IEEE Transactions E.I., Vol. 28,pp. 826-844,1993.

4 K. Kitagawa, G.Sawa, M.Ieda," Observation of Dielectric Breakdown Sites in Polyethylene thin film" Japan. J. Applied Physics., Vol. 19, pp 389-390, 1980.

5 K.Kitagawa, G. Sawa, M.Ieda, " Self-healing breakdown at Spherulite Boundaties of Polyethylene Thin Films" J. Applied Physics., Vol. 20, pp. 87-94, 1981.

6 A.K Jonscher, "Dielectric relaxation in solids", Chelsea Dielectric Press 1983, ISBN:0950871109.

7 Dissado L.A and Hill R.M, "Constant Phase Angle Response With Fractal Electrodes", Solid State Ionics 26, pp 295-297, 1988.

8 Dissado L.A and Hill R.M., "Constant- Phase Angle and Power Law Regimes in the Frequency Response of A General Determinate Fractal Circuit", The American Physical Society, Physical Review B, Vol37, pp3434-3439 1988.

9 J.M.Alison, "A high field pulsed electro-acoustic apparatus for space charge and external circuit current measurements within solid insulators", J.Meas.Sci and Technol. Vol.9, No. 10, pp1737-1750, 1998.

10 A. See, J.C. Fothergill, L.A. Dissado, J.M Alison, " Measurements of space charge distribution in solid insulators under rapidly varying voltage using high voltage high speed pulsed electro-acoustic (PEA) apparatus", J.Meas.Sci and Technol. Vol.12 , No. 8, pp. 1227-1234, 2001

11 A.see "High field space charge measurements in XLPE using a novel pulsed electro-acoustic system" PhD Thesis, University of Leicester, 2001.

12 Goupil. Norma.P," The use of Differential Scanning Calorimetry(DSC) in the prediction of metal composition and polymer characterisation, Ref. ITS/Gw-96.007. 1996.

13 McNaughton. J, Mortimer.C " Differential Scanning Calorimetry". Printed from IRS Physical Chemistry Series 2, Perkin-Elmer Corporation, Norwalk, Connecticut 068556.

14 J.R Fried, Polymer science and technology, London, Prentice-Hall International Editions ISBN 013685561x, 1995.

Chapter 4 References

1. L.A.Dissado and R.M.Hill, “Constant-phase-angle and power-law regimes in the frequency response of general determinate fractal circuit”, Physical Review B. Vol37.pp.3434-3439. 1988

2. A.K Jonscher, “Dielectric relaxation in solids”, Chelsea Dielectric Press 1983, ISBN:0950871109.

3. R.M. Hill, L.A. Dissado and R.R. Nigmatullin, “Invariant behaviour classes for the response of simple fractal circuits”, J. Phys. Condens. Matter, **3**, pp9773-9790. 1991.

4. R.R.Nigmatullin, L.A.Dissado, and N.N Soutougin” A fractal pore model for Aschie’s law in Sedimeutary Rocks” J.Physics.D ,Vol 25, pp 32-37, 1992.

5. Y. Sheiretov, M. Zahn, “Dielectric Measurements of Moisture Dynamics in Oil-impregnated Pressboard, IEEE Transaction on Dielectric and Electrical Insulation”, Vol. 2. pp329-351, 1995.

6. T.J.Lewis, J.J.Llewellyn, M.van der Sluijs, R.N.Hampton, “A new model for electrical ageing and breakdown in dielectrics”, Proc. IEE DMMA Conf., IEE Conf.Pub., vol 430, 220-224, 1996

7. P.H.F.Morshuis, F.H.Kreuger, P.P Leufkens, “The effect of Different Types of Inclusions on PE Cable Life”, IEEE Transaction on Electrical Insulation, Vol. 23, pp1051-1055, 1988.

8. H.P. Burgener and K. Frohlich, Probability of Partial Discharge Inception In Small Voids, Ann. Rep., CEIDP, pp298-302, 2001.

9. J.M.Alison, “A high field pulsed electro-acoustic apparatus for space charge and external circuit current measurements within solid insulators”, J.Meas.Sci and Technol. Vol.9, No. 10, pp1737-1750, 1998.

10. A.B.Wood, A text book of sound, G.bell and Sons Ltd, London, ISBN 54374532, 1964

11. T.J.Lewis, J.P, Llwellyn, M.J. vander Sluij, J.N. Hampton.” A new Model of Electrical Ageing and Breakdown in Dielectrics”, IEE. DMMA.pp.220-224. 1996.

12. B .Salvage.” Electric Stress in Gaseous Cavities in Solid Dielectrics”Proc. IEE, Vol 11, No 6, pp 1162-1172, 1964.

13. D.D Chang., T.S Sudarshan., and J.E Thompson.” Analysis of Electric Stress Distribution in Cavities Embedded Within Dielectric Structures” IEEE Transaction on Electrical Insulation, Vol. E-21, No 2, pp 213-219, 1986.

14. P.Connor, J.P Jones, J.P Llewellyn. And T.J Lewis.” A Mechanical Origin For Electrical Ageing And Breakdown In Polymeric Insulation.” IEEE International Conference on Conduction and Breakdown in Solid Dielectrics, pp 434-438, 1998.

15. C.H.Park, T.Kaneko, M.Hara, M. Akazaki, “The Effect of Mechanical Stress in The Dielectric Breakdown Strength of PET and FRP”IEEE Transaction on Electrical Insulation, Vol. EI-17, No.3, pp 234-240, 1982.

16. C.H.Park, T.Kaneko, M.Hara, M. Akazaki, “The Effect of Temperature and Voltage on Dielectric Breakdown Strengths of PET and FRP Under Mechanical Stress”IEEE Transaction on Electrical Insulation, Vol. EI-17, No.3, pp 546-553, 1982.

17. Parknelco product specifications, Electrochemical Corporation, 5 Dakota DriveLake Success, NY11042, see internet page www.parknelco.com

Content